AN INVESTIGATION OF SPRING SOURCES AND POTENTIAL ALTERNATIVE WATER SUPPLIES NEAR VIRGINIA CITY, MONTANA

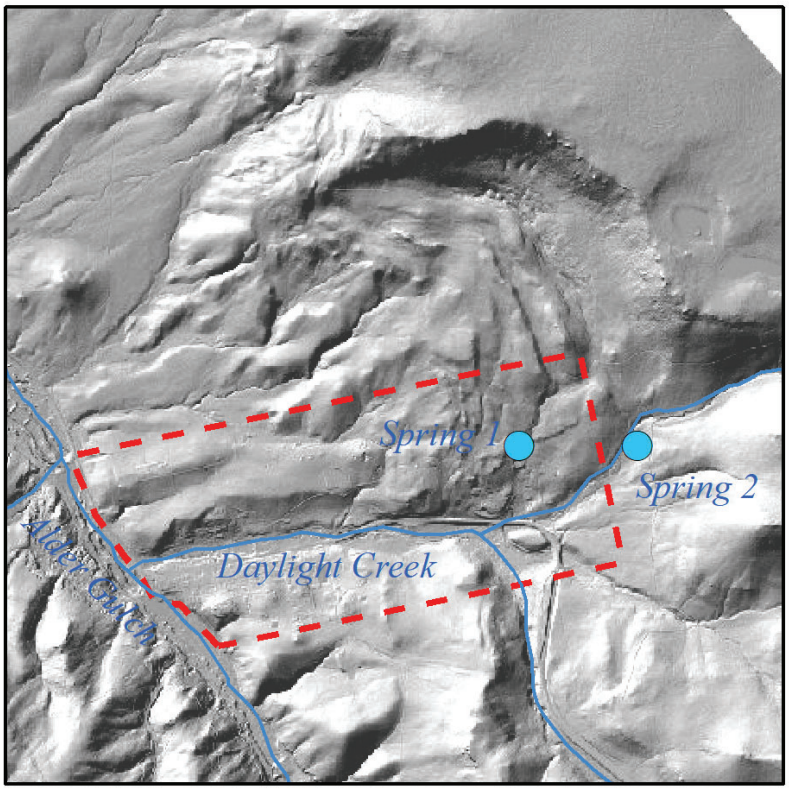

The Virginia City Springs are related to the landslide area northeast of the town center. Spring water that is not needed to supply the municipal system is discharged to ground surface. Photo by Andrew Bobst, MBMG.

Andrew Bobst,[1] Tom Michalek,[1,2] and Jesse Mosolf[1]

[1]Montana Bureau of Mines and Geology
[2]RESPEC, Bozeman, Montana

Ground Water Investigation Program

MBMG
Montana Bureau of Mines and Geology

AN INVESTIGATION OF SPRING SOURCES AND POTENTIAL ALTERNATIVE WATER SUPPLIES NEAR VIRGINIA CITY, MONTANA

Andrew Bobst,[1] Tom Michalek,[1,2] and Jesse Mosolf[1]

[1]Montana Bureau of Mines and Geology
[2]RESPEC, Bozeman, Montana

Ground Water Investigation Program

April 2022

Montana Bureau of Mines and Geology Report of Investigation 30

MBMG
Montana Bureau of Mines and Geology

TABLE OF CONTENTS

FIGURES

TABLES

PREFACE

The Ground Water Investigation Program (GWIP) at the Montana Bureau of Mines and Geology (MBMG) investigates areas prioritized by the Ground-Water Assessment Steering Committee (2-15-1523 MCA) based on current and anticipated growth of industry, housing and commercial activity, or changing irrigation practices. Additional program information and project-ranking details are available at: http://www.mbmg.mtech.edu/gwip/.

Products of the Virginia City Groundwater Investigation:

This **Interpretive Report** presents interpretations of the data and summarizes the project results. This report focuses on the study objectives: (1) to understand the source of the springs that Virginia City uses for their public water supply; (2) to evaluate the potential for residential and commercial development to impact these springs; and (3) to evaluate the potential for developing supplemental water supplies.

An **Aquifer Test Report,** summarizing the results of an aquifer test conducted in the landslide deposits near Spring 1 (Bobst, 2020).

A **Geologic Map** of the Virginia City quadrangle, which provides detailed information on the geologic formations and structures in the area (Mosolf, 2021).

A **Landslide Map** that provides a focused interpretation of where landslides have occurred in the area, based on LiDAR data (Mosolf and others, in prep.).

MBMG's Groundwater Information Center (GWIC) online database (http://mbmggwic.mtech.edu/) provides a permanent archive for the data from this study, including aquifer test reports, aquifer test data, stream stage, stream discharge, groundwater elevations, temperature measurements, and water-quality results. The sites monitored for this study, including their GWIC ID numbers, are listed in appendix A.

ABSTRACT

Virginia City is one of southwest Montana's oldest gold mining districts, whose colorful history draws over 300,000 tourists annually. Residents have become concerned that growing tourism and development will negatively affect the town's developed springs (named Spring 1 and Spring 2), which are the only developed sources of municipal water.

The objectives of this study were to (1) understand the source of the springs currently used for Virginia City's public water supply; (2) evaluate the potential effects of commercial and residential development on spring hydrology and water quality; and (3) identify and evaluate potential supplemental municipal water sources. This study focused on the area upgradient from the two springs, the Daylight Creek drainage (a spring-fed stream), and the area northwest of Virginia City where there are additional springs. Geologic mapping, geophysical measurements, remote sensing, surface-water and groundwater monitoring and sampling, drilling and well installation, and aquifer tests were used to achieve these objectives.

Results showed that the municipal springs are contact springs emitting from contacts between lava flow deposits and an underlying tuff. Spring flow and climate records suggest that in most years Spring 1 has median annual flows greater than 200 gallons per minute. Groundwater from perched aquifers feeds the springs, based on the presence of an unsaturated zone separating the springs from a deeper, regional groundwater system. Likely recharge areas for the municipal springs were delineated based on topography, the locations of other springs, and the conceptual model we developed for these systems. Spring 1 is on the south lateral edge of a landslide complex, which provides a large recharge area with high infiltration rates. Spring 2 is on a scarp at the upper edge of the landslide complex, so the lava flow units in its source area are undisturbed by landslide processes, and its source area is smaller than that of Spring 1. Since infiltration rates are high in both fractured lava

flow deposits and fractured landslide deposits, both springs are vulnerable to contamination from spills or septic discharges in their source areas.

Viable options for supplemental water supplies include: (1) a combination of two or more as yet undeveloped small springs; (2) surface water from Alder Gulch; (3) groundwater from the unconsolidated deposits aquifer along Alder Gulch; or (4) a combination of these options. While water quality is good at most locations, arsenic, a naturally occurring element, exceeds drinking water standards at some of the springs and wells sampled during this study.

INTRODUCTION

Background

Virginia City is located near the divide between the Ruby and Madison drainages in southwest Montana (fig. 1). Virginia City's municipal water supply is sourced from two springs located northeast of town (fig. 2). These springs have served as the primary water supply since 1876 (Great West Engineering, 2016). Land topographically above these springs, and potentially in the recharge area, has been recently purchased for residential and commercial development. This hydrogeologic investigation was nominated by the Ruby Watershed Council to address concerns from Virginia City residents that development near the springs could affect the quality and quantity of the spring water.

A recent water-system evaluation showed that Virginia City does not have a backup water supply adequate to meet the maximum daily demand if the largest spring (Spring 1) is out of service (Great West Engineering, 2016). That evaluation showed the current maximum daily demand is about 91 gallons per minute (gpm) or 131,000 gallons per day (gal/d), and maximum daily demand forecast for 2036 was 120 gpm (173,000 gal/d). This report found that the flow from both springs was about 250 gpm; however, Spring 2 produced about 40 gpm, so the maximum daily demand cannot be met with Spring 2 alone. A redundant supply is required under Montana Department of Environmental Quality Circular 1 (MDEQ, 2014).

Purpose and Timeframe

The objectives of this study were to (1) understand the source area for the springs currently used for Virginia City's public water supply; (2) evaluate the potential impact of residential and commercial development on spring flows and water quality; and (3) identify and evaluate potential supplemental municipal water sources.

This study was initiated in 2017 by establishing a hydrologic monitoring network, drilling several groundwater monitoring wells, and conducting geologic mapping and geophysical studies of the subsurface. Most field activities were completed by the end of 2018. Several sites were revisited in the summer of 2021 for additional spring-flow measurements at key locations.

Study Area

This study focused on the area topographically upgradient from Spring 1 and Spring 2, the Daylight Creek watershed (a spring-fed stream), and the area northwest of Virginia City, where there are additional springs in similar geologic settings (fig. 2). Geologic mapping and elevation data collection via light detection and ranging (LiDAR) were conducted over larger areas.

Physiography

Virginia City is located in the upper Alder Gulch watershed on the west side of a low mountain pass between the Madison and Ruby River Basins (fig. 1). The Tobacco Root Mountains are to the north, and the Greenhorn and Gravelly ranges are to the south. Alder Gulch, a tributary to the Ruby River, borders the western edge of Virginia City. Daylight Creek flows through Virginia City, and is tributary to Alder Gulch (fig. 2). Springs 1 and 2 lie in the hills to the east (fig. 2). The flat-lying plateau at the top of these hills is the drainage divide between the Ruby and Madison watersheds. Elevations in the area range from about 5,700 ft above mean sea level (amsl) near Alder Gulch, to 7,468 ft-amsl at the divide. Spring 1 is at an elevation of 6,205 ft-amsl, and Spring 2 is at 6,318 ft-amsl (table 1).

Climate

Virginia City has cold winters and mild summers. Data from the NOAA Climate Normals (1981–2010) for the Virginia City National Weather Service Station

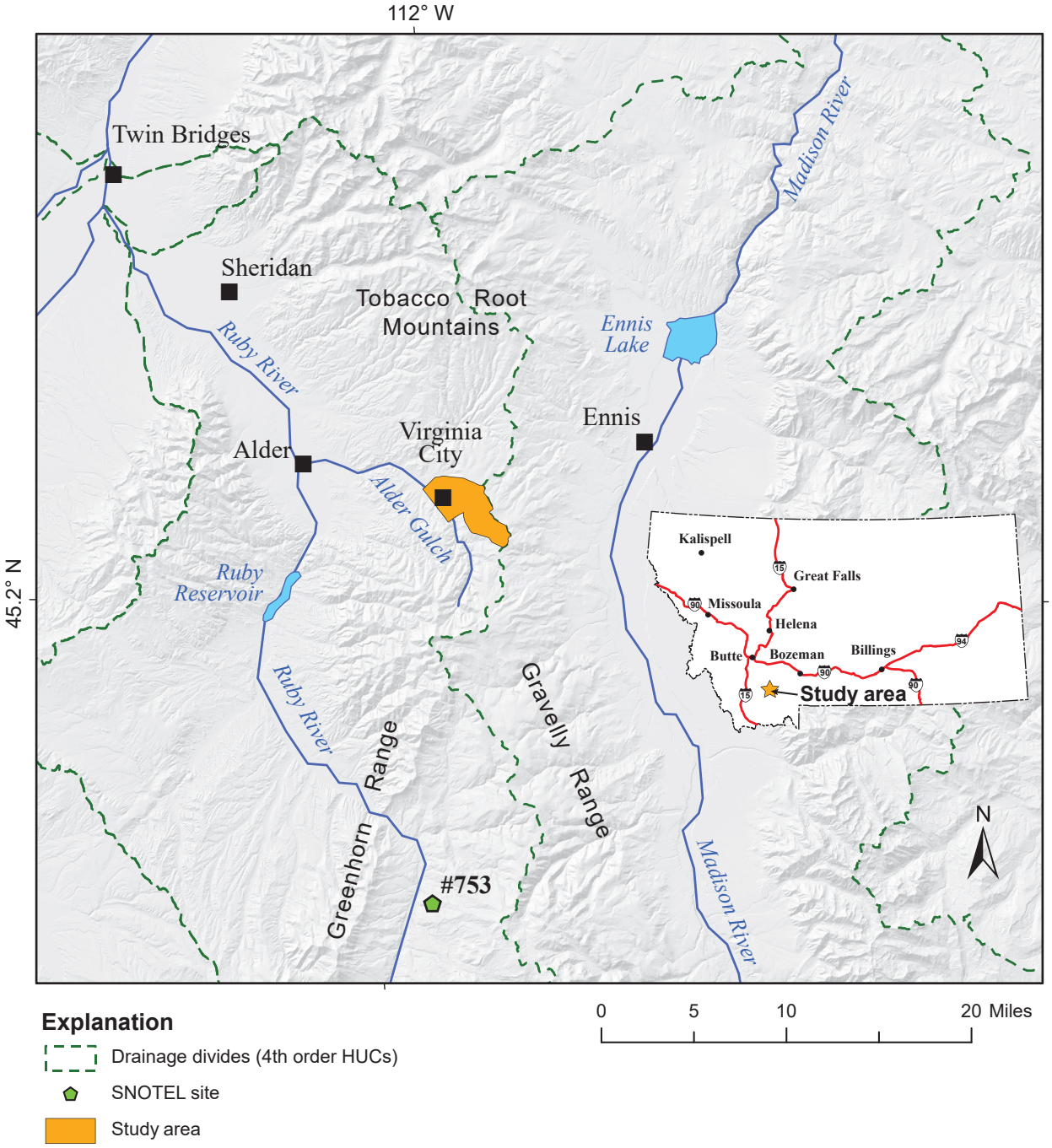

Figure 1. The Virginia City study area is located in southwest Montana, near the divide between the Madison and Ruby Valleys.

(USC00248597; located in the downtown area near Alder Gulch) show that December is the coldest month (average minimum temperature 12.2°F) and July is the warmest month (average maximum temperature 81.5°F). The mean annual temperature is 43.1°F. The highest monthly precipitation occurs in May and June (2.4 and 2.6 in on average, respectively), and total annual precipitation averages 15.30 in. Precipitation models (PRISM, 2018) indicate that mean annual precipitation within the study area ranges from 15 to 22 in, with precipitation increasing with elevation.

The Short Creek SNOTEL site (#753) is 21 mi south of Virginia City, on the western edge of the Gravelly Mountains, at an elevation of 7,000 ft (SNOTEL, 2018; fig. 1). The Short Creek site is located at an elevation between that of the Virginia City Springs and the top of the ridge east of town, and the Short Creek site and Virginia City are both located on the west side of the Ruby–Madison divide. Therefore, we used data from the Short Creek site as a proxy for precipitation and snow accumulation patterns in the area most likely to be feeding the spring systems. The aver-

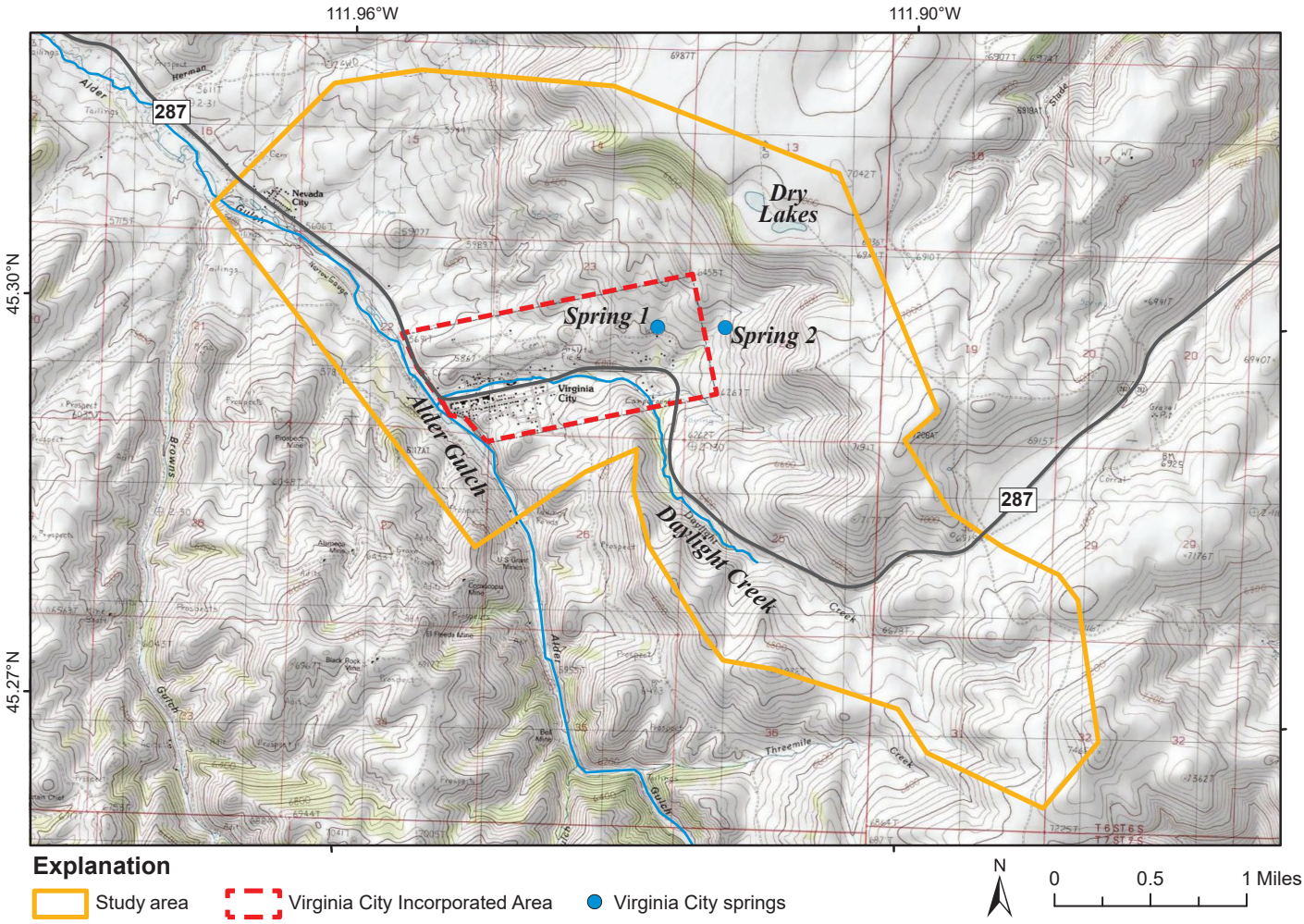

Figure 2. This study focused on the area topographically upgradient from Virginia City's springs, the drainage area of Daylight Creek, and the area north of Virginia City where there are several other springs.

age annual precipitation at the Short Creek site is 17.7 in, and in 2017 and 2018 it recorded 21.5 and 18.7 in/yr (121 and 106% of average; fig. 3A). From water year 2000 to water year 2021 total annual precipitation ranged from 14.0 to 22.2 in. The annual peak snow water equivalent (SWE) is the highest SWE recorded during any day over a water year. From 2000 to 2018 annual peak SWE ranged from 3.6 to 9.2 in (fig. 3B).

Water Infrastructure

In addition to Springs 1 and 2, other smaller springs and wells are used for residential and livestock water outside of the municipal service area. The Montana Bureau of Mines and Geology (MBMG) Ground Water Information Center (GWIC) database shows 19 wells within the Virginia City study area (MBMG, 2018). Septic systems are used to manage domestic waste water from homes located outside of the municipal service area. Within the service area, wastewater is managed through a centralized collection and treatment system. Effluent is used to irrigate hay near Nevada City (Great West, 2016).

Geologic Setting

The area southwest of Alder Gulch was mapped by Weir (1982). This map details the Archean rocks and the associated pegmatite and diabase dikes in that area. Weir (1982) did not map the area east of Alder Gulch in detail.

Previous geologic maps covering the area east of Alder Gulch, including Virginia City and the springs, offer conflicting interpretations of Virginia City's geology. Geologic mapping (1:100,000 scale) by Kellogg and Williams (2006) shows the Virginia City area to be underlain by Tertiary mafic lava flows and rhyolitic tuff (volcanic ash) that unconformably rest on Archean metamorphic rocks. In contrast, Ruppel and Liu (2004) show large parts of the Virginia City area to be underlain by landslide units formed in the Tertiary volcanic units. Both of these mapping efforts show

Table 1. Surface-water and groundwater monitoring network

Map No.	GWIC ID	Site Name	Ground Surface Elevation (ft-amsl)	Total Depth (ft-bgs)	Hydrogeologic Unit	Representative Groundwater Elevation (ft-amsl)	Representative Flow Rate (gpm)
Springs							
3	278204	VIRGINIA CITY * SPRING 2	6,320	NA	Lava Flows	NA	50
4	262623	VIRGINIA CITY * SPRING 1	6,205	NA	Landslide	NA	230
5	298083	GILBERT SPRING	6,202	NA	Landslide	NA	50
6	291688	SAWYER SPRING	5,737	NA	Landslide	NA	NA
7	291701	MASON SPRING	5,685	NA	Landslide	NA	NA
8	292170	NEVADA CITY SPRING	5,610	NA	Landslide	NA	20*
Stock and Domestic Wells							
9	108805	CHRISTMAN, RICH	5,960	99	Landslide	5,910	NA
10	289223	GRANITE CREEK RANCH	6,117	360	Landslide	5,900	NA
11	263446	KOCH, WILLIAM	5,767	318	Basement Rocks	5,760	NA
12	271932	MADISON COUNTY	5,665	109	Alluvium	5,653	NA
13	242217	NEVIN BUBBA	5,659	250	Basement Rocks	5,628	NA
14	236720	BOWLING, ROBERT	5,767	220	Landslide	5,719	NA
15	258455	BOWLING, ROBERT	5,714	550	Landslide	5,714	NA
16	236721	GRANITE CREEK RANCH	5,641	220	Landslide	5,587	NA
17	263878	GRANITE CREEK RANCH	5,687	320	Basement Rocks	5,633	NA
18	258457	BOWLING, ROBERT	5,662	195	Basement Rocks	5,603	NA
Monitoring Well Nest							
19	294417	MBMG BOWLING 1	6,280	155	Landslide	6,171	NA
20	294418	MBMG BOWLING 2	6,280	610	Volcanic Tuff	6,135	NA
21	294419	MBMG BOWLING 3	6,278	240	Landslide	6,171	NA
22	294421	MBMG BOWLING 4	6,283	240	Landslide	6,171	NA
Stream Sites							
23	291773	DAYLIGHT CREEK #1/MADISON SPRING	6,442	NA	Lava Flows	NA	30
24	291774	DAYLIGHT CREEK #2	5,863	NA	NA	NA	NA
25	291775	DAYLIGHT CREEK #3	5,737	NA	NA	NA	NA
26	291776	ALDER GULCH #1	5,773	NA	NA	NA	NA
27	291777	ALDER GULCH #2	5,680	NA	NA	NA	NA

Note. Site details are available at: http://mbmggwic.mtech.edu/. Map no. refers to fig. 7. Gpm, gallons per minute; ft-amsl, feet above mean sea level; NA, not applicable. ft-bgs, feet below ground surface.
*Estimated.

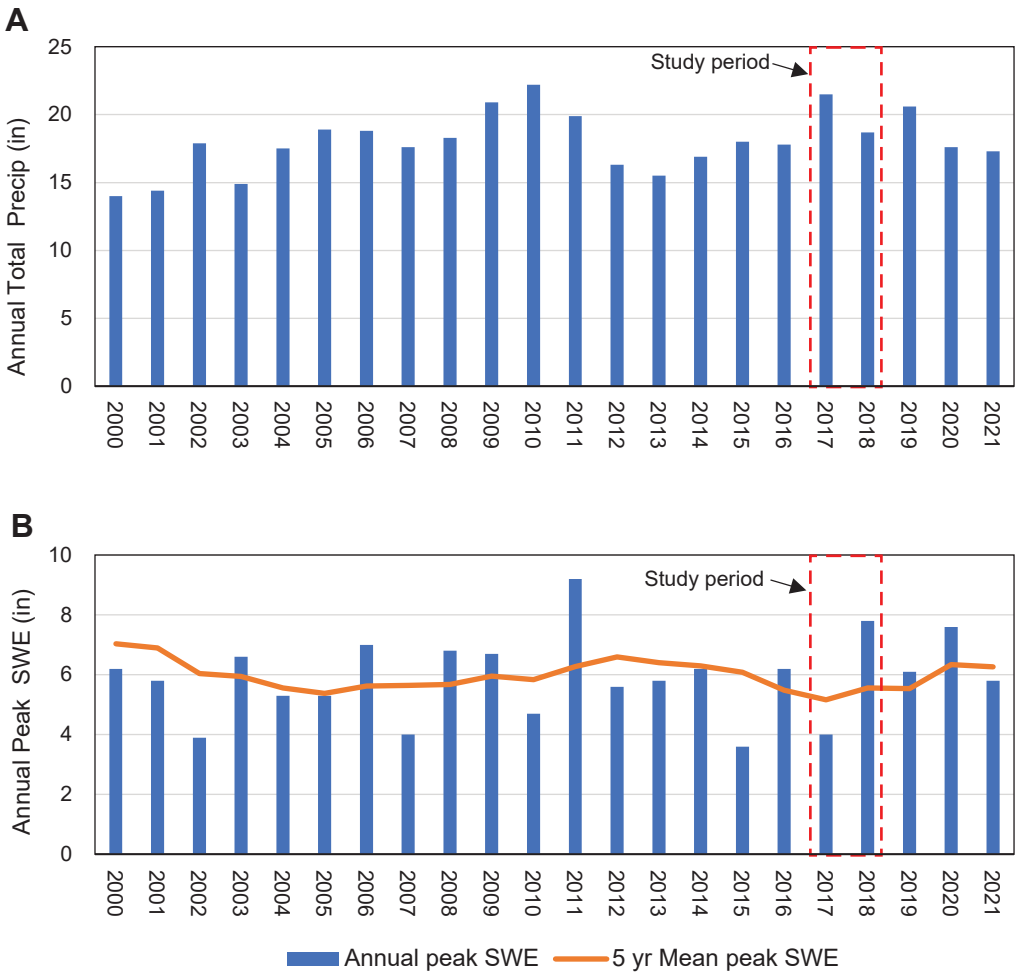

Figure 3. Annual precipitation (A) and annual peak snow water equivalent (SWE; B) recorded at the Short Creek SNOTEL site (#753). Note the highest and lowest precipitation years do not corollate with the highest and lowest SWE years.

that a northwest-trending, left-lateral fault system (the Virginia City fault zone) crosses the area near Alder Gulch, and deforms Archean metamorphic rocks and Tertiary volcanic units in the study area.

Hydrogeologic Setting

Previous hydrogeologic studies in the area focused on the source of water to Virginia City's springs, relying primarily on field reconnaissance and interpretations based on the general geology and geomorphology of the area.

Dunn (1977) noted that the Tertiary volcanic rocks include a sequence of several lava flows that are separated by clay layers, and a thick interval of tuff underlies the lava flow sequence. Based on this stratigraphy, he concluded that snowmelt and rainfall likely infiltrate the lava flows via vertical fractures, and the sub-horizontal clay layers and the contact at the top of the tuff divert a portion of this water to the surface as springs. The water that is not discharged to springs eventually discharges to streams. Dunn (1977) also noted that the larger springs in the Virginia City area form near the contact between the lava flows and the tuff.

Thomas Patton (MBMG, written commun. to Tichenor, 1991) confirmed the geology of the area as described by Dunn (1977), and concluded that groundwater flow to the springs is likely from the north and east. Patton suggested that the town remain aware of potential land-use changes in areas that could be in the recharge zone for the springs. He identified the likely recharge zone as being in areas generally topographically upgradient from the springs (fig. 4).

In 2000 a Source Water Protection Plan (SWPP) developed for the springs noted that the springs discharge from the lava flow deposits (Damschen-Entranco, 2000). The report concluded that due to the low overall evapotranspiration and the fractured nature of the lava flows, infiltration would be on the

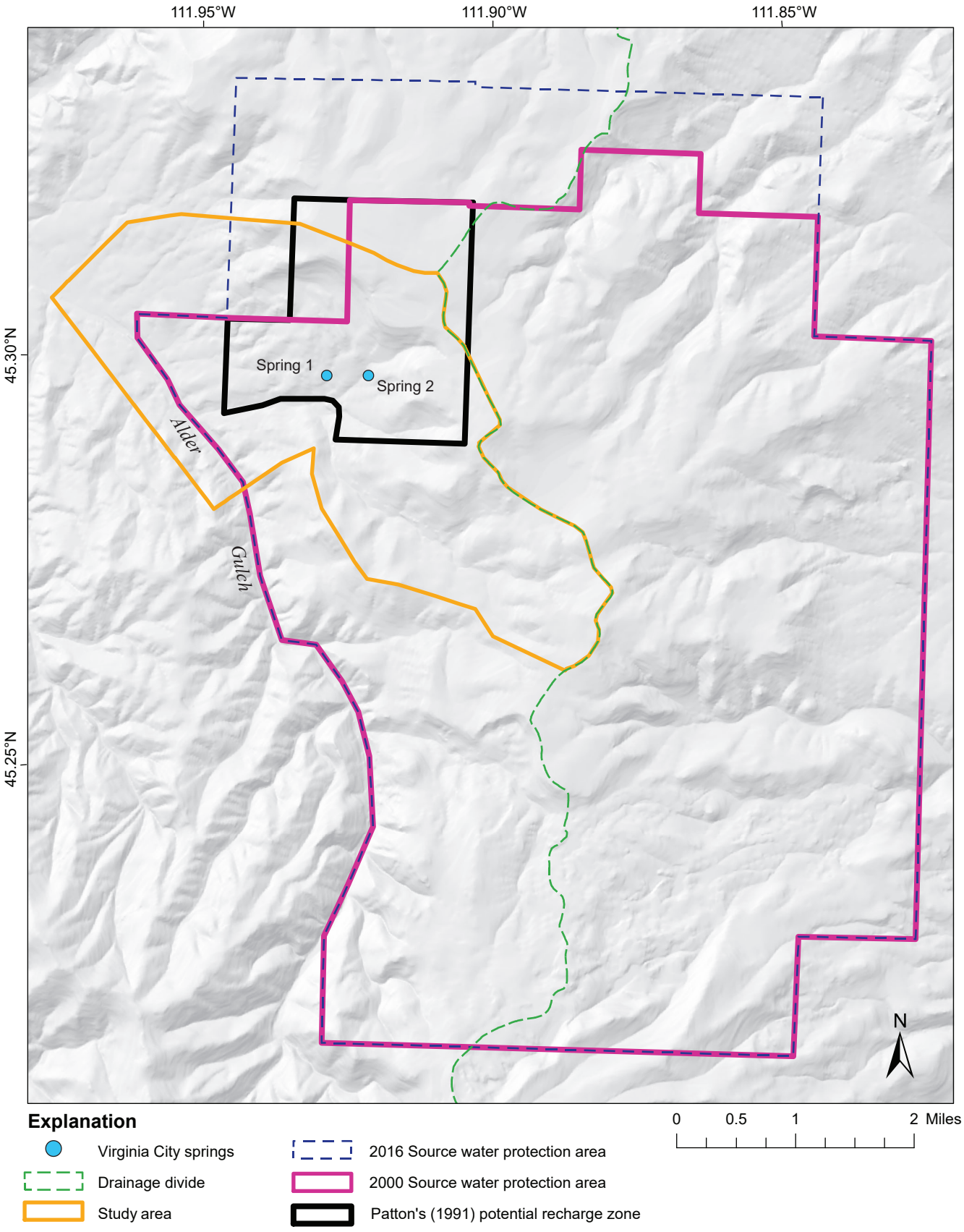

Figure 4. Patton (1991) identified the potential recharge area for the Virginia City springs as being generally the area topographically upgradient from them. Source water protection plans developed in 2000 and 2016 developed larger protection areas due to uncertainty regarding the source areas for the springs.

order of 50% of precipitation. The SWPP also states that "the highest portion of the basalt mass [lava flows], which forms a relatively flat-lying ridge top or plateau, is the primary source of recharge for the Virginia City municipal water system springs." The SWPP also notes that spring flow, temperature, and turbidity measurements collected for an analysis of the Virginia City water system (Damschen and Associates, 1996) showed little variation over time, and the temperature of the water from Spring 1 was about 10°F (5.6°C) warmer than the mean annual air temperature. These measurements suggest a flow system with enough storage to buffer flow and temperature, and to allow sufficient time in storage for geothermal heating of the water. They concluded that the springs appear to be fed by the area between the spring and the divide (Damschen-Entranco, 2000). Because of the uncertainty associated with the fractured nature of the flow system, they used a "conservative approach" and identified a source water protection area extending from Alder Gulch to approximately 5 mi east, 1.5 mi north, and 5.5 mi south of Spring 1, covering a total of 35.8 mi^2 (fig. 4).

The SWPP was updated in 2016 to evaluate new potential threats to the springs (Kline, 2016). The plan update noted that recharge for the springs "…is most likely occurring at the top of the basalt mass [lava flows] …." The increased potential for residential and commercial development in the area topographically above the springs due to recent land sales, and the associated potential for septic drain fields and groundwater extraction wells, were noted as threats to the springs. One of the objectives in this plan was to further characterize the source of Virginia City's springs so that the source area could be defined with more confidence. This update modified the source water protection area by expanding it approximately 1 mi to the north, to cover 41.4 mi^2 (fig. 4).

METHODS

Data Management

Data collected for the Virginia City GWIP project are archived in MBMG's GWIC database (http://mbmggwic.mtech.edu/). GWIC contains well completions, groundwater levels, water chemistry, aquifer tests, and other information. Sites monitored for this project, including GWIC ID numbers, are listed in table 1.

Geologic Framework

Several methods were used to refine the geologic framework in the vicinity of the springs, including collection of areal LiDAR elevation data, electromagnetic and seismic geophysical measurements, and geologic mapping.

LiDAR

A detailed digital elevation model (DEM) of the Virginia City area was compiled using LiDAR data obtained by a manned fixed wing aircraft (Aero-Graphics, Inc., 2017). A 30% overlap was used, yielding an average of 4 points per square meter to obtain QL2 quality/accuracy (Sugarbaker and others, 2014). Ground control points were surveyed to ensure geographic integrity and to test accuracy. The maximum elevation error was 0.29 ft.

Geophysical

A series of geophysical surveys was conducted to identify fracture zones in the area above Spring 1, to investigate lithologies near Springs 1 and 2, to estimate the thickness of the tuff and lava flow deposits, and to evaluate the thickness of the unconsolidated aquifer along Alder Gulch. Geophysical methods included 2D electrical resistivity tomography (ERT), very-low-frequency electromagnetics (VLF), and seismic profiles (figs. 5, 6). The Montana Tech Geophysical Engineering Field Camp performed the work in 2017 and 2018 and results were provided in a series of reports and papers (Khalil, 2017; Rutherford and Speece, 2017; Speece, 2018; Khalil and others, 2018).

Geologic Mapping

Geologic mapping was undertaken to define the geologic, stratigraphic, structural, and geomorphic relationships that control the area's hydrogeology (Mosolf, 2021). Field mapping of the Virginia City 7.5′ quadrangle was conducted during 2017 with reference to previous mapping and research in the region (Cordua, 1973; Weir, 1982; Ruppel and Liu, 2004; Kellogg and Williams, 2006). A 1:24,000-scale topographic base, high-resolution Google Earth areal imagery, and the newly acquired LiDAR data were used to assist field mapping.

Interpretation of the Tertiary volcanic stratigraphy and related intrusions was based on field relationships, petrography, geochemistry, and geochronology data.

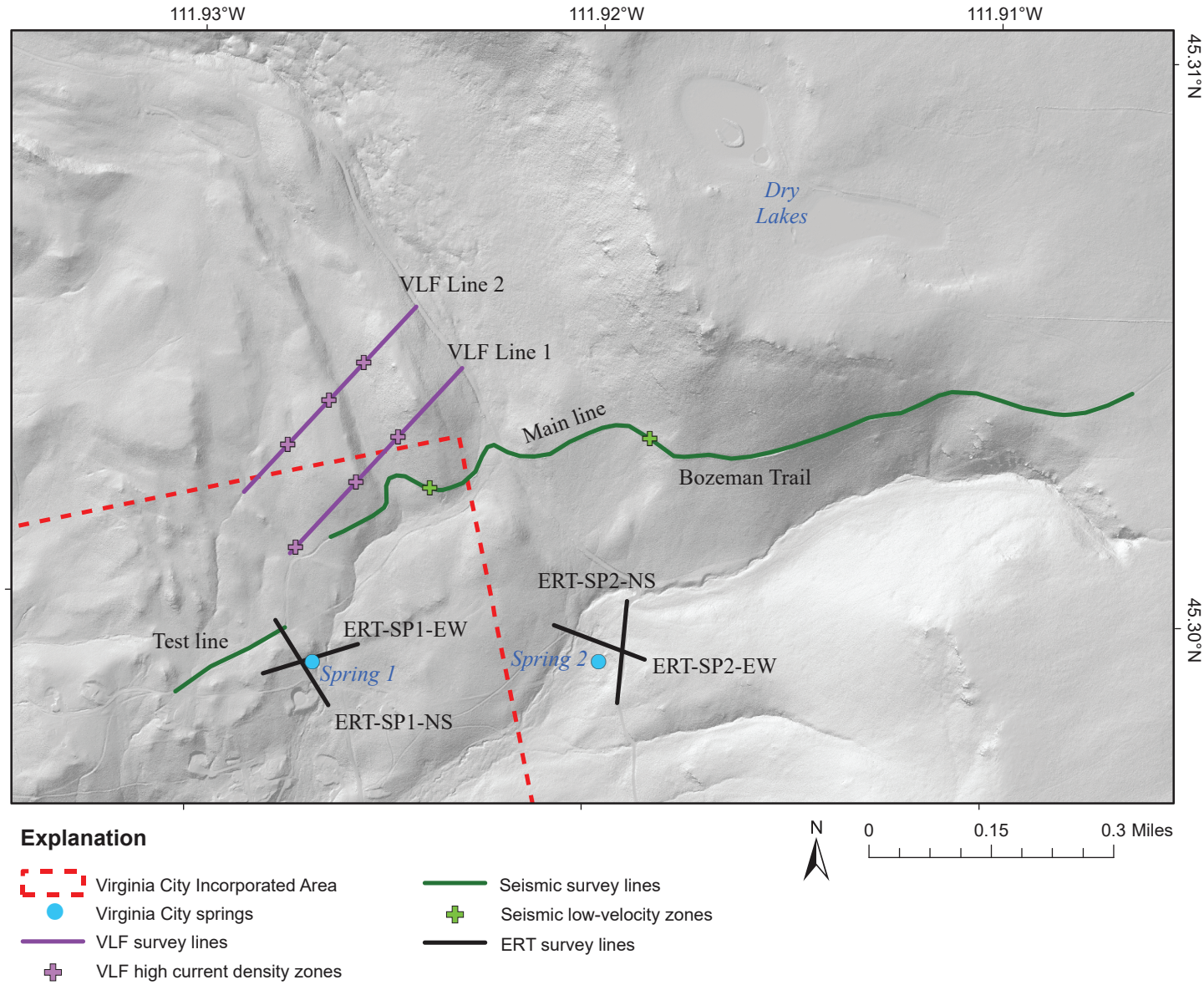

Figure 5. Geophysical surveys using ERT, VLF, and seismic profiles were conducted near the springs in 2017.

Unit descriptions for the Archean rocks were adapted from previous studies (Cordua, 1973; Wier, 1982; Ruppel and Liu, 2004). The LiDAR DEM hillshade model aided the mapping of extensive landslide deposits occurring throughout the study area. Field sheets were scanned and georegistered in ArcGIS, and the geology was subsequently digitized using the NCGMP09 geodatabase template, a cartographic standard jointly formulated by the U.S. Geological Survey and the Association of American State Geologists (Haugerud and others, 2018).

Water Monitoring and Sampling

Monitoring of flows, stages, and groundwater levels, and water sampling were conducted at precipitation sites, springs, wells, and surface waters. For convenience, each monitoring location was assigned a site number (fig. 7; table 1). Selected water-quality results are presented in appendix A, and the results of all water-quality analyses are available in GWIC.

Samples for major ions, trace elements, water isotopes, and nutrients were collected and analyzed following MBMG standard procedures (Timmer, 2020; Gotkowitz, 2022), and were analyzed by the MBMG Analytical Lab (appendix A, tables A1–A6). Samples for major ions, trace elements, and nutrients were filtered prior to collection using 0.45-µm filters. Samples for tritium, noble gases (^{3}He, ^{4}He, Ar, Ne, Kr, and Xe), and chlorofluorocarbons (CFCs) were obtained following sampling SOPs from Noble Gas Lab at the University of Utah (https://noblegaslab.utah.edu/), and were analyzed by that lab (appendix A, tables A7, A8).

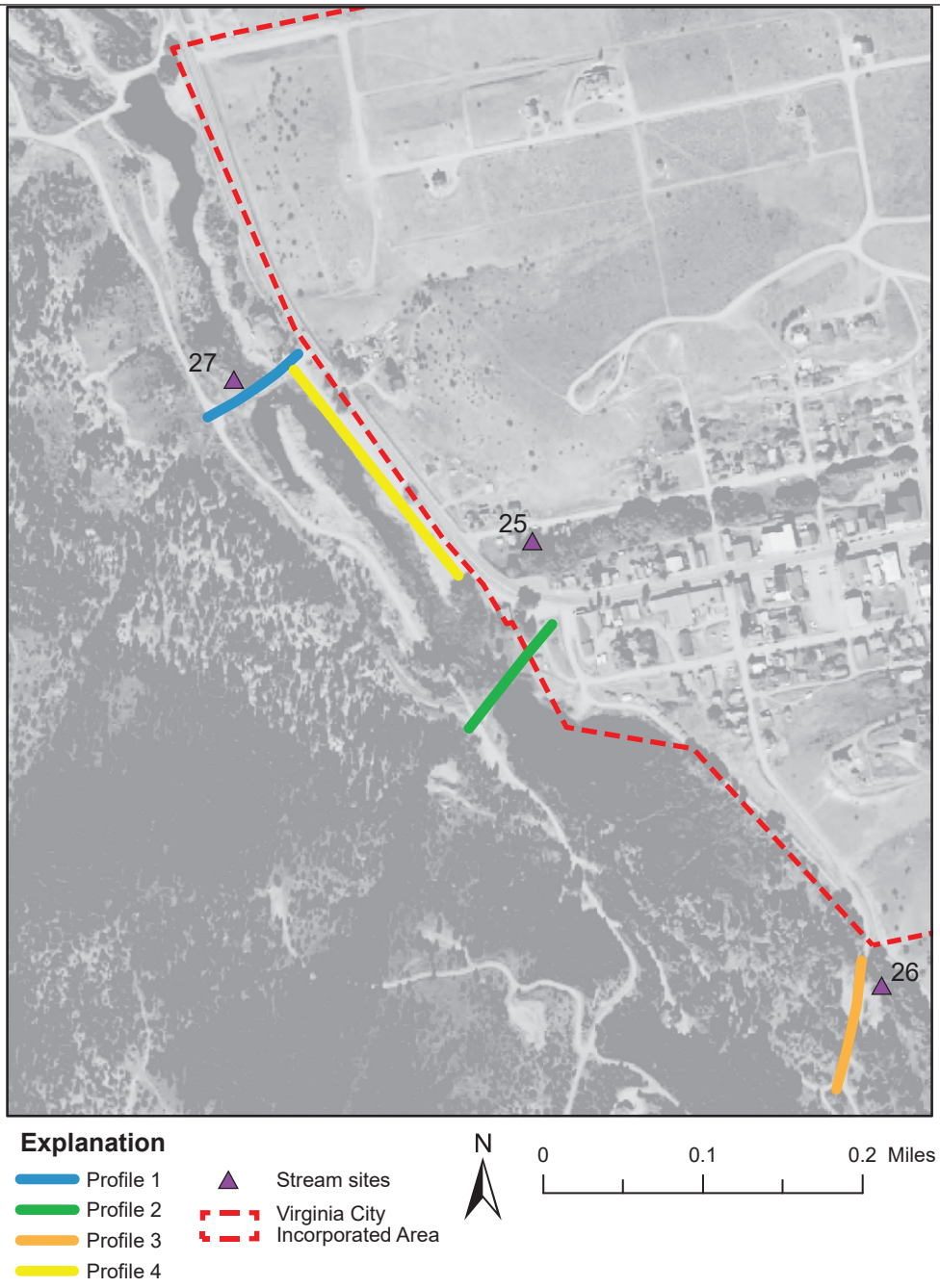

Figure 6. Seismic profiles were collected in 2018 along Alder Gulch. These data were used to evaluate the thickness and geometry of the unconsolidated mining dumps and alluvial deposits. Also shown are the basins along Alder Gulch.

Samples were collected from several wells and springs for analysis of ^{14}C, and were analyzed by Beta Analytics (Miami, FL). ^{14}C analysis supports interpretation of groundwater age (that is, the time since the water entered the groundwater system). These results were consistent with results of other age-dating methods, but due to the low resolution they did not provide additional insight. ^{14}C results are presented in appendix A (table A9), but are not further discussed in this report.

Precipitation

Precipitation samples were collected at two stations (sites 1 and 2; fig. 7) in the Virginia City area for water-isotope analyses (δD and $\delta^{18}O$) to develop a local meteoric water line (LMWL; appendix A; table A2). The LMWL can help identify the sources of water to springs, wells, and surface waters. The upper station (site 1) was located near the top of the ridge east of town at an elevation of 6,928 ft-amsl. The lower station (site 2), at an elevation of 5,777 ft-amsl, was located at the Virginia City weather station in

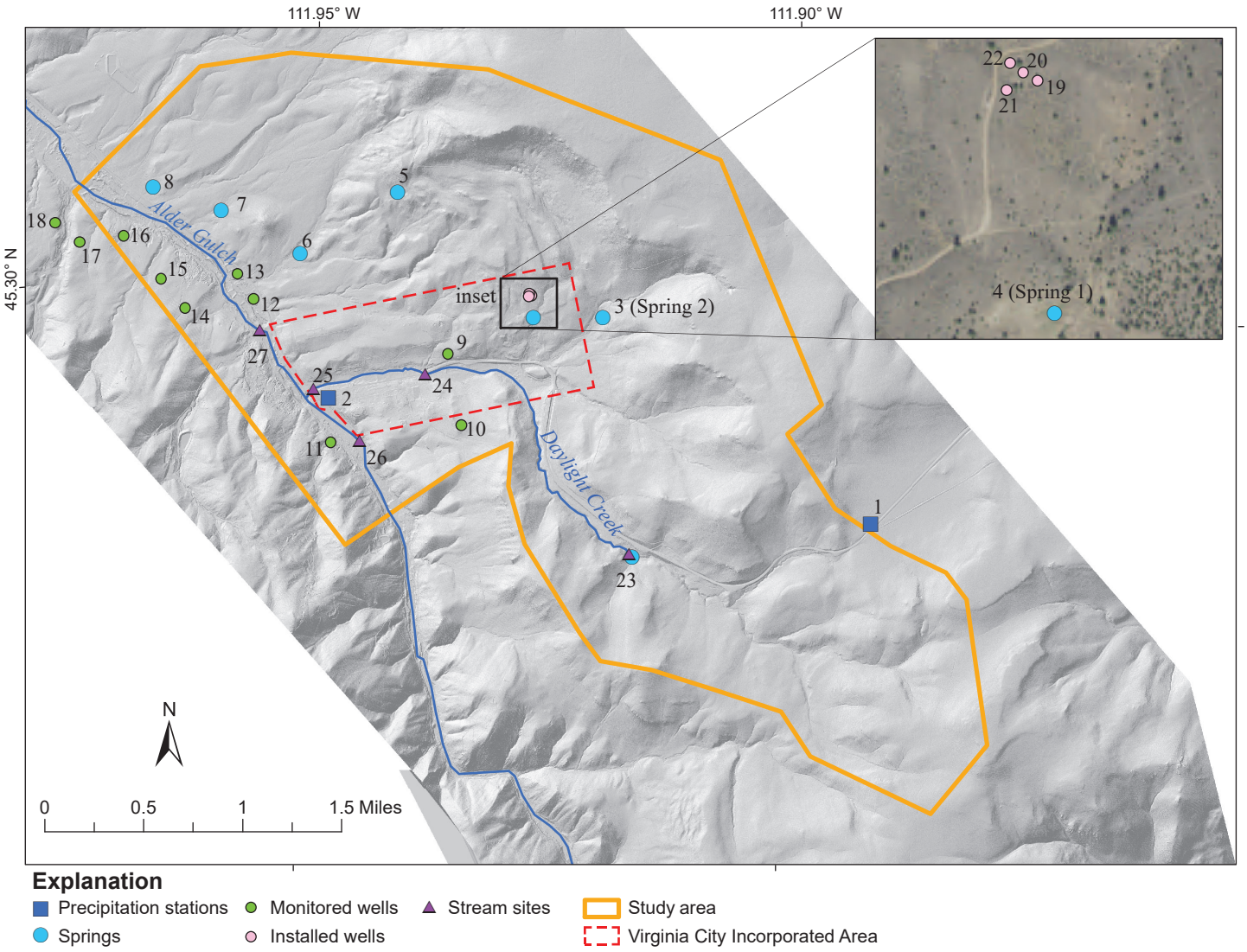

Figure 7. Map of monitoring sites, including precipitation stations (1 and 2), springs (3–8), wells (9–22), and surface-water sites (23–27). Site details, including GWIC IDs, are provided in table 1.

the downtown area, near the junction of Daylight and Alder Creeks. At the lower station, monthly samples were collected from March 2017 to October 2018. At the upper station, monthly samples were collected from April to October 2017, and in April, May, September, and October in 2018. Composite monthly precipitation samples were collected using PALMEX collectors (IAEA, 2002; Gröning and others, 2012), which isolate the samples from the atmosphere to prevent evaporation. The samples were weighed upon collection to allow the weighted mean composition of precipitation to be calculated for comparison to groundwater and spring waters. All results are reported relative to Vienna Standard Mean Ocean Water (VSMOW; Coplen, 1994).

During the winter months (November 2017–March 2018) both precipitation collectors were located at the lower station (site 2). One collector was deployed while the other was kept above freezing. The collectors were exchanged daily if there was snow, so that accumulated snow could melt and flow into the collector to prevent evaporation and sublimation. At the end of each month the contents of the two collectors were weighed and then combined to provide a representative composite sample for the month.

Springs

Virginia City obtains its water from Spring 1 and Spring 2 (fig. 8). The discharge from Springs 1 and 2 are both captured in galleries and then routed to concrete spring boxes. The water from Spring 2 flows through a pipeline for approximately 0.4 mi to the area near Spring 1, and then is either routed to the Spring 1 spring box, or discharged to a natural drainage. From 2013 to mid-July 2018, the Spring 1 spring

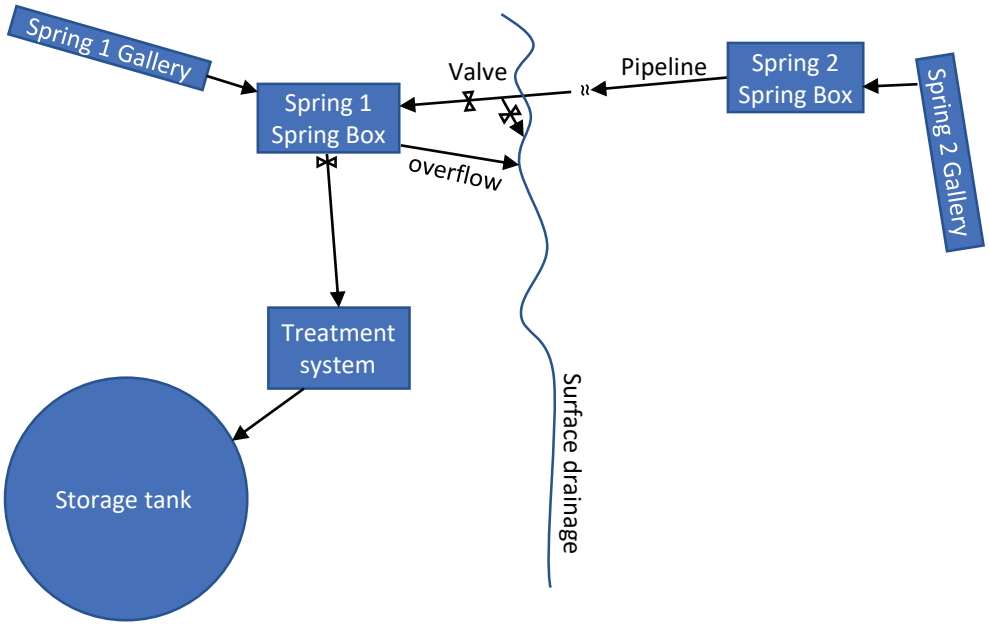

Figure 8. A schematic diagram of the Virginia City water supply (not to scale). When Springs 1 and 2 are both in use for municipal supply, flows are combined in the Spring 1 spring box and then routed to the treatment plant.

box collected only water from Spring 1 (R. Erdale, Water system operator, Virginia City, oral commun., 2018). Since July 2018, water from both springs has been flowing into the Spring 1 spring box. Water from the Spring 1 spring box is either routed to the water treatment plant (when needed), or discharged to a natural drainage, which flows to Daylight Creek. The treatment plant and water storage tank for the municipal system are located approximately 175 ft downhill from the Spring 1 spring box (fig. 8).

Spring 1 (site 3)

Periodic measurements of the flow from the Spring 1 spring box to the treatment system have been recorded by the water system operator since 2013. These measurements were made if water was flowing from the spring box to the treatment system during daily site visits. We used the non-parametric Kruskal–Wallis test to evaluate if median annual flow rates from Spring 1 were changing over time, and used the Wilcoxon rank-sum test, with the Benjamini and Hochberg correction (per Helsel and others, 2020; p. 190–191), to identify which years had statistically different flow rates.

The operator reported that flow rates varied depending on the time that the valve to the treatment system had been open. Therefore, we conducted a flow-rate test on March 14, 2017 to characterize the variability in measured flow rate caused by opening the value to the treatment system. Prior to this test the storage tank was allowed to drain to a low level to maximize the duration of the test. The valve was kept open for 398.5 min (6.6 h), and flow meter and totalizer readings were recorded at regular intervals to determine flow rates over time.

Hourly measurements of water stage, temperature, specific conductance (SC), pH, dissolved oxygen (DO), and turbidity were made in the Spring 1 spring box using a multi-parameter sonde (In-Situ Aqua Troll 600) from March 2, 2017 to July 2, 2018. Data collection with the sonde was discontinued prior to water from Spring 2 being routed into the Spring 1 spring box (mid-July, 2018). Water levels dropped to the bottom of the spring box when the valve to the treatment system was open, dewatering the sonde, and these dry readings were discarded. The sonde was checked against standards quarterly, and recalibrated if needed.

Water-quality samples were obtained from Spring 1 from March 2017 to May 2018 (appendix A, table A3). Monthly samples were collected for water isotopes (δD and $\delta^{18}O$). Quarterly samples were collected for major ions, trace elements, and nutrients.

We collected and analyzed samples for tritium, noble gases, and CFCs to evaluate the residence time of groundwater feeding Spring 1. Tritium and noble gases were sampled quarterly. CFCs were sampled in May and August 2017 (appendix A, tables A7, A8).

Spring 2 (site 4)

The water from Spring 2 flows through a partly filled pipe for 0.4 mi before reaching the sampling point (fig. 8). Spring 2 was not sampled for nitrogen gas, noble gases, and CFCs because samples could not be collected prior to exposure to the atmosphere. Flow was measured by bucket and stopwatch at the outfall. Water-quality samples were collected from March 2017 to April 2018 and analyzed for water isotopes (12 samples), major ions (4 samples), trace elements (4 samples), nutrients (4 samples), and tritium (3 samples; appendix A, tables A3, A7).

Other Springs

Other springs that are not part of the Virginia City water-supply system were evaluated for their potential to serve as supplemental water sources and to aid in understanding the hydrogeologic system.

Sawyer Spring, Mason Spring, and Nevada City Spring (sites 6, 7, and 8; fig. 7) were monitored periodically from April 2017 to June 2018. Field parameters were measured, and water isotope samples were collected during each visit. Due to the low flow conditions and the physical setting at these springs it was not possible to measure flows at these sites on a regular basis using standard equipment. Flow was measured at the Nevada City Spring (site 8) in August 2018 when flows were relatively high. Samples for major ions, trace elements, nutrients, and tritium were collected in May and August 2017 (appendix A, tables A4, A7). Noble gas samples were collected for Mason Spring and Nevada City Spring in May 2017 (appendix A, table A7).

Madison Spring (site 23; fig. 7) was monitored in the channel of Daylight Creek, immediately downstream of the spring. This is the start of the perennial portion of Daylight Creek, so except for during spring runoff, this site both represented Madison Spring and was the uppermost site on Daylight Creek. Like the other springs, it was not possible to measure the flow from this spring on a regular basis; however, flow was measured in August 2018. Supplemental flow measurements were made from late July to mid-September 2021 to assess low flows (appendix A, table A6).

Staff gages, stilling wells, and pressure transducers with data loggers were installed at Nevada City Spring and Madison Spring. This allowed for the collection of hourly stage and water temperature for these sites (appendix C).

Gilbert Spring (site 5; fig. 7) is a potential supplemental water source; however, it was not identified until the summer of 2018 following the primary data collection period for this project. Therefore, it was located and a site description was recorded in GWIC, but it was not sampled or monitored during the study period. Supplemental flow measurements were made in the summer of 2021 (appendix A, table A4).

Groundwater

Groundwater levels were measured monthly in 10 wells from March 2017 to June 2018 (wells 9 to 18; fig. 7; appendix B). These wells are used to supply domestic and stock water, so they may be influenced by pumping. A nest of four dedicated monitoring wells (wells 19 to 22; fig. 7) were drilled and constructed for this study and added to the monitoring network in August 2017 (appendix B). Pressure transducers and data loggers were installed in wells 10, 19, 20, and 22 to measure hourly water levels.

Groundwater-quality samples were collected from nine wells in May and August 2017 (appendix A, tables A5, A7). Samples were analyzed for water isotopes, major ions, trace elements, and nutrients. Samples from five wells were analyzed for tritium, and three of these wells were also sampled for analysis of nitrogen gas and noble gases (appendix A, table A7).

Streams

Surface-water data were collected at three sites on Daylight Creek (sites 23–25), and at two sites on Alder Gulch (sites 26, 27). A stilling well and staff gage were installed at each site with transducers that collected stage and temperature readings every hour during the ice-free period (April to November 2017, and April to June 2018; appendix C). Discharge and stage were measured manually at approximate 2-week intervals during the ice-free periods at all of the sites except for site 23, where flows were typically too low to measure using a flow meter (appendix A, table A6). The manual discharge and stage measurements were used to develop rating curves for each site, and the rating curves were used to calculate hourly discharge values.

Field parameters (pH, SC, and temperature) were measured during most site visits (appendix A, table A6). Grab samples were collected in May and August

2017 for analysis of major ions, trace elements, and nutrients. Water isotope samples were collected approximately monthly (appendix A, table A6).

On Alder Gulch there are several basins (pools) between the two monitoring stations (fig. 6). These basins are regulated using gates to either store or release water.

Well Installation and Aquifer Testing

The four monitoring wells installed for this project (described above) were constructed as a nest of co-located wells completed at various depths at a site topographically upgradient from Spring 1 (fig. 7, inset; table 1). The site is in an area of landslide deposits. The wells were used to conduct an aquifer test in May 2018 (Bobst, 2020). The shallowest well (well 19) was completed in the shallowest productive zone at 135–155 feet below ground surface (ft-bgs). The static water level in well 19 is about 30 ft below the contact between the surficial lava flow deposits and the underlying tuff, and that contact is at the same elevation as Spring 1. Well 20 was completed at 570–610 ft-bgs, below the elevation of Daylight Creek. Although the goal in drilling well 20 was to reach the bottom of the tuff, expected at ~600 ft, the base of the tuff was not encountered, and drilling ceased at 610 ft. Wells 21 and 22 were completed in an intermediate zone (the most productive zone encountered in well 20) at 200–240 ft-bgs.

RESULTS AND INTERPRETATIONS

Hydrogeologic Framework

The Virginia City study area is underlain by basement rocks composed of metamorphic and associated intrusive volcanic rocks that formed during the Archean to Proterozoic [2,700 to 1,700 million years ago (Ma)]. In the Tertiary (41.2–32.9 Ma) these basement rocks were overlain by volcanic tuff, and then by the mafic to intermediate lava flows of the Virginia City Formation (Mosolf, 2021). The Tertiary volcanic units are susceptible to landslides. Quaternary (2.6 Ma to present) gravels are associated with modern streams; however, in many areas these gravels have been disturbed by historical placer mining.

The geologic units were grouped based on their ability to store and transmit groundwater. The units include: (1) metamorphic and intrusive basement rocks, (2) volcanic tuff, (3) lava flows, (4) landslide deposits, and (5) unconsolidated alluvium and mine dumps. These hydrogeologic units are recharged in somewhat different ways. The basement rocks, tuff, lava flows, and landslide units are primarily recharged by diffuse infiltration of water into fracture networks, primarily during spring snowmelt. The unconsolidated units are recharged through multiple pathways including the exchange of water with streams, discharge of water from fractured bedrock, and infiltration of precipitation and snowmelt.

Basement Rocks

The Archean metamorphic rocks and associated Proterozoic dikes make up the oldest hydrogeologic unit in the area, the basement rocks. The metamorphic rocks are composed of gneiss, amphibolite, marble, quartzite, and small bodies of ultramafic rock. Dikes composed of pegmatitic granite and diabase intruded the Archean rocks, likely along preexisting brittle faults and fractures. These units crop out near Virginia City on the west side of Alder Gulch (Agfg, Au, and dikes on fig. 9). These units also occur on the north, west, and south sides of the Virginia City volcanic field, and are believed to underlie the volcanic deposits (Mosolf, 2021; fig. 10).

The metamorphic and intrusive rocks have very low primary porosity, and the movement and storage of groundwater is dependent on fractures. The productivity of wells completed in this unit are variable, ranging from 8 to 50 gpm (MBMG, 2018). Well yields depend on the number of fractures intersected by the well bore, the aperture of those fractures, and the degree to which the intersected fractures are connected to the overall fracture network.

Volcanic Tuff

The oldest Tertiary unit in the map area is a 41 Ma fine-grained tuff exposed near Nevada City (Tnct; fig. 9; Mosolf, 2021); however, its stratigraphic relationship with the overlying units is uncertain due to the extensive landslide deposits. The next oldest mapped unit is also a fine-grained rhyolitic tuff exposed south of Virginia City (Tagf; fig. 9; 35 Ma). The tuff deposits are typically poorly lithified. The glassy components of these ash-derived deposits are often altered to clay.

The only known well completed in the tuff where it has not been modified by landslides is well 20, installed during this study at the aquifer test site. This

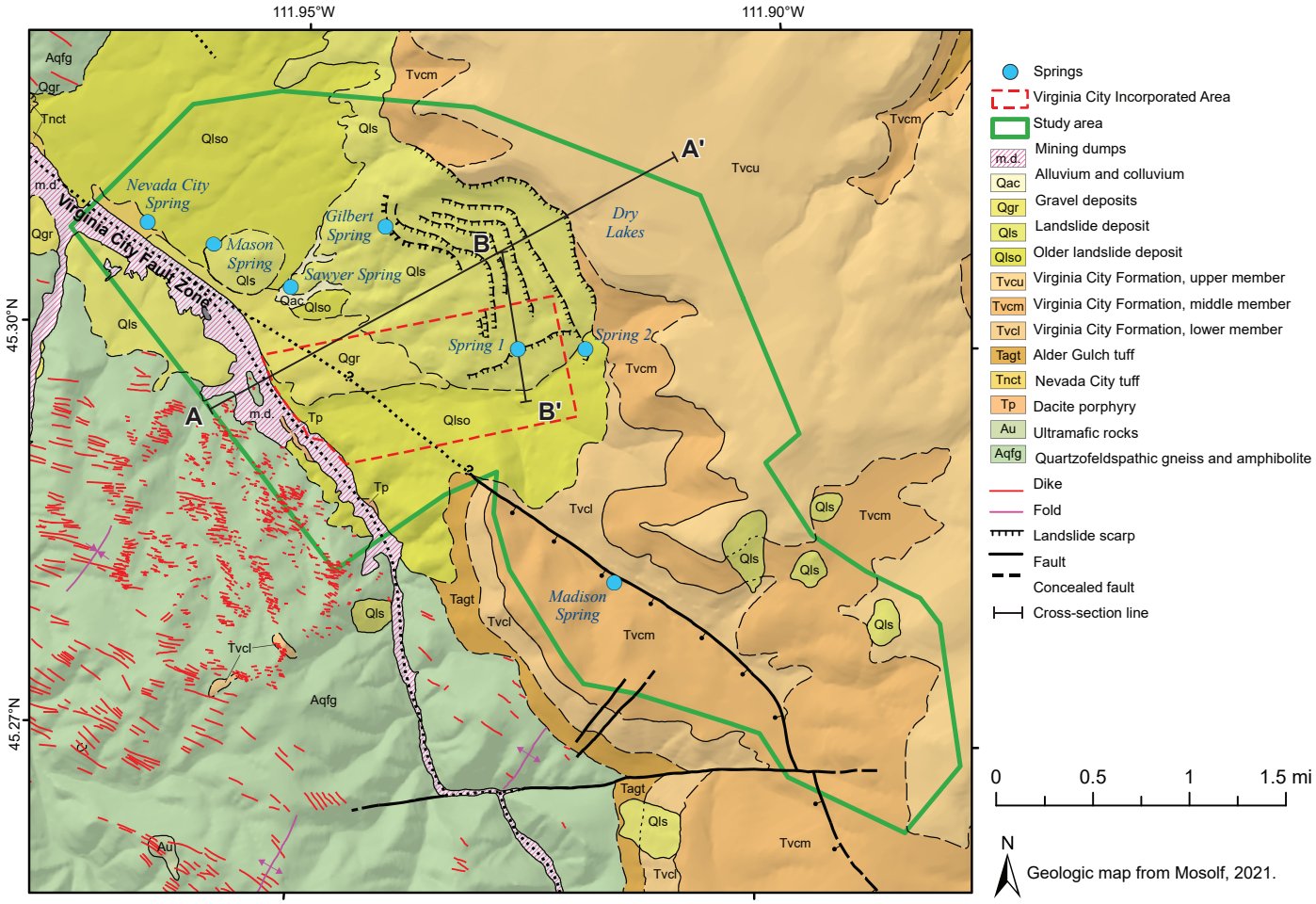

Figure 9. This composite geologic map of the Virginia City area was developed for this study (Mosolf, 2021). The springs are all located at landslide ruptures, bedrock faults, and mapped contacts, suggesting that geologic structures drive spring development. Cross sections A–A' and B–B' are shown in figure 10.

well was screened from 570 to 610 ft-bgs in a poorly cemented zone with no apparent fractures (fig. 10B), and it produced less than 1 gpm.

Lava Flows

The tuff is overlain by a ~650-ft-thick sequence of mafic-to-intermediate lava flows of the Virginia City Formation (Tvcl, Tvcm, and Tvcu; fig. 9; 35–32.9 Ma). The lower, middle, and upper members of this formation were differentiated for geologic mapping (Mosolf, 2021); however, we combined them into a single hydrogeologic unit. This unit forms the prominent mesas north and east of Virginia City (figs. 9, 10).

Lava flows generally have low primary permeability, but they are typically highly fractured and brecciated (Walker, 1971; Anderson and Bowers, 1995). Intervals of autobreccia typically delineate individual lava flows, and the coherent, non-brecciated flow interiors are commonly fractured by cooling joints. The fractured nature of the lava flows, and the thin soils covering them, allow for significant water infiltration. In the Virginia City area, the lava flows lie above the regional water table and there are no records of wells being completed in them. Given the presumed high permeability of the lava flows, if saturated zones exist, wells completed in them would likely be productive; however, such zones have not been located in the study area.

Although perched zones have not been identified during drilling, our conceptual model is that the contact between the relatively permeable lava flows and the underlying low-permeability tuff causes perched aquifers to form at the contact, some of which discharge to springs. These perched aquifers, if they exist, are likely thin due to the relatively high permeability of the lava flows, and laterally discontinuous due to the topography of the top of the tuff.

Spring 2 is located on the main scarp of the landslide northeast of Virginia City (fig. 11). Surface map-

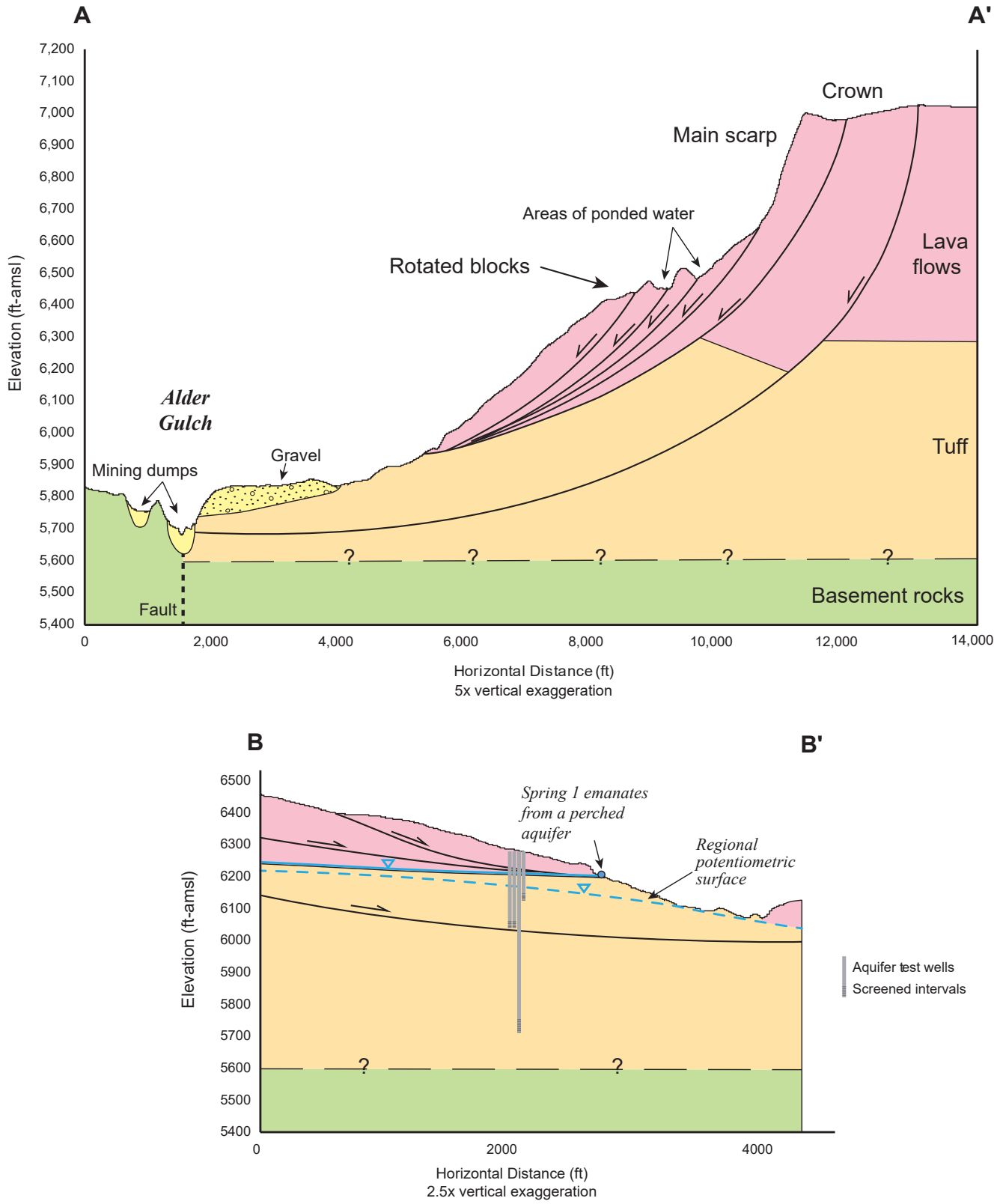

Figure 10. Conceptual cross-sections through the Virginia City Landslide. Mass movements have affected the geometry of the near-surface geologic units near Virginia City (A–A'). Cross section B–B' illustrates well depths at the aquifer test site and the perched aquifer that discharges at Springs 1.

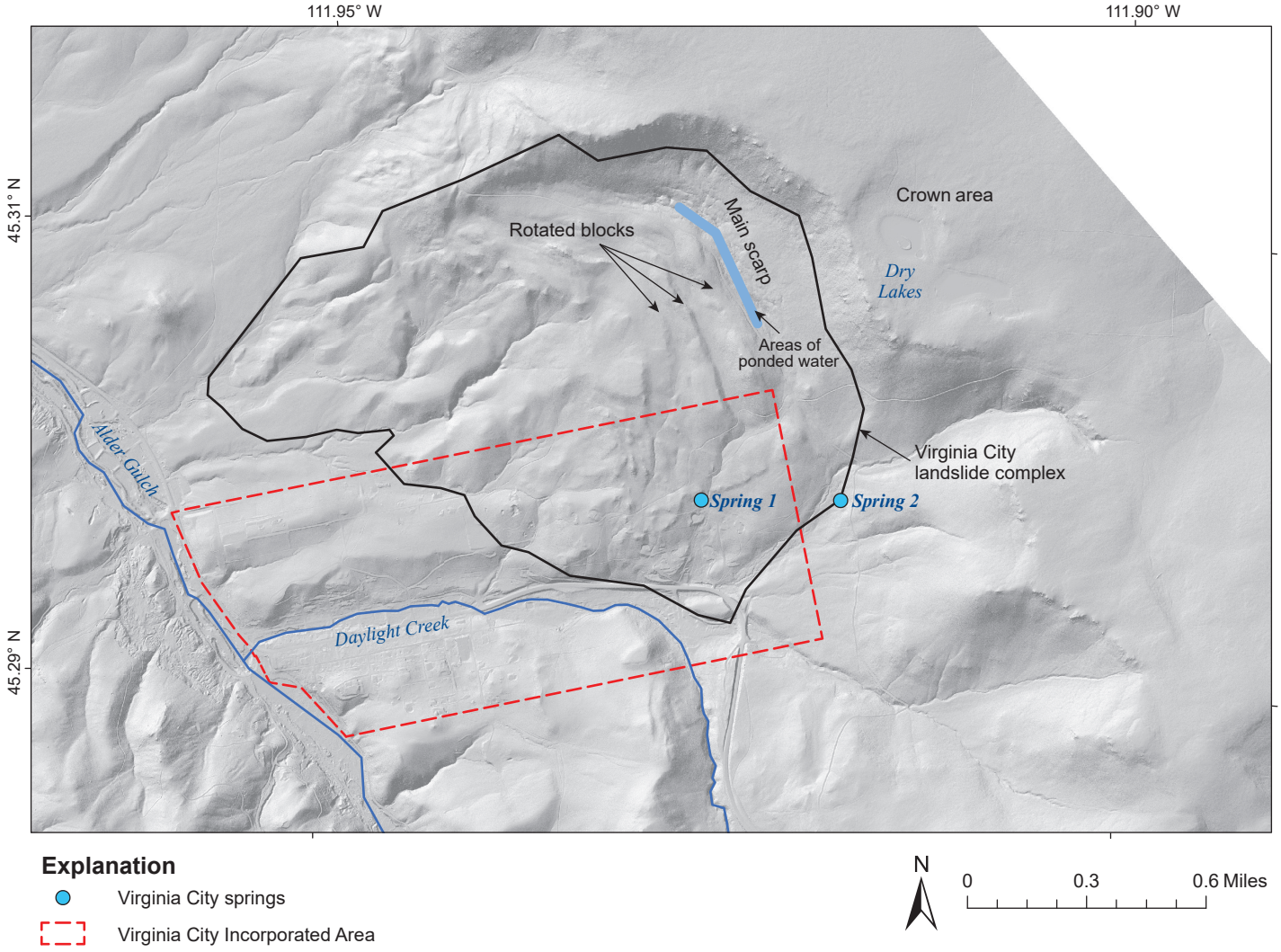

Figure 11. The LiDAR-based hillshade model shows features of the landslide complex northeast of Virginia City. These features are also illustrated in figure 12.

ping and ERT profiles show that the location of Spring 2 is coincident with a contact between lava flow materials topographically above the spring and tuff below (Khalil, 2017; Khalil and others, 2018; Mosolf, 2021). The lava flows and tuff in the area above Spring 2 have not been modified by landslides. As such, it appears that Spring 2 directly discharges from a perched zone at the contact between the lava flows and the underlying tuff.

Landslide Deposits

There are several large rotational and translational landslides and debris flow deposits that rim the high-standing volcanic mesas (Qls and Qlso; figs. 9, 10, 11; Mosolf, 2021). Many of the landslides appear to have been triggered by failure within the tuff intervals (Tnct and Tagf), which likely have low shear strength. Competent blocks of the overlying lava flow units were rotated and transported downslope (fig. 10). These units exhibit many recognizable landforms associated with landslides, including crowns, scarps, fissures, slump blocks, and toes (figs. 11, 12).

In the landslide areas the lava flow units slid and rotated over the tuff (fig. 10), resulting in trough-like features at the surface, which lie between the rotated blocks (fig. 11). These troughs are internally drained basins; there are no streams flowing out of these areas. The landslide area has thin soils underlain by fractured lava flow materials. This combination results in high infiltration. The Dry Lakes area (fig. 11) is also an internally drained basin in the crown area of the landslide that is underlain by lava flow units. Standing water is only seasonally observed in the basins, suggesting high infiltration rates.

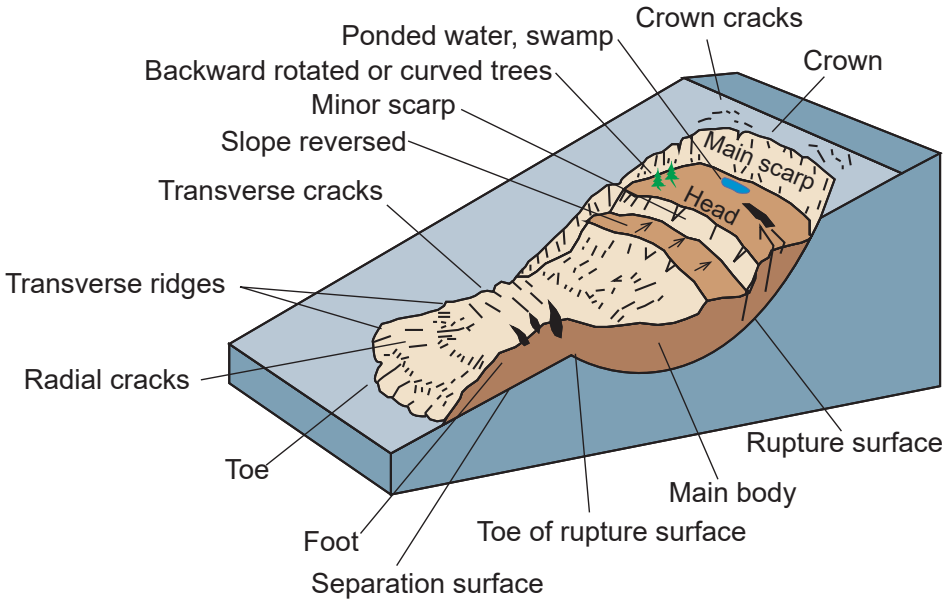

Figure 12. Schematic diagram of a rotational landslide. Rotational landslides are a type of mass movement in which the mass (sediment or rock) moved along a concave rupture surface. The main body of the slide rotated toward the upslope part of the rupture surface, and the toe moved beyond the rupture surface (from Vuke, 2013).

The fracturing associated with landslide activity created secondary porosity and permeability in the tuff and lava flow units. Relatively high porosity increases the potential storage volume within these units. Since the major fracturing associated with landslides occurs along planes adjacent to the rotated blocks, preferential flow paths are likely created. While the intact tuff has low permeability and the observed yield was less than 1 gpm, where it has been fractured by landslide activity it is able to produce up to 20 gpm (Bobst, 2020).

The geophysical surveys conducted in the landslide area provided insight into the internal structure of these materials. The two VLF profiles within the landslide deposits north of Spring 1 (fig. 5; Khalil, 2017; Khalil and others, 2018) reveal zones of fractured volcanic rocks. The fracture zones align with the troughs in the landslide units (fig. 5). Seismic data collected along the Bozeman Trail (fig. 5; Rutherford and Speece, 2017) reveal fracture zones along the main landslide scarp, and bounding the rotated landslide blocks.

Spring 1 is located on the lateral edge of the Virginia City landslide complex (figs. 10, 11). The hillshade model from LiDAR DEM data shows an area of secondary movement within the complex (fig. 11), likely triggered by Daylight Creek eroding the edge of the landslide deposits. Spring 1 discharges at the scarp of this secondary slide (fig. 11). ERT profiles and geologic mapping near Spring 1 (fig. 5; Khalil, 2017; Khalil and others, 2018; Mosolf, 2021) confirm that, like Spring 2, there is a geologic contact coincident with the spring. Although the area near Spring 1 has been influenced by landslide movement, the spring is overlain by lava flows and underlain by tuff (fig. 10). As such, Spring 1 appears to be discharging from a perched aquifer formed at the contact between the overlying lava flow materials and the underlying tuff, but these materials have both been modified by landslides.

Aquifer Test Site

The aquifer test site and well nest was located 0.1 mi topographically above Spring 1 (fig. 7), and within the landslide area (fig. 9). The landslide deposits include extensive blocks of lava flow materials at the surface. The general stratigraphy at this site is fractured lava flows from 0 to 75 ft-bgs, weathered tuff (clay) from 75 to 120 ft-bgs, semi-consolidated tuff with fractured zones from 120 to 240 ft-bgs, and semi-consolidated tuff from 240 to 610 ft-bgs (Bobst, 2020). Wells 19, 21, and 22 (figs. 7, 10B; table 1) were screened in the fractured volcanic tuff, which we interpret as being fractured by landslide movement. Well 20 was completed at 610 ft-bgs in unfractured tuff,

which did not appear to be affected by landslide activity. Seismic results (Rutherford and Speece, 2017) suggest that well 20 was completed close to the underlying contact between the tuff and a more consolidated unit (likely basement rocks; fig. 10B). The contact between the lava flow and the top of the tuff at this site is at 6,205 ft-amsl, the same elevation as Spring 1 (table 1). Static groundwater levels in wells 19, 21, and 22, completed in the fractured tuff, were about 110 ft-bgs (fig. 10B). These water levels are about 35 ft below the contact between the lava flow and the tuff. We did not observe a saturated zone at the base of the lava flows during drilling and well construction. The surface of the tuff is expected to be somewhat irregular due to erosional patterns, and modification by lava flows and landslides. We hypothesize that perched aquifers form in depressions on this surface, with spillways between these saturated pockets.

The three wells completed in fractured tuff had well yields ranging from 8 to 20 gpm. The most productive zone encountered during drilling (200 to 240 ft-bgs) produced about 20 gpm during short-term tests, and therefore was selected as the pumping zone for the aquifer tests. The aquifer tests showed that this zone could sustain a pumping rate of about 20 gpm for several days; however, several months would be needed for water-level recovery. As such, this pumping rate is not a long-term sustainable yield. This slow recovery is likely due to the limited extent of the local fracture network (Bobst, 2020).

Unconsolidated Deposits

Unconsolidated alluvium and mine dumps (placer deposits or spoils from dredging operations) lie along Alder Gulch and its tributaries [Qgr, Qac, and mining dumps (m.d.) in fig. 9; Mosolf, 2021], including the lower end of Daylight Creek. The deposits generally consist of poorly sorted cobbles and pebbles that are rounded to subrounded. Elevated terraces flank the alluvial floodplain along Alder Gulch (Qgr in fig. 9), but these older gravels are likely unsaturated. Most of the alluvial stream deposits in Alder Gulch have been disturbed by extensively dredged placer workings (m.d. in fig. 9). The mining dumps are composed of excavated, transported, processed, and emplaced rock and gravel. Well records in GWIC show only one well (well 12) completed in the unconsolidated deposits within the study area. It is 109 ft deep, with a reported completion in clay and a yield of 8 gpm.

The unconsolidated alluvial and mine dump materials likely have zones of high permeability and porosity, and are likely productive aquifers where saturated. However, the groundwater may be affected by residual mining contaminants. The alluvium and Alder Gulch are hydrologically connected. Alder Gulch meets drinking water maximum contaminant levels (MCLs); however, it is listed as impaired on the Montana Department of Environmental Quality's 2020 303d list (http://svc.mt.gov/deq/dst/#/app/cwaic; accessed 12/10/21) due in part to levels of lead, manganese, and mercury in the water that exceed the standards for aquatic life and recreation. The identified probable sources for lead, manganese, and mercury are mill tailings and mine tailings. Alder Gulch also exceeds the recreation standard for nitrate, with near-stream livestock grazing identified as the probable source.

The seismic profiles along Alder Gulch suggest that the saturated thickness of the unconsolidated deposits varies from about 30 to 100 ft between profiles 1 and 3 (fig. 6; Speece, 2018). The groundwater surface and the land surface were relatively flat; however, there was variation in the bedrock surface. Profile 4 (fig. 6) suggests that the saturated thickness is greatest near the mouth of Daylight Creek. The saturated thickness appears to exceed 100 ft on the north end of profile 3, and on the southeast end of profile 4.

Monitoring

Springs

Spring 1 (site 4)

The spring flow test conducted on March 14, 2017 showed that flow rates decreased substantially over the duration of the 6.6-h test (fig. 13). Flow rates as high as 579 gpm were recorded at the start of the test, and dropped to 150 gpm by the end of the test. Flow rates decreased quickly during the first 3 min of the test, reflecting drainage of the spring box and gallery (fig. 8). After 3 min the flow rates declined logarithmically, as expected for groundwater flow to a constant head boundary (Jacob and Lohman, 1952). After the first 3 min, the time-weighted mean flow rate for this test was 183 gpm. These results show that individual measurements taken in the treatment area as the tank fills (discussed below) are influenced by the timing of measurements relative to the tank filling cycles. Measurements made immediately after the valve opened will be high, while measurements made several hours

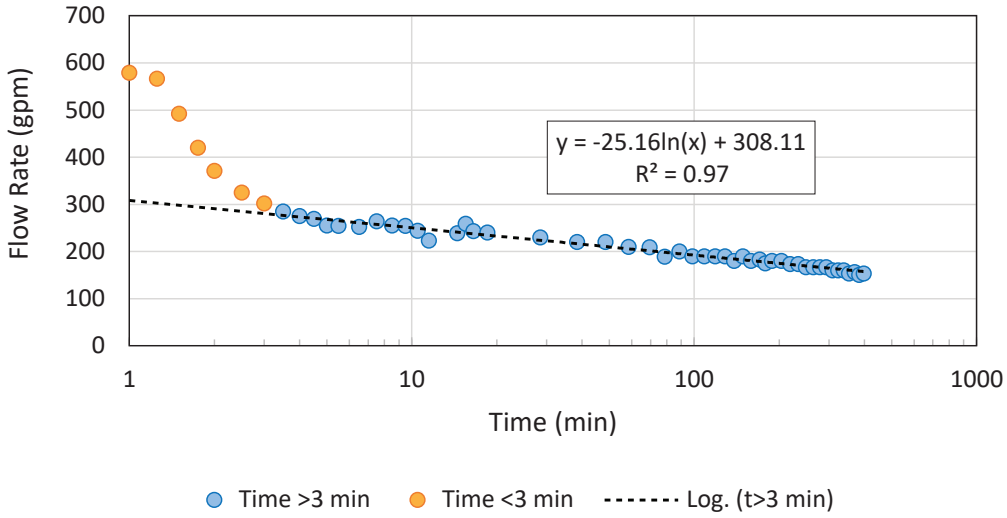

Figure 13. Discharge of Spring 1 was measured on March 14, 2017, with the valve open for 6.6 h.

after the valve opened, and measurements taken when the system had not fully recovered from the previous tank-filling cycle, will be low. We used non-parametric statistics to minimize the effect of these outlier measurements when evaluating the operator-recorded spring-flow data below (Helsel and others, 2020).

Operator-recorded flow rates to the treatment system from the Spring 1 spring box (fig. 8) between 2013 and 2020 were used to evaluate patterns in the flow rate of Spring 1 (fig. 14). Starting in mid-July 2018, measurements included discharge from Spring 2 (fig. 8). The average flow from Spring 2 during this study (2016–2017) was 50 gpm (see below), so we subtracted this amount from measurements collected after mid-July 2018 to remove the influence of Spring 2. A scattering of measurements was particularly high, which we attribute to the measurement being collected soon after the valve opened (figs. 13, 14A). Clusters of relatively low flow rates, particularly during the summers of 2016–2020 (fig. 14A), are attributed to readings collected when the valve was open for a long duration, or from periods where the valve reopened before the system had fully recovered from the previous tank-filling cycle. Both situations are more likely to arise in the summer. Since higher flows (similar to winter values) were also recorded on some days during these dips, it appears that the clusters of lower measured flows in the summer reflect system management rather than reduced spring productivity.

The flow rates for Spring 1 decreased from 2013 to 2016, and then were generally stable from 2016 to 2020 (fig. 14B). Median annual flows from 2013 to 2020 did not remain the same (Kruskal–Wallis rank sum test: p-value <0.001). The flows during 2013, 2014, and 2015 differed from each other and later years (Wilcoxon pairwise rank sum test: all p-values <0.001), with median flows of 348, 292, and 261 gpm, respectively. Flows from 2016 to 2020 were generally similar, with medians flows ranging from 223 to 240 gpm.

Median annual flow rates for Spring 1 were compared to precipitation and snow pack information at the Short Creek SNOTEL site (site #753; figs. 1, 3) to evaluate relationships between weather and variations in flow. We found the strongest correlation between the median annual flow from Spring 1 and the 5-yr mean peak SWE (fig. 15). The isotopic composition of the water from Spring 1 also supports that groundwater discharging at Spring 1 is dominantly recharged during snowmelt (see below). There appears to be a piecewise linear relationship between the 5-yr mean peak SWE and the median annual discharge from Spring 1, with a break in slope at about 6.2 in of SWE. Spring flows show little variation when the 5-yr peak SWE is less than 6.2 in; the slope of the relationship (1.8 gpm/in) is not statistically different from zero (p-value = 0.889). The median annual flow from Spring 1 responds more strongly when the 5-yr mean peak SWE is greater than 6.2 in (slope is 290 gpm/in), and the slope is statistically different from zero (p-value = 0.016). This correlation also suggests that the median annual flow from Spring 1 should remain above 200 gpm unless there are dramatic changes to the system.

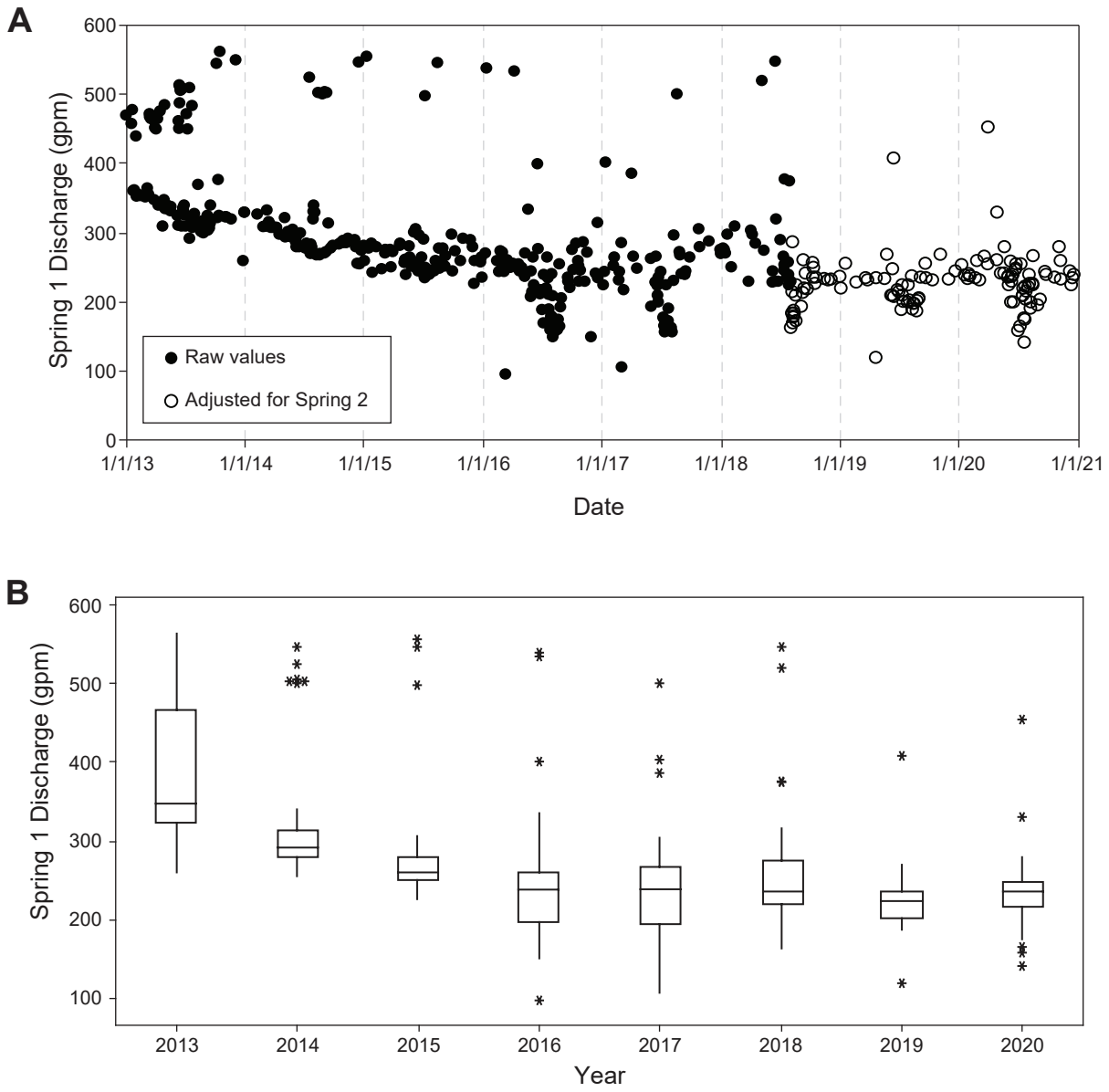

Figure 14. Spring 1 discharge measured by the municipal system operator (A). Recorded values from after mid-July 2018 were reduced by 50 gpm to account for flow from Spring 2 into the treatment system. The box and whisker plot (B; Helsel and others, 2020, p. 22–26) shows these measurements grouped by calendar year. (B) The boxes show the interquartile ranges (25th to 75th percentiles), the central lines show the medians, whiskers show the range of values within 1.5 times the interquartile range, and asterisks (*) show outliers.

Spring 2 (site 3)

The measured flows from Spring 2 ranged from 24 to 89 gpm with an average of 50 gpm (fig. 16 and appendix A, table A3). Maximum flow occurs in the springtime (April/May), with lower flows in August. This suggests that Spring 2 responds to seasonal variations in water availability.

Nevada City Spring (site 8)

As noted in the methods section, data collection at the Nevada City spring was limited to hourly stage readings during the ice-free period (appendix C). We used the stage record to evaluate flow dynamics. Spring stage readings during 2017 showed little variation (0.33 to 0.45 ft). A slight response to large rain events is attributed to surface runoff collecting at the spring. The stage was also stable (0.48 to 0.61 ft) in 2018, but was on average 0.14 ft higher than in 2017. Groundwater levels and surface-water flows in Daylight Creek and Alder Gulch were also higher during 2018 (see below). Therefore, the higher flow at the Nevada City spring likely resulted from greater snow pack in water year 2018. Discharge measured from

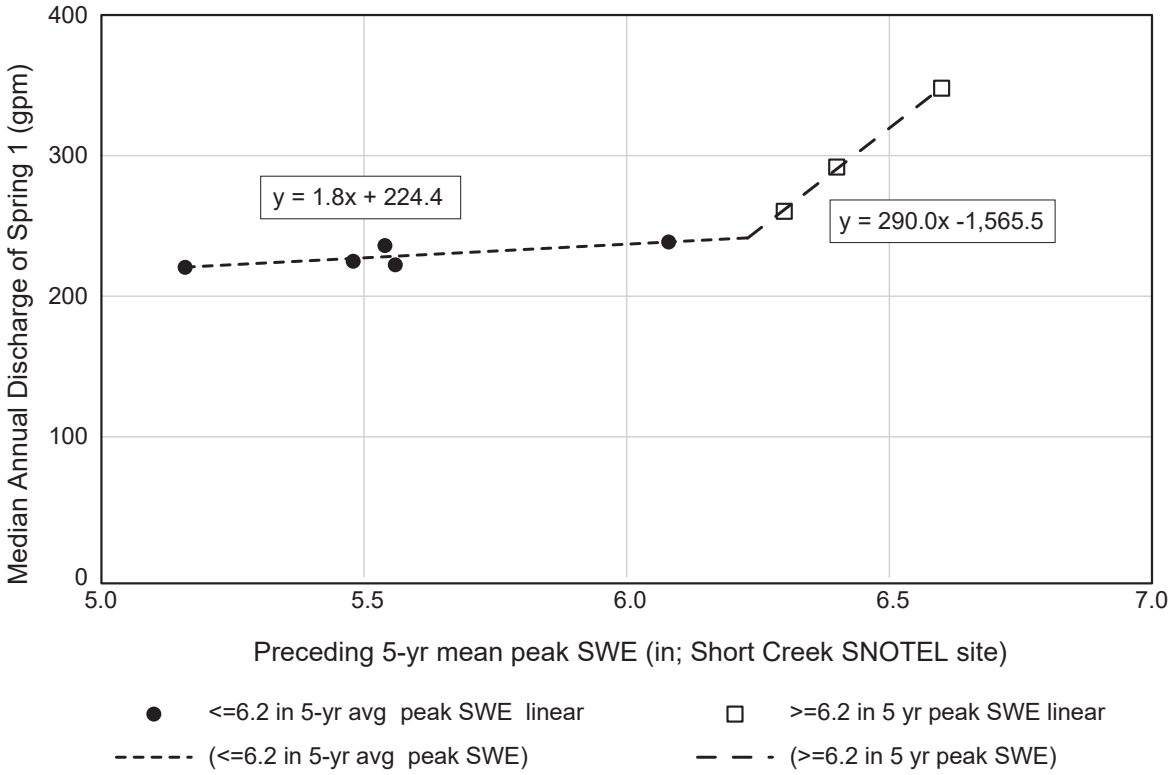

Figure 15. There is a relationship between the 5-yr mean peak snow water equivalent at the Short Creek SNOTEL site (x-axis; fig 3) and the median annual discharge from Spring 1. This is a piecewise linear relationship, with a break in slope at a 5-yr mean peak SWE value of about 6.2 in.

Nevada City spring on August 13, 2018 was 108 gpm with a stage of 0.49 ft.

Madison Spring (site 23)

Stage was measured hourly in the channel of Daylight Creek immediately downstream of Madison Spring from April to November 2017 and from April to June 2018 (appendix C). Daylight Creek originates at Madison Spring except during periods of substantial surface runoff. Therefore, the variations in stage at site 23 reflect changes in spring flow except for periods of snowmelt and large rain events. The stage at site 23 showed little short-term variation (from 0.58 to 0.78 ft, with an average of 0.69 ft) from April to November 2017. In April 2018, variation in stage increased, ranging between 0.76 and 2.06 ft, in response to snowmelt draining to this site via Daylight Creek. Short-term variation in stage decreased during May and June 2018, and stage declined through early June, followed by a rise through the end of monitoring in early July. This appears to reflect declining runoff, followed by a lagged increase in spring discharge. 2018 stages exceeded those in 2017, with an average stage during May and June of 0.88 ft. The discharge at site 23 was measured at 130 gpm on August 13, 2018, at a stage of 1.00 ft. Supplemental discharge measurements during the summer of 2021 ranged from 17 to 38 gpm (appendix A, table A6).

Gilbert Spring (site 5)

Gilbert Spring was visited on July 30, 2018, and flow was visually estimated at about 30 gpm. During supplemental monitoring in the summer of 2021, discharge ranged from 49 to 60 gpm (appendix A, table A4). Geologic mapping and field reconnaissance indicate this spring lies within the landslide deposits. The spring emits at a scarp inside the Virginia City landslide (fig. 9), where the contact between the overlying lava flows and underlying tuff is exposed, similar to Spring 1. Gilbert Spring is also at the same elevation as Spring 1 (table 1).

Groundwater

Groundwater Elevations

The well monitoring network for this project included wells completed in basement rocks, tuff, landslide deposits, and unconsolidated deposits (table 1).

Wells in the basement rocks (wells 11, 13, 17, and 18; table 1) generally showed higher water levels

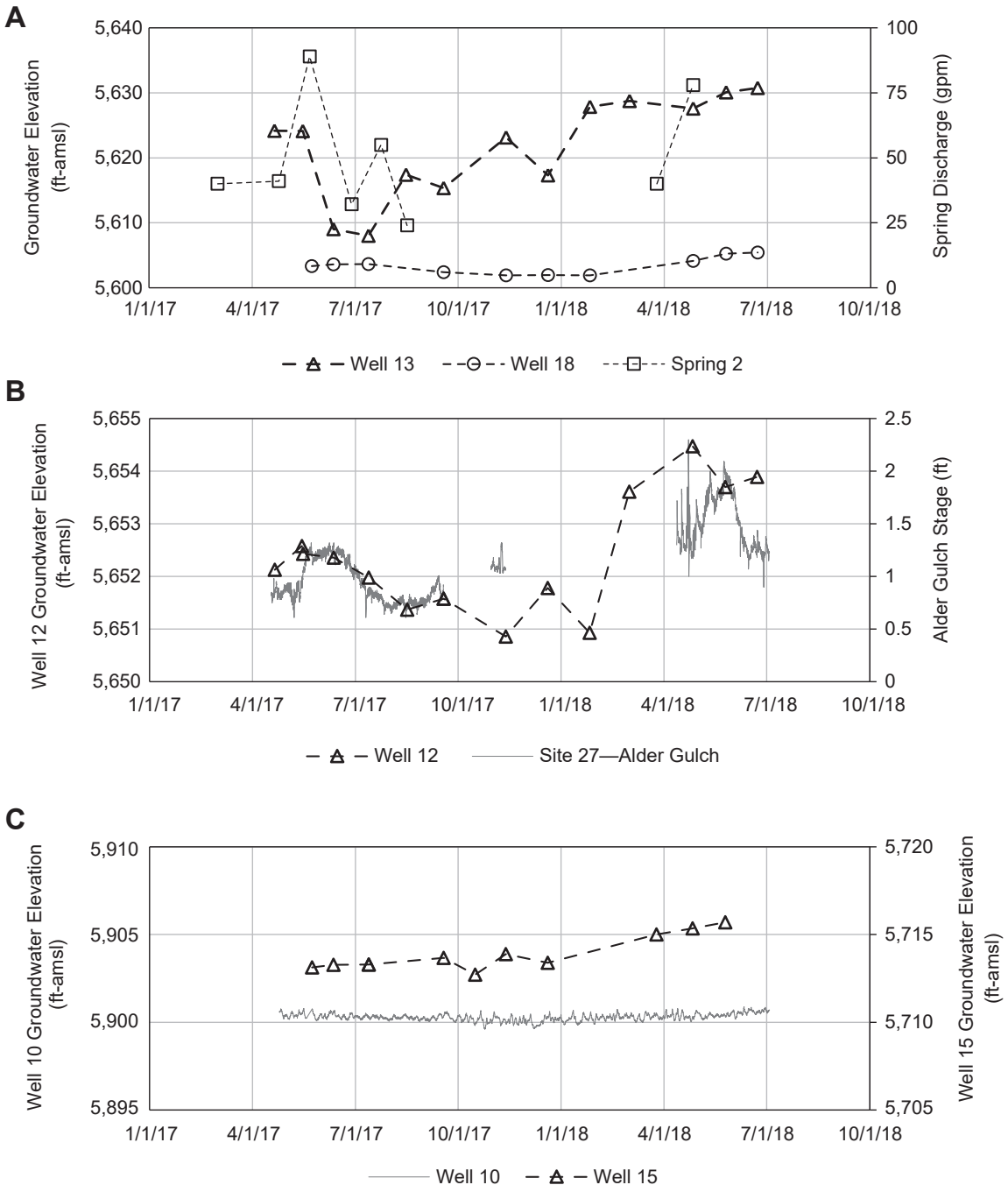

Figure 16. Discharge from spring 2 compared to groundwater levels in the basement rock (A). The highest spring flow rates were measured in the springtime each year. Groundwater levels in wells completed in basement rocks (A) declined through the summer of 2017, and then rose in the spring of 2018, similar to the flows in Spring 2. Groundwater levels in well 12, completed in the alluvium (B), followed stream stage. Wells 10 and 15, completed in the landslide deposits (C), had stable groundwater levels through 2017, and then rose in the spring of 2018; however, the magnitude of increases varied by well.

in the spring of 2017 and 2018 (appendix B and fig. 16A). Summer groundwater levels were more variable in used (pumped) wells due to higher summer use (e.g., well 13 vs. well 18; fig. 16A). Spring 2 has its source area in intact lava flows, and the observed flows from Spring 2 show a pattern similar to that of the groundwater levels in basement wells (fig. 16A), suggesting that the basement wells and this lava flow sourced spring are similarly influenced by springtime recharge.

Three of the four wells in the aquifer test site well nest (wells 19, 21, and 22; table 1) were completed in the landslide deposits. The deep well at this site (well

20) was completed in the underlying tuff, which did not appear to be affected by the landslide movement. The vertical gradient is downward at the site, with heads in the landslide unit exceeding those measured in the underlying tuff (fig. 17). The landslide deposit wells, completed between 155 and 240 ft-bgs, had static groundwater elevations at about 6,171 ft-amsl. Well 20, with a total depth 610 ft-bgs, had a static groundwater elevation at about 6,135 ft-amsl. This relatively large difference is consistent with the results of the aquifer test (Bobst, 2020), which showed pumping from a landslide well (well 21) caused drawdown in the other two landslide wells (19 and 22), but no measurable response in well 20. The hydrographs for the landslide wells at this site (fig. 17) were flat from the fall of 2017 until the end of March 2018. Water levels in landslide wells then rose from late March to early May, but the rise was arrested by the aquifer test at this site (pumping from 5/9/18 to 5/17/18; Bobst, 2020). Following the aquifer test, groundwater levels recovered until the end of monitoring (5/17/18 to 7/2/18; fig. 17A). Well 20 (tuff) showed a slight rise from the fall of 2017 until the spring of 2018, was strongly drawndown during development and sampling, was slow to recover from pumping, and was not influenced by the aquifer test in the overlying landslide deposits (fig. 17B).

Other wells completed in the landslide deposits (wells 9, 10, 14–16; table 1; appendix B; fig. 16C) responded similarly to those at the aquifer test site. Groundwater levels were stable through 2017, and then rose in the spring of 2018, but the magnitude of increases varied by well.

The hydrograph from well 12, completed in the alluvium, is similar to that of the Alder Gulch stream

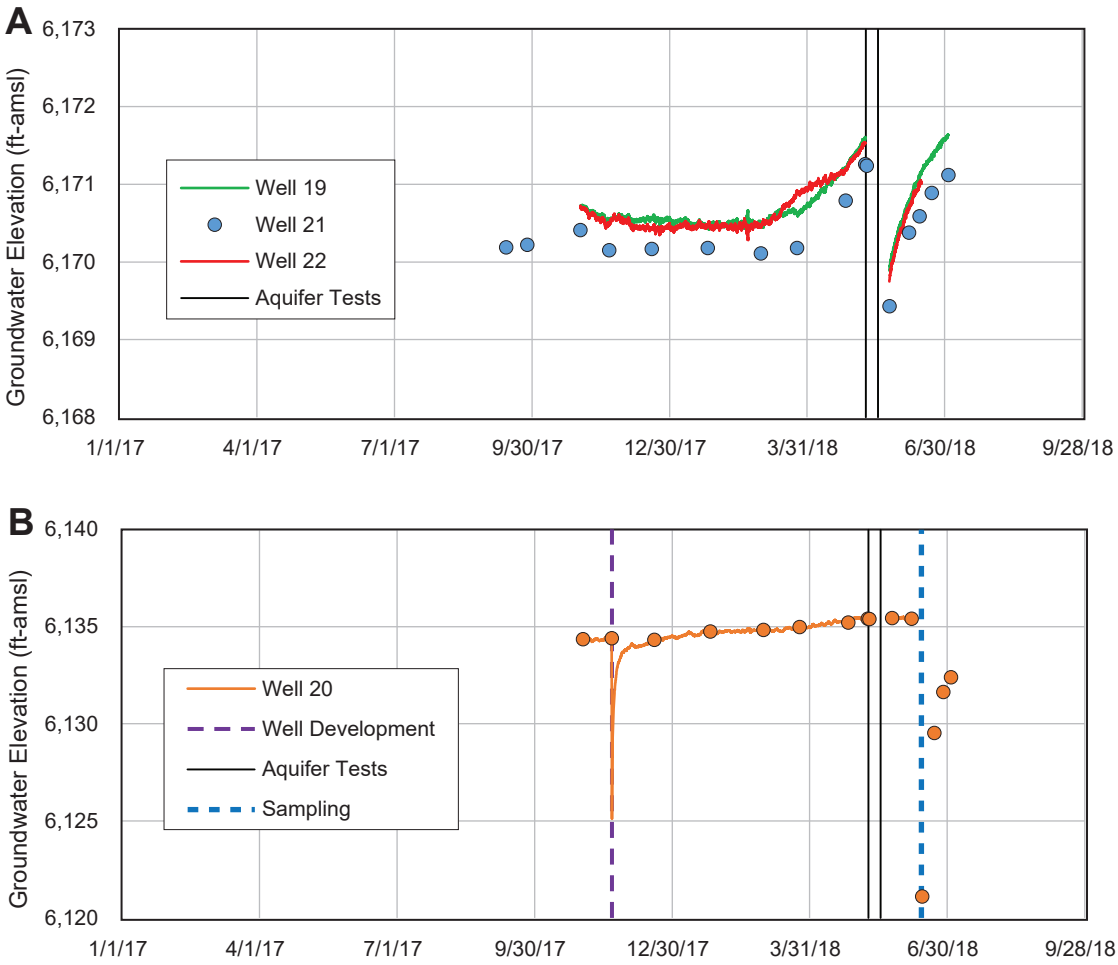

Figure 17. Hydrographs for the well nest at the aquifer test site show that groundwater levels were stable through the fall and winter of 2017–2018 and then began rising in the spring of 2018. The aquifer test conducted at this site truncated the rise, and recovery from the test took over a month. Well 20 was not influenced by the aquifer test, and it was very slow to recover from pumping for development and sampling. Comparison of A and B shows that there is a downward gradient at this site.

stage (site 27; fig. 16B). The hydrographs decline through summer and fall of 2017, stabilize during the winter, and increase during the spring of 2018. Groundwater levels were about 1 ft higher in the first half of 2018 than those recorded for the same period in 2017.

Streams

Stream stage was measured at three sites (sites 23, 24, and 25) on Daylight Creek, and two sites on Alder Gulch—one above (site 26) and one below (site 27) the confluence with Daylight Creek. Stream discharge was calculated hourly at sites 24 and 25 on Daylight Creek and at both Alder Gulch sites. Discharge calculations were based on stage-discharge measurements from ice-free periods in 2017 and 2018 (appendix A, table A6). At site 23, the most upstream site on Daylight Creek just below Madison Spring, discharge was measured on August 13, 2018 with supplemental measurements collected during the summer of 2021 (appendix A, table A6).

The highest stream stages were generally recorded from April to early June (fig. 18; appendix A, table A6; appendix C). Stages during 2018 were higher than in 2017. Peak stages were 0.9 to 1.3 ft higher in 2018 on Daylight Creek, and 1.0 to 1.1 ft higher on Alder Gulch. High-frequency changes in stage during April 2018 recorded at all stations on Daylight Creek are attributed to snowmelt and possibly formation of ice dams. Pulses of high flow also occurred at the Alder Gulch station (site 27) downstream of the confluence with Daylight Creek.

Synoptic discharge measurements were made at all three sites on Daylight Creek on August 13, 2018, when there were no apparent surface-water inflows. Flow in the creek increased from 0.3 cfs at site 23, to 1.1 cfs at site 24. This reflects gaining conditions from a series of small springs between sites 23 and 24. Daylight Creek flows into the main town area between sites 24 and 25, where the creek transitions from flowing across tuff to flowing across unconsolidated materials. The creek lost about 0.3 cfs in this area during the synoptic gaging event. Over the longer project monitoring period, hourly discharge measurements show that this lower reach of Daylight Creek was near neutral (neither losing nor gaining flow) during the relatively low flows in 2017 (fig. 19; appendix C), but this reach was generally losing during higher discharge conditions in 2018. The loss of streamflow to groundwater during higher flows is at least partly due to increased stream stage.

There are two basins on the main channel of Alder Gulch, between sites 26 and 27, along the reach that includes the confluence with Daylight Creek (figs. 6, 7). Upstream flows (site 26) were more variable than downstream (site 27), because the downstream location reflects buffering from storage in the intervening basins (appendix D). Discharge measured at the two stations in 2017 indicated a net reduction in streamflow, suggesting that this portion of the stream was losing water to the underlying aquifer. During the spring and early summer of 2018, conditions varied from net gains to net losses, reflecting a buffering of streamflows by the intervening basins (fig. 19B).

Water Chemistry

Isotopic Composition of Precipitation

The isotopic composition of precipitation is affected by season, elevation, latitude, and distance from the ocean (Faure, 1991). We collected precipitation for isotopic analysis from a station in Virginia City (site

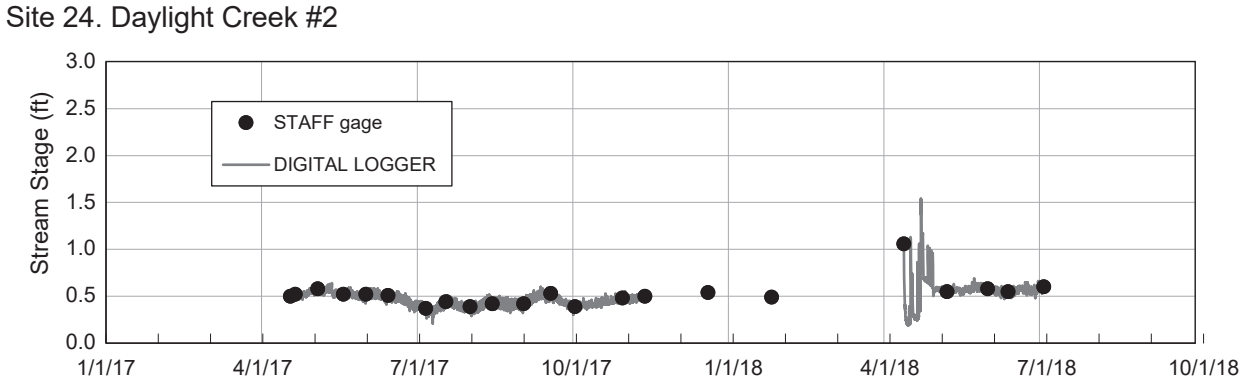

Figure 18. A stage hydrograph for site 24 on Daylight Creek shows that peak water levels in 2018 were about 1 ft higher than in 2017, and baseflow stages were slightly higher.

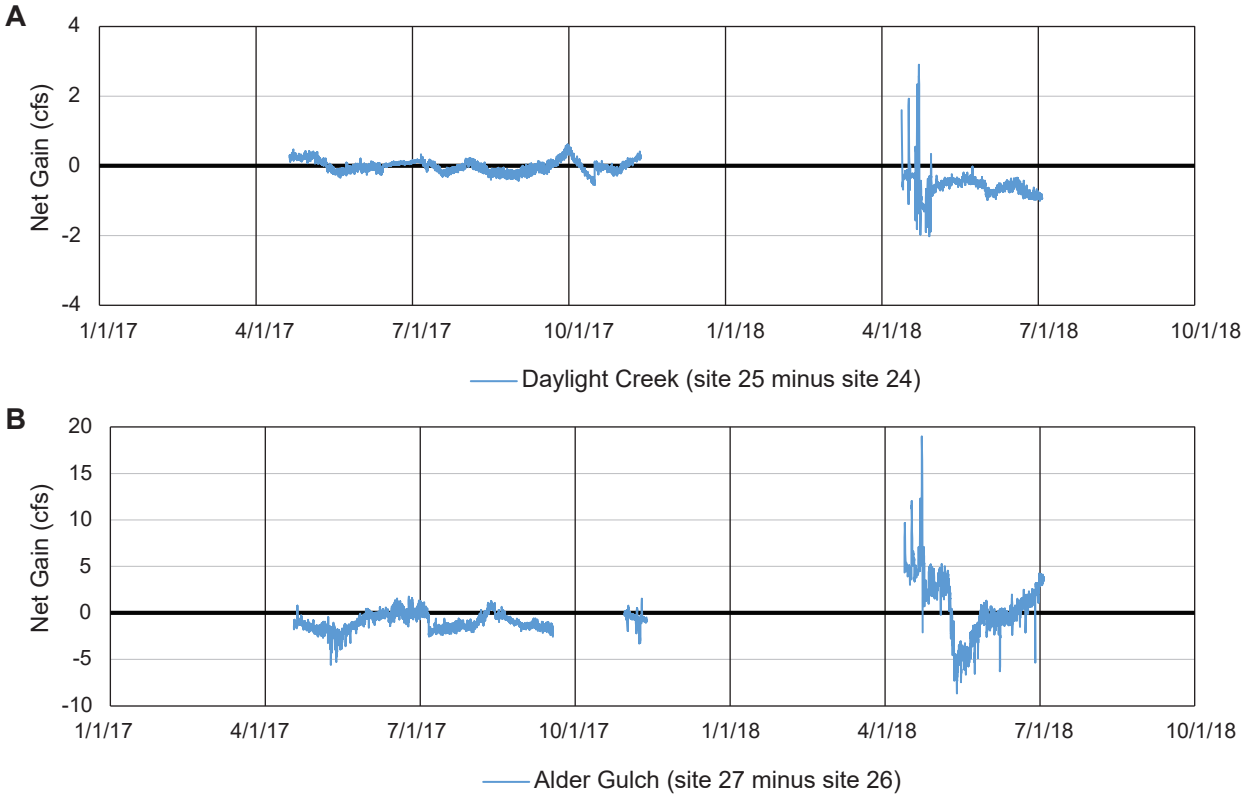

Figure 19. These charts show the net change in flow between two stations on Daylight Creek (A) and Alder Gulch (B). Positive values show increase in flow and negative values indicate decreases. There was little net change streamflow during the relatively low flows observed in 2017. In 2018 net gains during the spring were higher, reflecting surface inflows (runoff). On Daylight Creek (A) stream stage was higher in 2018 than in 2017 (fig. 17), resulting in greater net loss to the underlying alluvial aquifer. On Alder Gulch (B) it appears that the on-stream basins (fig. 6) stored water during high streamflow in 2018 (negative net gains), and then released that water back to the stream during low flows (positive net stream gains).

2; fig. 7), and from a station located about 2.8 mi east and about 1,150 ft higher in elevation (site 1; fig. 7). Composite monthly values for $\delta^{18}O$ and δD from site 1 were consistently lower than those at site 2, indicating depletion rates of about 1.0‰ and 4.7‰ per 1,000 ft, respectively (0.31‰ and 1.6‰ per 100 m; appendix A, table A2). These values are consistent with findings of other studies in the region (Kharaka and others, 2002; Gammons and others, 2006) and worldwide (Clark and Fritz, 1997).

The $\delta^{18}O$ and δD composition of precipitation also depends on temperature, with lower values corresponding to cooler weather and higher values reflecting warmer weather. Temperature changes the degree of fractionation during evaporation and precipitation, and causes samples taken throughout the year at a location to plot along a local meteoric water line (LMWL; fig. 20; Faure, 1991). The data from both stations fall along a similar line (fig. 20). We constructed the LMWL from site 2 data because samples were not collected during the winter at site 1 (appendix A, table A2). The Virginia City LMWL is similar to that developed for Butte, MT (56 mi NW of Virginia City; Gammons and others, 2006; appendix A, table A2). The slope and intercept of the Virginia City LMWL were lower than the global meteoric water line (fig. 20; Rozanski and others, 1993), which is typical for continental areas like Virginia City (Gammons and others, 2006).

The seasonal temperature dependence of $\delta^{18}O$ and δD values causes more depleted values in the winter (fig. 21B). The weighted average annual precipitation (May 2017 to April 2018) at site 2 yielded $\delta^{18}O$ and δD values of -16.3‰ and -127‰, respectively (fig. 20). We also calculated the winter weighted mean (fig. 20; November 2017 to March 2018) $\delta^{18}O$ and δD values, -19.3‰ and -148‰, respectively, because most groundwater recharge near Virginia City likely occurs during snowmelt.

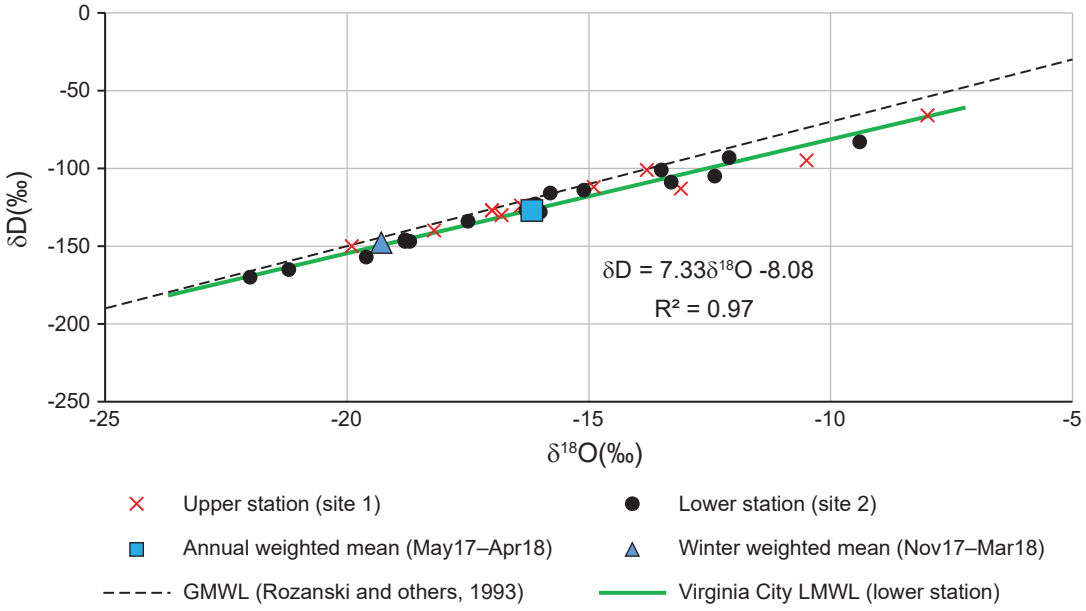

Figure 20. A local meteoric water line (LMWL) for Virginia City was derived from precipitation samples collected at the low-elevation station (site 2; appendix A, table A2). This LMWL has a lower slope and intercept than the global meteoric water line (GMWL).

Springs

Spring 1

Water chemistry characteristics of Spring 1 were used to evaluate seasonal variability in spring chemistry, to evaluate general water quality, to infer relationships between groundwater and surface waters, and to estimate the residence time of groundwater that discharges at the spring.

Water isotopes. The isotopic composition of the water from Spring 1 showed little temporal variation. Values for δD and $\delta^{18}O$ ranged from -152 to -149‰, and from -19.4 to -18.7‰, respectively (figs. 21C, 22C; appendix A, table A3). These values are similar to the winter weighted mean precipitation (fig. 22C), which is consistent with snowmelt providing the primary source of recharge to Spring 1. The lack of variation in the isotopic composition of Spring 1 water relative to precipitation suggests that the groundwater system discharging at Spring 1 has sufficient storage to buffer seasonal variations in recharge composition, the primary source of recharge is relatively homogeneous (as may be the case for snowmelt), or both.

Temporal variation in field parameters. Hourly measurements of temperature, SC, pH, DO, water stage, and turbidity were collected in the spring box for Spring 1 (figs. 8, 23). These measurements ended before water from Spring 2 was introduced to the spring box. Given that the isotopic composition of Spring 1 water is similar to that of snowmelt, we considered the timing of snowmelt with respect to the temporal records from the spring. Snowmelt at the Short Creek SNOTEL site in 2017 primarily occurred from March 17th to April 7th, and from April 19th to May 8th in 2018 (fig. 23A). The timing of snowmelt in the vicinity of Spring 1 was likely similar.

Temperature in the spring box ranged from 9.7 to 10.8°C and averaged 10.5°C (fig. 23B). This was 4.3°C (7.7 °F) warmer than the average air temperature reported for Virginia City (6.2°C; 1981–2010 normal data; NOAA, 2018). The elevated spring water temperature relative to the average air temperature suggests that the groundwater feeding the spring has sufficient residence time to reflect geothermal heating. The spring water temperature was relatively stable from the start of measurements through the end of August 2017. The temperature declined gradually from September 2017 to mid-April 2018, but declined sharply during snowmelt in late April 2018. The 2018 snowmelt cooling pulse suggests that some local flow paths feed the spring during snowmelt; however, spring temperature did not drop during the relatively low snowpack in 2017. The rapid decrease and rise in 2018 also suggests that the Spring 1 flow system has sufficient groundwater storage to buffer temperatures during most of the year, but that local flow paths contribute during snowmelt.

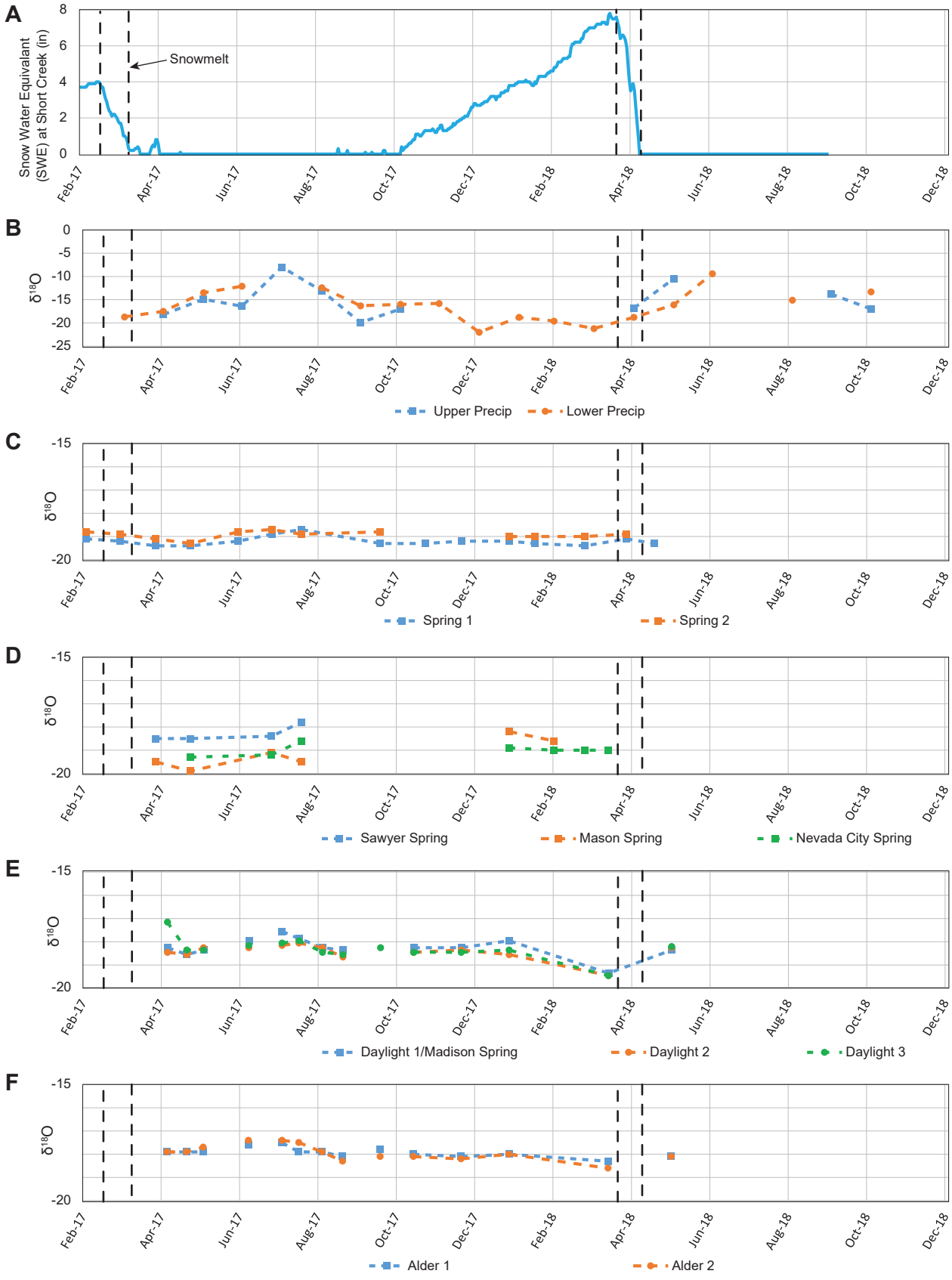

Figure 21. Isotopic compositions over time. Note that the y-axis scales for C, D, E, and F are different than for B. See text for discussion of these patterns.

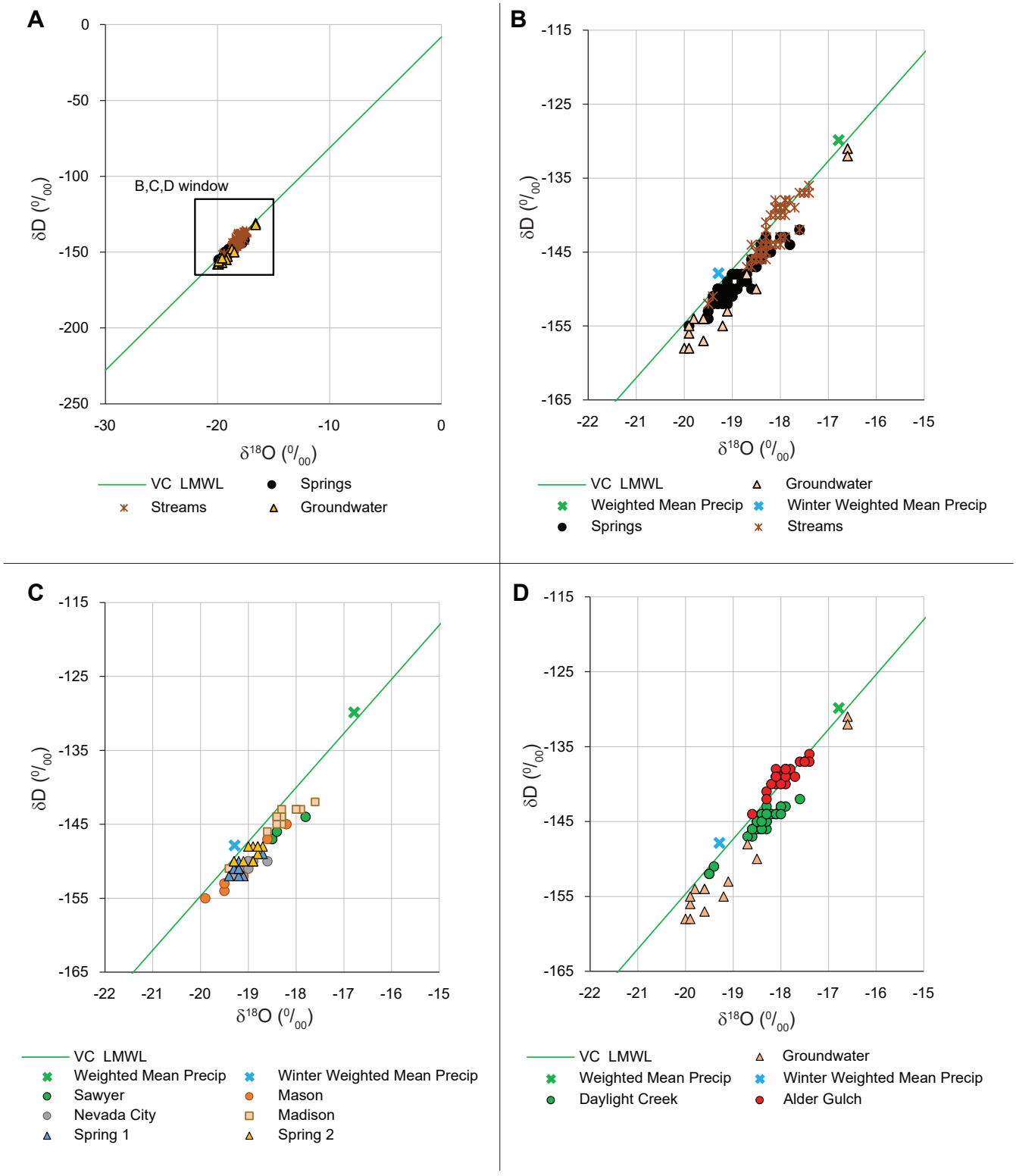

Figure 22. All samples (A) generally follow the LMWL. Most of the groundwater (wells and springs) are similar to the winter weighted mean, while streams are intermediate between weighted mean precipitation and winter weighted mean precipitation (B). The springs have similar isotopic compositions (C), which are also similar to the winter weighted mean precipitation. Daylight Creek has more depleted values than Alder Gulch (D), suggesting that it receives more bedrock groundwater. The two highest groundwater values (δD ~ -131) are both from an alluvial well (well 12).

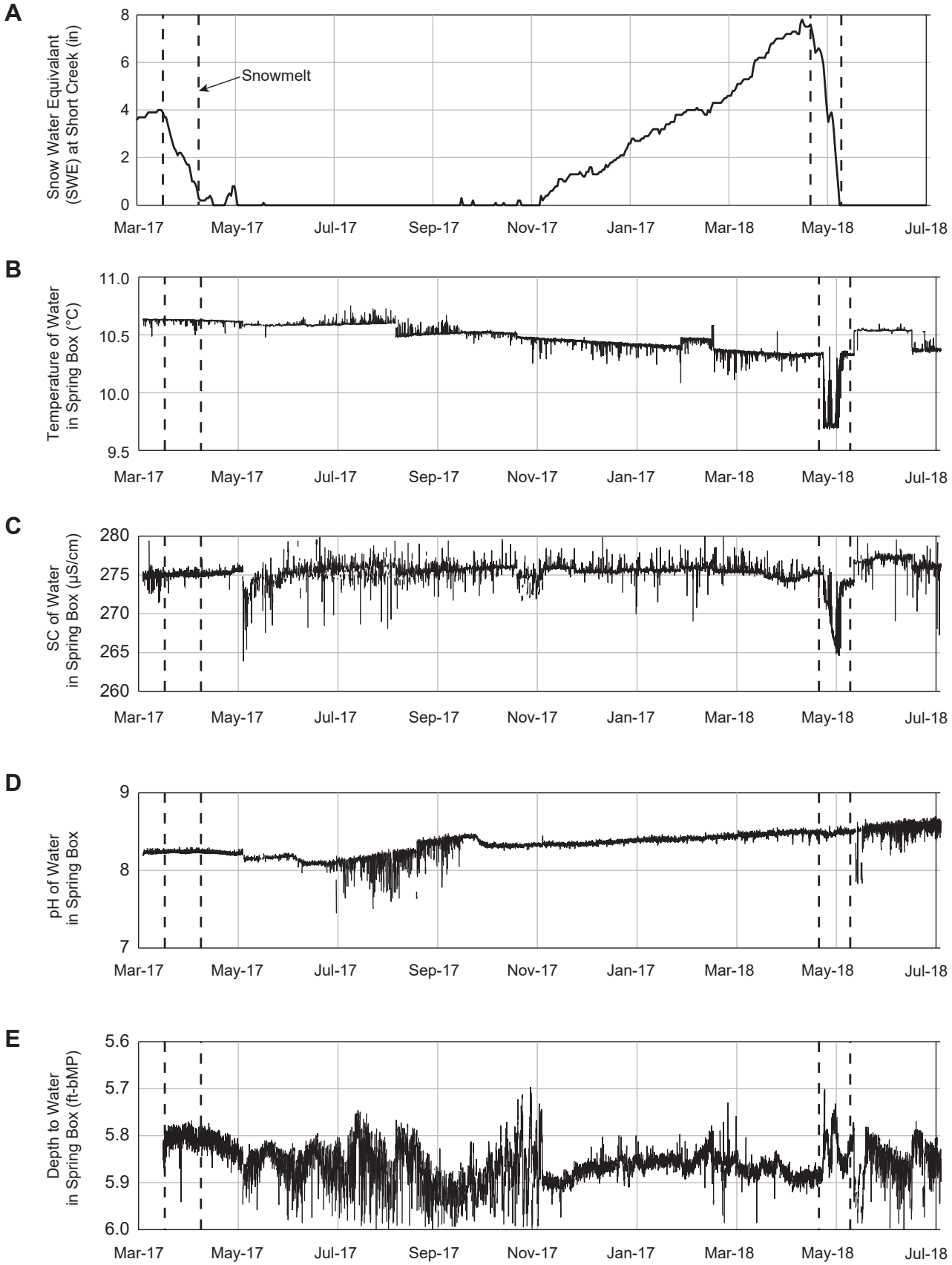

Figure 23. A comparison of SWE (A) to temperature (B), SC (C), pH (D), and water level (E) in the Spring 1 spring box. The Short Creek SNOTEL site (#753; A) data show periods of snowmelt in the spring of 2017 and 2018. The Short Creek data also provide an indication of the amount of available water during snowmelt. See text for discussion of these patterns.

SC of the Spring 1 water ranged from 265 to 280 microSiemens per centimeter (μS/cm), and averaged 275 μS/cm (fig. 23C). SC was stable at about 275 μS/cm from early March 2017 through early May, followed by a sharp drop to 265 μS/cm for a short period. This drop occurred approximately 1 mo after snowmelt. After this dip SC recovered to about 275 μS/cm until a decline during 2018 snowmelt. Similar to the temperature data, this pattern in SC suggests that local flow paths contribute fresh water to Spring 1 during snowmelt in years with higher snow pack. Snowmelt is expected to have a low SC, and the relatively small magnitude of the SC dips suggest that a larger flow system is dominant.

The daily average pH of the water in the spring box ranged from 8.0 to 8.6, and averaged 8.3 (fig. 23D). There are high-frequency fluctuations in recorded pH values during periods when the spring box was frequently drained; we interpret these variations as air bubbles forming on the probe. The pH decreases from about 8.2 in early March to about 8.1 in mid-June 2017. There is an increase in pH from mid-June to late September 2017, with pH reaching 8.4, and then dropping to 8.3. From late September 2017 on, the pH steadily increases to reach 8.6 in early July 2018.

DO saturation ranged from 93 to 104%, and averaged 97%. The spring discharge is well aerated, consistent with a thin, perched saturated zone discharging at a contact spring.

Turbidity was consistently low, with an average of 0.2 nephelometric turbidity units (NTU). Turbidity was often higher following tank filling (up to 18.9 NTU), likely due to air bubbles that formed on the instrument during rewetting cycles. The lack of a seasonal turbidity signal suggests that Spring 1 is not fed by short flow paths, such as in karst systems, that would introduce sediments (Fournier and others, 2007).

General water quality. Six water-quality samples showed that the water from Spring 1 was a calcium-bicarbonate (Ca-HCO_3) water type (figs. 24, 25; appendix A, table A3). Total dissolved solids (TDS) concentrations averaged 185 mg/L. The water chemistry of Spring 1 is consistent with the weathering of volcanic rocks (Hounslow, 1995).

Trace elements. The six water-quality samples from Spring 1 showed that the concentrations of trace elements were low, and none exceeded MCLs (MDEQ, 2019). Arsenic ranged from 2 to 3 μg/L (appendix A, table A3), well under the MCL of 10 μg/L.

Water age. Tritium concentrations in samples from Spring 1 ranged from 0.14 (± 0.11) to 0.62 (± 0.03) tritium units (TU; appendix A, table A7). Using the criteria developed by Lindsey and others (2019), these tritium values indicate Spring 1 discharge is composed of a mixture of "modern" (post-1953) and "premodern" (pre-1953) water sources (appendix A, table A7).

Noble gas concentrations were very low or non-detect, consistent with air stripping due to aeration of the water, which is also reflected in the high DO. We attribute aeration of the groundwater feeding the spring to flow through a relatively thin perched aquifer on top of the tuff in some portions of the contributing area. The tritium-helium dating method could not be applied to Spring 1 due to the loss of helium by air stripping.

CFC-11 ($CFCl_3$), CFC-12 (CF_2Cl_2), and CFC-113 ($C_2Cl_3F_3$) are anthropogenic chemicals that can also be used to estimate the time since water was last in contact with the atmosphere (Cook and Solomon, 1995; Cook and others, 1995; Oster and others, 1996). CFCs, which are not naturally occurring, were first produced in the 1940s. Atmospheric concentrations of CFCs increased until about 1995 and then either declined (CFC-11) or stabilized (CFC-12 and CFC-113; Chambers and others, 2019). Groundwater age is calculated based on historical atmospheric CFC concentrations and the solubility of the CFCs in water. CFC concentrations ranged from 175 to 182 parts per trillion by volume (pptv) for CFC-11, from 492 to 550 pptv for CFC-12, and from 46 to 56 pptv for CFC-113 (appendix A; table A8). These CFC values suggest that on average the water from the spring was last in contact with the atmosphere 21 to 40 yr ago.

These age dating techniques reflect mixing of water along various flow paths in the capture zone. A variety of decay processes may affect each method (microbial or radiometric decay, volatilization, etc.). Taken as a whole, these results suggest groundwater that discharges to Spring 1 recharged on average about 20 to 60 yr ago, with some of the water being older (premodern; Lindsey and other, 2019) and some younger.

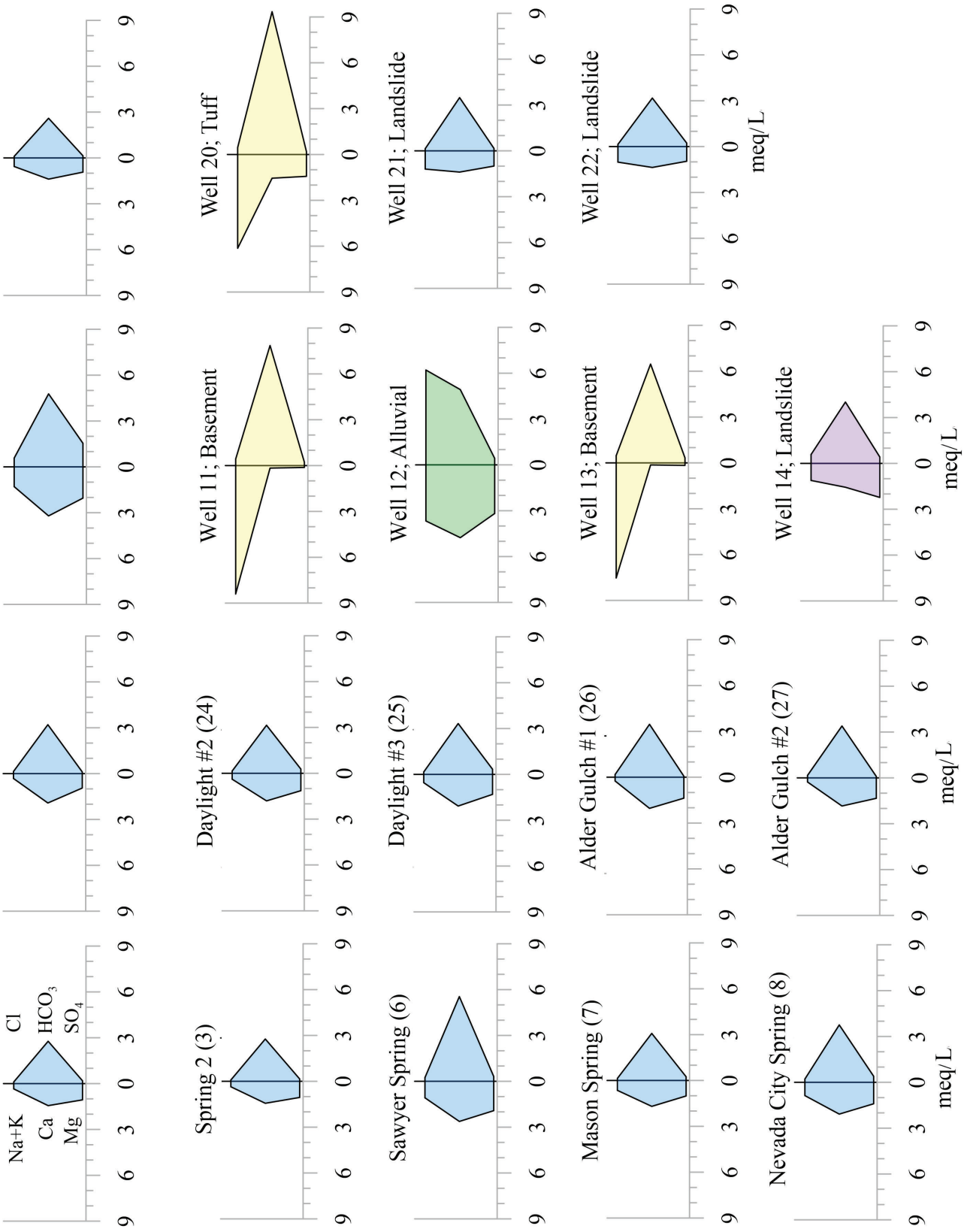

Figure 24. Stiff plots showing major ion chemistry of springs, surface waters, and wells. Polygon color reflects the dominate cation and anion, with Ca-HCO_3 shown as blue, Na-HCO_3 as yellow, Ca-Cl as green, and Mg-HCO_3 as purple.

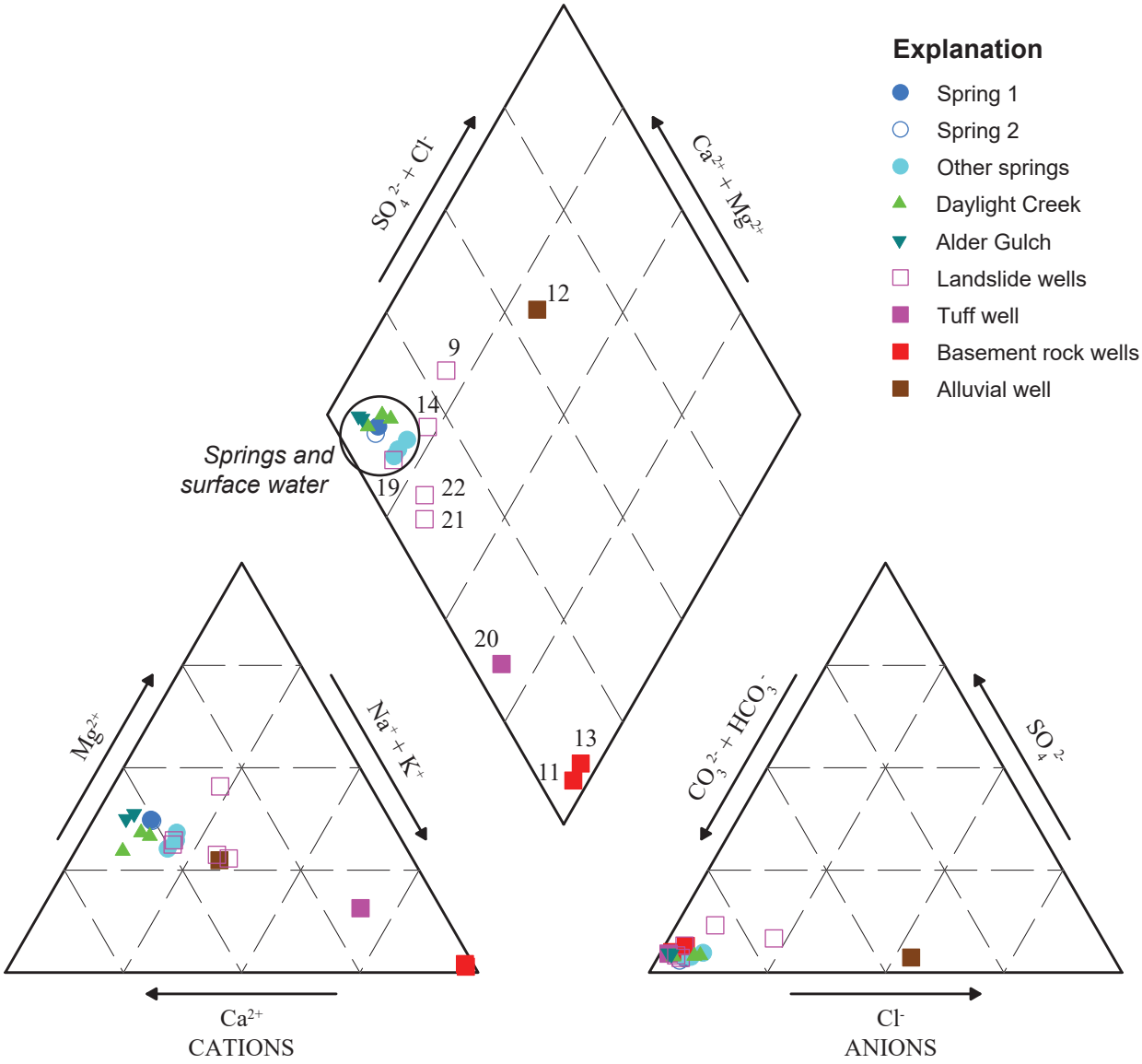

Figure 25. All springs and surface waters (circled on graph) were Ca-HCO_3 type waters. The major ion chemistry of groundwater in wells was more variable. Wells installed above Spring 1 (sites 19, 20, 21, and 22) became more sodic with depth. The basement rocks (wells 11 and 13) have a Na-HCO_3 water type. Data points are labeled with site numbers (fig. 7, table 1).

Spring 2

Since Spring 2 was monitored at the end of its pipeline, near Spring 1, the thermal properties and some of the chemical characteristics of the water may have been affected en route to the discharge point. In particular, CFCs and noble gas samples were not collected due to the aeration.

Water isotopes. The isotopic composition of the water from Spring 2 was analyzed 12 times over the course of this study, and showed little seasonal variation (fig. 21C; appendix A, table A3). Values for δD and $\delta^{18}O$ ranged from -150 to -148‰, and from -19.3 to -18.7‰, respectively (fig. 22C). These ranges are similar to winter precipitation and to Spring 1. The data are consistent with snowmelt as the primary source of recharge to Spring 2.

Field parameters. Field parameters were measured at the Spring 2 outfall seven times during this study (appendix A, table A3). SC averaged 307 µS/cm, with a range of 273 to 333 µS/cm. SC values showed a weak to moderate downward trend during the study (Pearson's correlation coefficient r = -0.50). pH ranged from 7.7 to 8.3, with an average of 8.0. The pH values did not show systematic variation with time.

General water quality. Four water-quality samples were analyzed for Spring 2 (appendix A, table A3). Spring 2 was a calcium-bicarbonate (Ca-HCO_3) water

type (figs. 24, 25). TDS averaged 177 mg/L. The water chemistry is consistent with the weathering of volcanic rocks (Hounslow, 1995), and is similar to Spring 1.

Trace elements. Similar to Spring 1, the water-quality samples from Spring 2 showed that trace elements were low, and none exceeded MCLs. Arsenic concentrations ranged between 2 and 3 µg/L, well below the MCL of 10 µg/L (appendix A, table A3).

Water age. Three tritium samples from Spring 2 showed little variation, ranging from 0.83 (±0.05) to 0.85 (±0.11) TU (appendix A, table A7). Using the criteria developed by Lindsey and others (2019), these tritium values indicate Spring 2 discharge is composed of a mixture of modern and premodern water sources. The tritium values for Spring 2 are greater than for Spring 1, which suggests that a greater proportion of the water from Spring 2 is from modern sources.

Other Springs

We also sampled Sawyer Spring, Mason Spring, Nevada City Spring, and Madison Spring (sites 6, 7, 8 and 23, respectively). Madison Spring was measured at site 23 (D1/Madison Spring), which also channels runoff during snowmelt. Isotopic values, SC, and temperature all show that snowmelt dominated the measurements taken at site 23 on April 11, 2018, and these data were not included in evaluating the spring. Data from site 23 are presented in appendix A in table A6, while data for the rest of the springs are presented in table A4.

Water isotopes. The isotopic composition of the water from Sawyer Spring showed slight temporal variation (figs. 21D, 22C). Values for δD and $\delta^{18}O$ ranged from -147 to -144‰, and from -18.5 to -17.8‰, respectively, somewhat heavier than those at Springs 1 and 2 and heavier than the mean winter precipitation. The heavier water and the slight variations suggest some incorporation of non-snowmelt water.

Madison Spring showed slight variations in isotopic composition (figs. 21E, 22C). Values for δD and $\delta^{18}O$ ranged from -146 to -142‰, and from -18.6 to -17.6‰, respectively, somewhat heavier than those at Springs 1 and 2 and heavier than mean winter precipitation. As at Sawyer Spring, the heavier water and the slight variations suggest some incorporation of non-snowmelt water.

The isotopic composition of the water from Mason Spring showed more variation than at the other springs (figs. 21d, 22C). δD and $\delta^{18}O$ ranged from -155 to -145‰, and from -19.9 to -18.2‰, respectively. These ranges encompass the ranges observed for Springs 1 and 2, and fall above and below the mean winter precipitation value.

The Nevada City Spring showed little variation in isotopic composition (figs. 21D, 22C). δD and $\delta^{18}O$ ranged from -152 to -150‰, and from -19.3 to -18.6‰, respectively. These ranges are close to those from Springs 1 and 2, and similar to mean winter precipitation.

Field parameters. Madison, Mason, and Nevada City springs temperatures averaged between 7.8 and 10.2°C (appendix A; tables A4, A6). Temperature ranges from these springs ranged from 5.5 to 8.7°C, compared to ranges of 1.2°C at Spring 1 and 1.4°C at Spring 2. The wider temperature ranges suggest that these springs are fed from shorter and shallower flow paths compared to Springs 1 and 2. Data collection at Sawyer Spring (site 6) was limited to spring and summer, and data are not considered here.

SC measured at Sawyer, Mason, Nevada City, and Madison springs averaged 609, 425, 424, and 340 µS/cm, respectively (appendix A, tables A4, A6). Madison Spring is similar to Springs 1 and 2 (275 and 303 µS/cm, respectively), while the other springs had higher SC values. Sawyer Spring's SC was elevated relative to the other springs, suggesting the presence of soluble minerals in its recharge area.

Average pH values for the four springs ranged between 7.5 and 8.4 (appendix A, tables A4, A6). pH at Sawyer and Mason springs was lower than at Springs 1 and 2, and the Nevada City and Madison Springs pH values were similar to those at Springs 1 and 2.

General water quality. Each of the springs was sampled twice. All springs had Ca-HCO_3 water types (figs. 24, 25; appendix A, tables A4, A6). TDS averaged 344, 227, 263, and 192 mg/L at Sawyer, Mason, Nevada City, and Madison Springs, respectively. The water chemistry is consistent with the weathering of volcanic rocks (Hounslow, 1995) and is generally similar to that at Springs 1 and 2. With the exception of Madison Spring, TDS was higher than at Springs 1 and 2, particularly at Sawyer Spring. The elevated

TDS may indicate dissolution of soluble minerals in the shallow subsurface.

Trace elements. The concentrations of trace elements in water from the Mason, Nevada City, and Madison Springs were low (appendix A, tables A4, A6). Arsenic concentrations varied from 1 to 4 µg/L at these springs. Sawyer Spring's arsenic concentration, at 12.54 µg/L, exceeded the MCL (10 µg/L).

Water age. Tritium samples were collected and analyzed twice for Sawyer, Nevada City, and Mason Springs. Average tritium values were 1.74, 0.72, and 0.20 TU, respectively (appendix A, table A7). The Sawyer and Nevada City results are classified as a mixture of modern and premodern waters (Lindsey and others, 2019). Mason Spring results suggest a source with little modern influence.

Sawyer Spring was distinct in several ways. It had the highest tritium values, the highest SC, the highest TDS, and the highest arsenic concentration. Together this suggests that the water from Sawyer Spring is relatively young, but there are soluble minerals in the recharge zone. Given the elevated arsenic concentrations, these minerals may be hydrothermal in origin.

Groundwater

Water Isotopes

The isotopic composition of groundwater samples from various hydrogeologic units plot near the LMWL (fig. 22D; appendix A, table A5). The alluvial well had the heaviest signature ($\delta D \approx -131‰$; $\delta^{18}O \approx -16.6‰$), similar to the mean annual precipitation (fig. 22D; appendix A, table A5), suggesting that groundwater in the alluvium receives recharge year-round. Wells completed in the landslide or bedrock units had δD values ranging from -158 to -148‰, and $\delta^{18}O$ values from -20.0 to -18.5‰ (fig. 22D; appendix A, table A5). The non-alluvial groundwater is similar in isotopic composition to the mean winter precipitation (fig. 22D), suggesting that these wells receive most recharge during snowmelt. For those wells sampled in both May and August 2017, the isotopic composition was similar between sampling events (appendix A, table A5).

Field Parameters

Temperature, pH, and SC were measured during well sampling events (appendix A, table A5). Groundwater temperature ranged from 9.6 to 12.8°C. The largest seasonal temperature change (from May to August) occurred in the alluvial aquifer adjacent to Alder Gulch, at well 12. Well 13, completed in the basement rock, had the highest temperature during both sampling events. pH values ranged from 6.6 to 8.9. SC values ranged from 269 to 1,279 µS/cm; the lowest SC value was from the shallowest well installed above Spring 1 (well 19), whereas the highest value was recorded in alluvial well 12.

General Water Quality

The major ion chemistry for groundwater varied primarily based on the hydrogeologic unit the well was completed in (figs. 24, 25; appendix A, table A5).

Wells 11 and 13, completed in the basement rocks, had Na-HCO_3 type water with little Ca or Mg (figs. 24, 25). This chemistry likely reflects the relatively sodic composition of the gneiss (Mosolf, 2021).

Four of the five wells completed in the landslide deposits (wells 9, 19, 21, and 22) had Ca-HCO_3 type waters, similar to the springs (figs. 24, 25). Well 14, located on the west side of Alder Gulch, had a Mg-HCO_3 water type (figs. 24, 25), perhaps reflecting basalt-dominated mineralogy (i.e., more Mg-rich rocks).

Well 20, completed in the tuff at a depth of 610 ft, had distinctly different groundwater chemistry from wells completed in the overlying landslide unit (wells 19, 21, and 22; figs. 24, 25). The tuff had a Na-HCO_3 water type, but with Ca and Mg concentrations similar to wells in the landslide deposits. Well 20 also had an elevated SC compared to the overlying landslide wells (average 933 µS/cm). The tuff groundwater (well 20) is similar to groundwater from the metamorphic basement rocks and differs from wells in the overlying landslide deposits (figs. 24, 25).

Groundwater in the unconsolidated alluvium along Alder Gulch (well 12) had a mixed water type (Ca-Na-Mg-Cl-HCO_3; figs. 24, 25). This groundwater had higher nitrate than other wells and springs in the area, with concentrations of 3.4 and 4.8 mg/L. The chemistry of alluvial water is typically similar to that of the stream water; however, in this case it is distinctly different (figs. 24, 25), with Cl as the dominate anion. Elevated chloride and nitrate may indicate effects of a nearby road salt storage area or historical septic systems.

Trace Elements

Arsenic (As) was the only trace element that exceeded MCLs in groundwater (appendix A, table A5). Arsenic concentrations increased with well depth, and 8 of 10 samples (5 of 6 wells) from wells over 200 ft deep exceeded the MCL (10 µg/L). All samples from wells less than 200 ft deep were less than the 10 µg/L. Well 14, completed in the landslide deposits on the west side of Alder Gulch (figs. 7, 9), was the one well more than 200 ft deep to have arsenic below the MCL. Wells at the aquifer test site also illustrate increasing arsenic in groundwater with depth (appendix A, table A5), with well 20 having the highest arsenic concentrations for any samples collected for this study (65 and 75 µg/L).

Groundwater Age

Tritium samples were collected from five wells, and nitrogen and noble gas samples (^{3}He, ^{4}He, Ar, Ne, Kr, and Xe) were collected for three of these (appendix A, table A7).

Three of the wells (wells 11, 13, and 14) are classified as having premodern water (ND to 0.12 TU). Noble gas samples for these wells resulted in calculated radiogenic ages greater than 60 yr (calculated using the excess air model), consistent with the premodern ages indicated by tritium.

Wells 12 and 21, which were not sampled for noble gases, had higher tritium (5.60 to 6.57 TU), and are classified as modern water (Lindsey and others, 2019). These wells produce groundwater from Alder Gulch alluvium (well 12; 109 ft deep) and the landslide deposits above Spring 1 (well 21; screened from 200 to 240 ft-bgs). Surprisingly, well 21, completed at a depth of 210 ft, had a tritium concentration of 6.57 TU (modern; Lindsey and others, 2019), while Spring 1 had a maximum tritium concentration of 0.62 TU (mixed). These results indicate that groundwater discharging from Spring 1 through a perched aquifer is on average older than groundwater from the underlying landslide (fractured tuff) deposits (fig. 10). This suggests that the fractured tuff in the landslide unit is recharged along preferential pathways, such as a fracture network, that transmit groundwater more rapidly than flow paths through the perched aquifer that discharge at Spring 1.

Streams

Water Isotopes

Stream isotope results generally plotted near the LMWL (fig. 22D; appendix A, table A6). The isotopic composition of the water at each site showed seasonal variations, with slight dips in the spring, likely due to snowmelt (fig. 21). The slight seasonal variation suggests that groundwater is the primary source of water in these streams. All sites had isotopic signatures between the mean winter and mean annual precipitation, reflecting that groundwater recharged by snowmelt makes up a disproportionate fraction of streamflow. The stream water $\delta^{18}O$ values were about 1‰ heavier than the water samples from Springs 1 and 2 (fig. 22), indicating that some stream water is generated from other sources (e.g., runoff and soil water) while the springs are fed exclusively from groundwater.

Field Parameters

Temperature at all stream sites followed patterns similar to air temperatures, but with buffering (appendix A, table A6). The upstream site in Alder Gulch showed a more pronounced diel temperature signal than the downstream site, likely due to buffering of the temperature signal by the basins between the sites. Average pH values were between 8.5 and 8.6 on Daylight Creek, and 8.3 and 8.4 for Alder Gulch. SC increased along Daylight Creek, averaging 344, 381, and 444 µS/cm for sites 23, 24, and 25, respectively. SC also increased downstream along Alder Gulch, due in part to the inflow of Daylight Creek between the sites. SC averaged 353 and 361 µS/cm at sites 26 and 27, respectively.

General Water Quality

All surface-water samples were Ca-HCO_3 type waters, similar to Springs 1 and 2 (figs. 24, 25; appendix A, table A6). TDS values averaged between 177 mg/L (site 26) and 252 mg/L (site 25). This chemistry is consistent with the weathering of volcanic rocks (Hounslow, 1995).

Trace Elements

The concentrations of trace elements in surface waters were low, with no exceedances of MCLs (appendix A, table A6). Arsenic in Daylight Creek ranged from 1 to 4 µg/L, and was less than 2 µg/L on Alder Gulch.

DISCUSSION

Potential for Supplemental Water Supplies

One objective of this study was to identify and evaluate potential supplemental sources of municipal water supply. A recent study forecast 120 gpm as a projected maximum daily demand for 2036 (Great West Engineering, 2016). We recorded a minimum flow rate of 24 gpm from Spring 2 during peak water demand (August), so an additional 96 gpm would be needed to meet a projected demand of 120 gpm if Spring 1 was unavailable. A summary of potential supplemental water supplies is shown in table 2. This evaluation focuses on physical availability without addressing water rights, engineering, or right-of-way requirements. The Upper Missouri River Basin is closed to new appropriations, so water-rights challenges may be formidable.

Another aspect of water supply development involves use of the existing treatment and storage system near Spring 1. Although beyond the scope of this study, other treatment and storage options could be considered. For example, Great West Engineering (2016) identified water pressure issues that could be addressed through changing the location of treatment and storage. For our evaluation we assume the existing treatment and storage system would be used.

Springs

Gilbert Spring, Madison Spring, and Nevada City Spring have the greatest potential for development. Sawyer Spring and Mason Spring are not considered here due to their relatively low flow rates. None of the springs independently would meet the total projected demand.

Gilbert Spring

Gilbert Spring (site 5) historically supplied water to a brewery and some homes in Virginia City until about 1980 (R. Williams, Virginia City Water Department, oral commun., 2018), through a gravity-fed pipeline. Gilbert Spring is located approximately 1.1 mi from the existing treatment system.

Monitoring in 2021 showed minimum flows for Gilbert Spring of approximately 50 gpm. Gilbert Spring is at approximately the same elevation as Spring 1 (6,202 ft-amsl), and emanates from the contact between the lava flow blocks and underlying tuff within the landslide area. The water quality at Gilbert Spring was not tested for this study, but it may have similar characteristics to Spring 1, given the similarity in hydrogeologic setting.

Madison Spring

Madison Spring (site 23) is an undeveloped spring that emerges at a fault within the lava flows. It is located about 1.4 mi from Spring 2, and lies about 70 ft higher. Madison Spring discharged 126 gpm on August 13, 2018; however, the stage on that day was 0.3 ft higher than the stage in August 2017. Thus, the 2018 flow measurement is likely not representative of long-term conditions. Flows measured in the summer of 2021 averaged 30 gpm, and the minimum was 17 gpm.

Table 2. Estimated properties of potential supplemental water sources.

Source	Yield (gpm)	TDS (mg/L)	As (mg/L)	Miles to Existing Infrastructure
Gilbert Spring	50	185*	3*	1.1
Madison Spring	30	191	1	1.4
Nevada City Spring	20	264	2	2.4
Basement Rock Wells	15	475	20	---
Tuff Wells	<1	550	70	---
Landslide Wells	10+	200 to 400	1 to 30	---
Alluvial Wells	120	200	1	1.3
Alder Gulch	150	200	1	1.3

Note. Highlight indicates exceedance of MCL. --- means the source could be developed at the treatment plant site, depending on well depth (fig. 8).
*Estimated based on similarity to Spring 1.
+Due to slow recovery, the landslide wells could only be used for about 1 month per year.

Samples collected at site 23 (Madison Spring at the start of Daylight Creek) had water quality similar to that at Springs 1 and 2 (figs. 24, 25), with no exceedances of MCLs.

Nevada City Spring

The spring at Nevada City (site 8) is undeveloped, although a partial trench dug immediately uphill from the spring indicates a past attempt to develop the spring. The Nevada City Spring is located 2.4 mi from the existing infrastructure, and emits at an elevation of about 5,610 ft-amsl, about 600 ft below the current treatment system.

The spring discharge was 108 gpm on August 13, 2018, at a stage about 0.1 ft higher than during most of 2017. Therefore, this flow is likely greater than long-term minimum flows. Based on measurements collected at other springs in August 2018 and during the summer of 2021, the long-term minimum flow for the Nevada City Spring is estimated to be approximately 20 gpm. More measurements would be needed to adequately characterize typical minimum flow, prior to development.

Nevada City Spring water quality is similar to that at Springs 1 and 2 (figs. 24, 25), and did not exceed MCLs.

Groundwater

We considered the potential for wells to supply groundwater from the basement rocks, tuff, lava flow deposits, landslide units (composed of fractured tuff and lava flow materials), and unconsolidated deposits (alluvium and mine dumps, fig. 9). Based on conversations with the Virginia City Water Department, we focused on the east side of Alder Gulch.

Basement Rocks

The metamorphic bedrock provides groundwater to domestic and stock wells on the west side of Alder Gulch; however, this unit is not exposed on the east side of Alder Gulch, nor are there reports of wells completed in it within that area. Metamorphic bedrock likely underlies the volcanic tuff on the east side of Alder Gulch (figs. 9, 10). It was not encountered during drilling well 20, to a depth of 610 ft (bottom hole elevation 5,670 ft-amsl). Reported yields from 11 wells completed in the metamorphic bedrock near the study area range from 1.5 to 60 gpm, with a median value of 15 gpm. Groundwater from wells 11 and 13, completed in the basement rocks, exceeded the arsenic MCL (appendix A, table A5).

Volcanic Tuff

The volcanic tuff was the only saturated bedrock unit identified by drilling on the east side of Alder Gulch that had not been altered by landslide activity. Well 20, the deepest well at the aquifer test site, was completed in this unit. We did not find records of any other wells screened in this unit. Well 20 produced less than 1 gpm, and groundwater contained arsenic above the MCL (appendix A, table A5).

Lava Flows

The lava flow deposits overlie the tuff and form the high mesas east and north of Virginia City (figs. 9, 10). Wells have not been reported in this unit. Due to the high secondary permeability of this unit, and the contrast in permeability with the underlying tuff, there are likely thin, laterally discontinuous saturated zones at the base of this unit. Such zones would be difficult targets to identify for drilling new wells. These zones appear to feed springs, such as Spring 2, where they outcrop.

Landslide Units

The landslide units are composed of the tuff and lava flow deposits, which have been subjected to additional fracturing due to mass movement (fig. 10). There are no records of wells completed in the lava flow portion of these units. There are likely areas where perched aquifers are present near the contact between the lava flows and the underlying tuff within the landslides; however, none have been identified by drilling. Such perched saturated zones in the landslide units are believed to feed Spring 1.

Wells in the fractured tuff within the landslide deposits have reported yields between 0.25 and 20 gpm. Three of the wells at the aquifer test site were completed in this unit. Aquifer test results indicate that pumping from individual wells would cause well interference, and water levels would recover very slowly following pumping. Analysis of aquifer test results (Bobst, 2020) showed that pumping a single well at 20 gpm for 12 h/d for 31 days would result in 60 ft of drawdown in the pumping well, and 28 ft of drawdown in a well 70 ft away. This suggests that two pumping wells located about 30 ft apart would result

in ~90 ft of drawdown and lower the water table to near the top of the screen. Water levels would recover to about 1 ft of pre-pumping levels approximately 200 d after the cessation of pumping. Using this pumping schedule (an average of 10 gpm per well for 31 d followed by 200 d of recovery), 10 wells could supply 96 gpm for about 1 mo per year.

Wells completed in the most productive zone of the fractured tuff (yield ~20 gpm) at the aquifer test site had arsenic concentrations above the MCL (appendix A, table A5). The shallowest well completed in the fractured tuff had an arsenic concentration below the MCL, but its yield was only 8 gpm.

Unconsolidated Deposits

The seismic surveys conducted near Alder Gulch indicated that the unconsolidated materials (alluvium and mine dumps; figs. 6, 9) have a saturated thickness of more than 100 ft on both the north side of profile 3 and the southeast side of profile 4 (fig. 6). Assuming a hydrologic conductivity representative of sand and gravel (~100 ft/d; Heath, 1983), the transmissivity would be about 10,000 ft^2/d. Pumping from an unconfined aquifer with a transmissivity of 10,000 ft^2/d, a storativity of 0.1, at a rate of 175,000 gal/d (350 gpm for 500 min/d; equivalent to a continuous rate of 121 gpm) would result in approximately 9 ft of drawdown after 31 d. Therefore, it is likely that a well in the unconsolidated deposits along Alder Gulch could supply an adequate quantity of water.

The one alluvial well sampled for this study, well 12 (appendix A, table A5), did not exceed any of the MCLs; however, it exceeded the aesthetic, or secondary, standard for iron. Although purged at the time of sampling, elevated iron in groundwater from the well may be due to infrequent well use or a deteriorated or rusty casing. Nitrate and chloride concentrations were below MCLs, but were higher than in the other hydrogeologic units. The aquifer at this site may be vulnerable to effects from road salt storage and/or historical septic systems located in hydraulically upgradient areas.

The aquifer characteristics near Alder Gulch are based on a geophysical survey and literature values. An aquifer test is the preferred method to confirm aquifer productivity and groundwater quality. Given that these units have been modified by historical placer mining, and they are adjacent to a major highway, the deposits are susceptible to contamination from spills and road salt. Installing a well upgradient from Virginia City (near site 26; fig. 7) would avoid influences from roads and other activities in developed areas. Site 26 is located approximately 1.3 mi from the existing treatment system.

Surface Waters

Alder Gulch above the confluence with Daylight Creek appears to be the most promising surface-water source. Daylight Creek has much lower flows, and if Spring 1 became unusable, the lower reach of Daylight Creek, and Alder Gulch below the confluence with Daylight Creek, might also be affected since Spring 1 is tributary to Daylight Creek. An upstream location would also be upstream of Virginia City and Highway 287, so it would not be susceptible to impacts from spills or other activities in those areas.

Flows in Alder Gulch appear to be sufficient to meet the needed 96 gpm. The water rights and ecological implications of such a diversion is beyond the scope of this study. Monitoring at site 26 (fig. 7; upstream of Virginia City) from June to November 2017 and from April to July 2018 indicated that discharge varied from 1.8 to 39 cfs (800 to 17,500 gpm), with an average of 9.9 cfs (4,500 gpm). To assess likely long-term low flow rates in Alder Gulch, results from this study were evaluated with flow estimates based on the USGS's StreamStats program (McCarthy and others, 2016; http://water.usgs.gov/osw/streamstats/). StreamStats uses physical and climatic characteristics of the drainage basin such as drainage area, mean annual precipitation, and land cover to estimate stream flow statistics. We used StreamStats to estimate flow statistics for site 26 on Alder Gulch, which resulted in an estimated mean annual flow of 10.2 cfs. This estimate compares well with the 9.9 cfs average from our monitoring. Low flows for site 26 were also estimated using StreamStats, where the 7Q10 flow (the lowest flow that would be expected for 7 consecutive days over any 10-yr period) was 0.34 cfs (150 gpm).

Water quality at site 26 met all MCLs when sampled in May and August 2017. However, historic upstream mining activity could alter water quality at times, particularly during high flow events. MDEQ has identified this portion of Alder Gulch as not fully meeting standards for aquatic life and recreation; however, it does meet drinking water MCLs (MDEQ,

2018). The MDEQ identified probable causes of impairment, including alteration in streamside vegetation, chlorophyll-a, lead, manganese, mercury, total nitrogen, substrate alterations, and sedimentation-siltation. In general, surface-water sources have higher treatment requirements than groundwater or groundwater-derived spring sources (E. Regensburger, MDEQ, written commun., 2020).

Summary of Potential Supplemental Water Supplies

Options for supplemental water supplies include springs, surface water from Alder Gulch from upstream of town, a well in the unconsolidated deposits along Alder Gulch upstream from town, or some combination of these options. All options require consideration of additional infrastructure, including conveyance pipelines and water treatment facilities. Surface water from Alder Gulch and groundwater from wells in the unconsolidated deposits may require additional monitoring and treatment.

Spring 1

Likely Source Area

The source area for Spring 1 was estimated based on geologic mapping, geomorphology, drainage divides, and the locations of other springs (fig. 26). This source area is interpreted to be the landslide complex and the internally drained area formed on the volcanic mesa east–northeast of Virginia City (~548 acres). The landslide complex is generally characterized by hummocky topography with internally drained basins underlain by fractured lava flow blocks that were rotated and transported downslope.

This source area has little surface-water runoff, suggesting that the groundwater system captures a large proportion of precipitation and snowmelt. Based on PRISM data (PRISM, 2018), this area receives about 20 in/yr of precipitation. About 35% of this water is required to feed Spring 1 at an average rate of 200 gpm (fig. 14). We hypothesize that recharge to the system feeding Spring 1 occurs primarily during spring snowmelt when saturated flow occurs through the soil/root zone.

Once groundwater infiltrates the fractured lava sequence on the mesa and within the landslide complex, it flows downward to the contact with the underlying tuff. We hypothesize that groundwater flows laterally along this contact, likely in thin discontinuous zones. Assuming the average age (residence time) of the water is about 40 yr, the flow rate of the spring (~200 gpm), and an assumed fractured porosity of 0.2, a storage zone averaging 120 ft thick over the recharge area could maintain flow to the springs. These storage zones would likely be discrete pockets of fractured lava flow and tuff materials, perhaps adjacent to rotated blocks in the landslide. These pockets of fractured materials would essentially function as a series of buckets, with one overflowing into the next until the last discharges at the spring. This hypothesis accounts for a groundwater age of approximately 20 to 60 yr, groundwater that is well-aerated, and spring flows that correlate with peak snow pack over the past 5 yr.

The other 65% of the annual precipitation that is not feeding Spring 1 returns to the atmosphere via evaporation and transpiration by plants (evapotranspiration), or recharges the underlying regional aquifer. Recharge of the reginal aquifer could occur by seepage through the base of the perched zone. Also, since the perched zone is interpreted to be laterally discontinuous due to the topography of the top of the tuff, the regional aquifer could be directly recharged where the perched zone is not present (potentially through fracture zones).

The estimate of about 35% of precipitation feeding Spring 1 compares favorably with TerraClimate data from Climate Engine (https://app.climateengine.com/climateEngine; Abatzoglou and others, 2018). Using the TerraClimate information, average evapotranspiration in the landslide area from 1991 to 2020 was about 14 in (70% of precipitation). This also suggests that on average most of the water received as precipitation either flows to Spring 1 or is used for evapotranspiration, and so recharge to the reginal aquifer primarily occurs in wetter years.

Vulnerability to Development

Spring 1 is a contact spring discharging from a perched aquifer. Therefore, pumping wells installed in the underlying aquifer for residential or commercial development are unlikely to affect spring flow. However, wells constructed without annular seals could provide a conduit for groundwater from the perched zone to the deeper regional groundwater system. Depending on the geometry of such a well in relation to the spring, this could reduce discharge of perched groundwater to Spring 1.

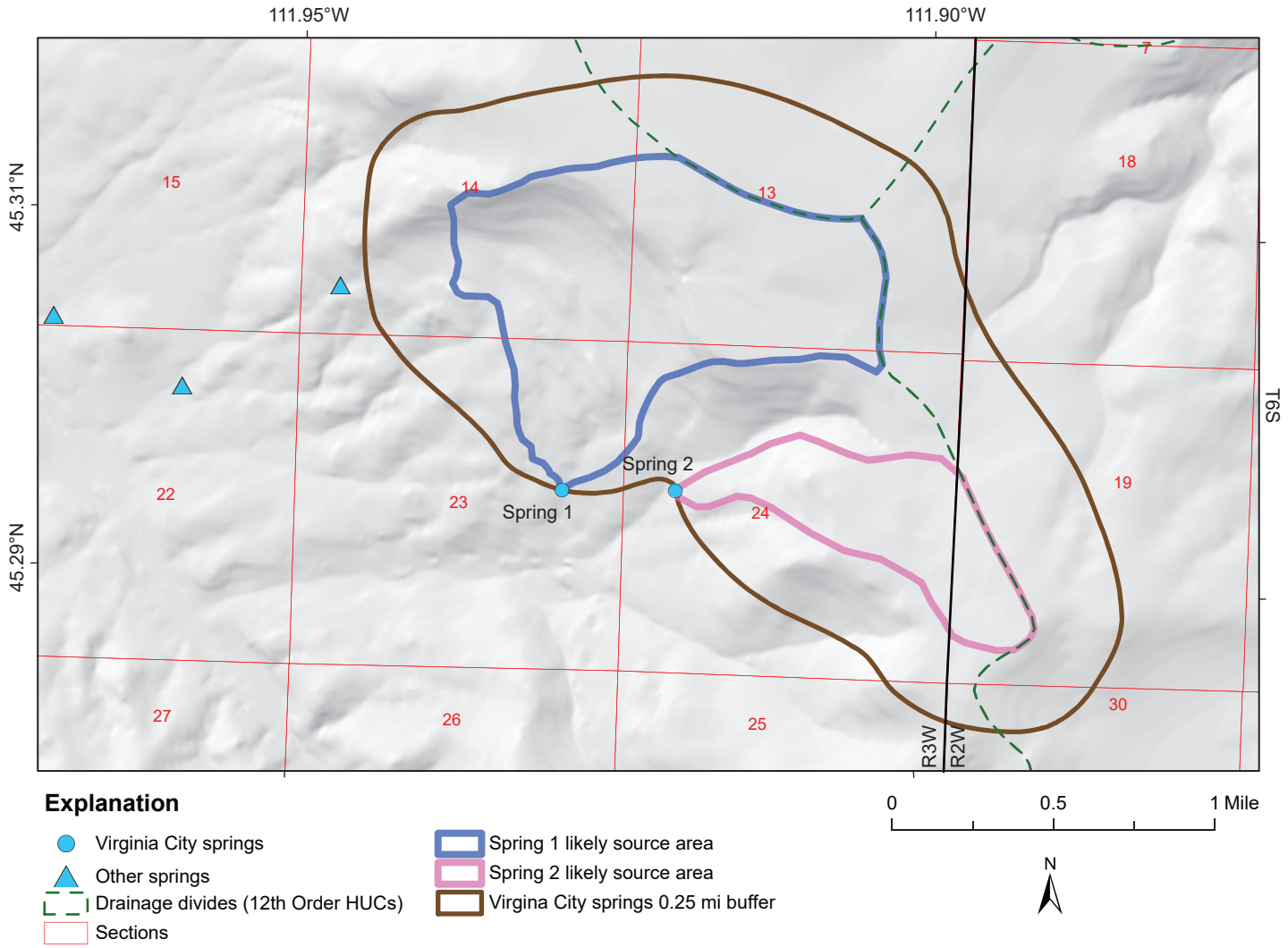

Figure 26. This figure shows the likely source areas for Springs 1 and 2. Geologic mapping, geomorphology, drainage divides, and the locations of other springs were used to estimate the source areas. The source area for Spring 1, 548 acres, includes the landslide area upslope from it, and the internally drained portion of the top of the mesa (the dry lakes area). The source area for Spring 2, 206 acres, includes the intact bedrock area upslope from Spring 2. Due to uncertainty associated with potential heterogeneity in the fracture network, a 0.25-mi buffer was extended beyond the interpreted source areas to provide a safety factor based on professional judgment.

If development occurs within the spring's source area, spills and septic system effluent could infiltrate through the fractured lava flows to the flow system of Spring 1. The concentration of dissolved contaminants (e.g., nitrate) are contingent upon the amount of material released relative to the spring flow, and degradation along the flow path. Biological contaminants (bacteria, viruses, and parasites) can move several miles through fractured rock aquifers (Butler and others, 1954; Allen and Morrison, 1973; Yates and others, 1988), and their concentration is controlled by the transport, survival, and reproduction of microorganisms in the subsurface.

Spring 2

Likely Source Area

Spring 2 emerges from the main landslide scarp. Similar to Spring 1, the source area for Spring 2 was estimated based on geologic mapping, geomorphology, drainage divides, and the locations of other springs (fig. 26). We interpret its source area to be from an area of intact (unaffected by landslide movement) volcanic bedrock located upslope of the spring (~206 acres). The recharge area is characterized by fractured and brecciated lava flows that are not internally drained. Based on the flow rate of Spring 2, and assuming 20 in/yr average precipitation in the source area (PRISM, 2018), about 24% of precipitation flows

to Spring 2. Similar to Spring 1, the water infiltrates into the basalt fractures until reaching the contact with the tuff, where it then flows laterally along this contact until discharging at Spring 2.

Vulnerability to Development

Similar to Spring 1, Spring 2 is fed by a perched aquifer and is unlikely to be affected by pumping wells completed in the underlying aquifer; however, it would be susceptible to contamination by spills and septic systems developed within its source area. Therefore, impacts to Spring 2 from residential and commercial development would be most likely to take the form of changes in water quality.

RECOMMENDATIONS

Land use within the spring source areas for Spring 1 and Spring 2 (fig. 26) should be monitored because these springs are susceptible to impacts from the infiltration of contaminants (e.g., spills or septic effluent). Spring 1 is a critical source of high-quality water for the town, with flow rates that meet current and projected water demands.

Planning for an alternative water supply would add redundancy in case Spring 1 is negatively affected by upgradient activities or natural phenomena. The cost of development, water rights, and rights of ways are also considerations, but are beyond the scope of this study. Alternatives to increasing water supply include measures to reduce demand, such as system maintenance to reduce water loss or water conservation programs.

Landslides cover much of the area near Virginia City. The LiDAR data collected for this study in 2017 contributed to mapping these landslides, but LiDAR does not provide information on landslide history or the timing of movement in these areas. A similar LiDAR survey could be performed in about 10 yr, and compared to these data to evaluate the landslide hazard based on the magnitude and geographic distribution of land movements (Jaboyedoff and others, 2012). Although outside the scope of this groundwater investigation, such an analysis would provide a geologic hazard/landslide assessment for this area.

ACKNOWLEDGMENTS

This study would not have been possible without the assistance of the landowners in the Virginia City area. They provided access to their property, and to their wells and springs.

The town of Virginia City provided much assistance with this study. They aided in developing the scope of the study, contacting landowners, providing historical information, and collecting samples. In particular, Robert Erdale and Roger Williams provided extensive support and assistance.

Montana Tech student Kira Overin provided support for both the field and office aspects of this study. Montana Tech's Geophysical Field Camp (supervised by Mohamad Khalil and Marvin Speece) collected and analyzed geophysical data. Jeremy Crowley from the MBMG assisted with LiDAR data collection and surveying. Susan Smith and Susan Barth from the MBMG assisted with figure preparation, editing, and report layout.

REFERENCES

Abatzoglou, J.T., Dobrowski, S.Z., Parks, S.A., and Hegewisch, K.C., 2018, TerraClimate, a high-resolution global dataset of monthly climate and climatic water balance from 1958–2015, Scientific Data, v. 5, no. 170191, doi: 10.1038/sdata.2017.191.

Aero-Graphics, 2017, Virginia City aerial survey: Madison County, Montana: Technical Project Report for the Montana Bureau of Mines and Geology, 15 p., available at: https://ftpgeoinfo.msl.mt.gov/Data/Spatial/MSDI/Elevation/Lidar/Reports/MADISON_2017_VirginiaCty.pdf [Accessed April 2022].

Allen, M.J., and Morrison, S., 1973, Bacterial movement through fractured bedrock: Groundwater, v. 11, no. 2, p. 6–10.

Anderson, S.R., and Bowers, B., 1995. Stratigraphy of the unsaturated zone and uppermost part of the Snake River Plain aquifer at Test Area North, Idaho National Engineering Laboratory, Idaho: U.S. Geological Survey Water-Resources Investigations Report 95-4130.

Bobst, A.L., 2020, Virginia City aquifer test: Montana Bureau of Mines and Geology Open File Report 726, 17 p.

Butler, R.G., Orlob, G.T., and McGauhey, P.H., 1954, Underground movement of bacterial and chemical pollutants: Journal American Water Works Association, v. 46, no. 2, p. 97–111.

Chambers, L.A., Gooddy, D.C. and Binley, A.M., 2019, Use and application of CFC-11, CFC-12, CFC-113 and SF6 as environmental tracers of groundwater residence time: A review: Geoscience Frontiers, v. 10, no. 5, p. 1643–1652.

Clark, I., and Fritz, P., 1997. Environmental isotopes in hydrogeology: New York, Lewis Publishers.

Cook, P.G., Solomon, D.K., Plummer, L.N., Busenberg, E., and Schiff, S.L., 1995, Chlorofluorocarbons as tracers of groundwater transport processes in a shallow, silty sand aquifer: Water Resources Research, v. 31, no. 3, p. 425–434.

Cook, P.G., and Solomon, D.K., 1995, Transport of atmospheric trace gases to the water table: Implications for groundwater dating with chlorofluorocarbons and krypton 85: Water Resources Research, v. 31, no. 2, p. 263–270.

Coplen, T.B., 1994, Reporting of stable hydrogen, carbon, and oxygen isotopic abundances (technical report): Pure and Applied Chemistry, v. 66, no. 2, p. 273–276.

Cordua, W.S., 1973, Precambrian geology of the southern Tobacco Root Mountains, Madison County, Montana: Bloomington, Indiana University, PhD dissertation, 147 p.

Damschen and Associates, Inc., 1996, Water system analysis, Virginia City, Montana: Unpublished document submitted to the Montana Department of Environmental Quality Permitting and Compliance Division, 37 p., 6 plates.

Damschen-Entranco, 2000, Town of Virginia City public water supply source water protection plan (PWSID#00353), 20 p.

Dunn, D., 1977, Preliminary water resources investigation, Virginia City, Montana: memo to Mr. Hadleigh Stoltz, 15 p.

Faure, G., 1991, Principles and applications of inorganic geochemistry: Upper Saddle River, N.J., Prentice Hall.

Fournier, M., Massei, N., Bakalowicz, M., Dussart-Baptista, L., Rodet, J., and Dupont, J.P., 2007, Using turbidity dynamics and geochemical variability as a tool for understanding the behavior and vulnerability of a karst aquifer: Hydrogeology Journal, v. 15, p. 689–704.

Gammons, C.H., Poulson, S.R., Pellicori, D.A., Reed, P.J., Roesler, A.J., and Petrescu, E.M., 2006, The hydrogen and oxygen isotopic composition of precipitation, evaporated mine water, and river water in Montana, USA: Journal of Hydrology, v. 328, p. 319–330.

Gotkowitz, M.B., ed., 2022, Standard procedures and guidelines for field activities: Montana Bureau of Mines and Geology Open-File Report 746, 96 p.

Great West Engineering, 2016, Town of Virginia City preliminary engineer report: Water/wastewater system improvements, 137 p.

Gröning, M., Lutz, H.O., Roller-Lutz, Z., Kralik, M., Gourcy, L., and Pöltenstein, L., 2012, A simple rain collector preventing water re-evaporation dedicated for $\delta^{18}O$ and $\delta^{2}H$ analysis of cumulative precipitation samples: Journal of Hydrology, v. 448, p. 195–200.

Haugerud, R.A., Richards, S.M., Soller, D., and Thoms, E.E., 2018, GeMS (Geologic Map Schema)—A standard format for digital publication of geologic maps, available at https://ngmdb.usgs.gov/Info/standards/GeMS/docs/GeMSv2_draft7g_ProvisionalRelease.pdf [Accessed February 18, 2019].

Heath, R.C., 1983, Basic ground-water hydrology: U.S. Geological Survey Water-Supply Paper 2220.

Helsel, D.R., Hirsch, R.M., Ryberg, K.R., Archfield, S.A., and Gilroy, E.J., 2020, Statistical methods in water resources: U.S. Geological Survey Techniques and Methods, book 4, chap. A3, 458 p., doi: https://doi.org/10.3133/tm4a3.

Hounslow, A.W., 1995, Water quality data, analysis and interpretation: CRC Press, Boca Raton, Fla., 397 p.

IAEA, 2002, A new device for monthly rainfall sampling for GNIP: Water & Environment Newsletter, International Atomic Energy Agency, Special Issue on the Global Network of Isotopes in Precipitation, Issue 16, October 2002, p. 5, available at http://www-naweb.iaea.org/napc/ih/IHS_resources_publication_newsletter.html [Accessed April 2022].

Jaboyedoff, M., Oppikofer, T., Abellán, A., Derron, M.H., Loye, A., Metzger, R., and Pedrazzini, A., 2012, Use of LIDAR in landslide investigations: A review: Natural Hazards, v. 61, no. 1, p. 5–28.

Jacob, C.E., and Lohman, S.W., 1952, Non-steady flow to a well of constant drawdown in an extensive aquifer: Transactions, American Geophysical Union, v. 33, no. 4, p. 559–569.

Kellogg, K.S., and Williams, V.S., 2006, Geologic map of the Ennis 30′ x 60′ quadrangle, Madison and Gallatin Counties, Montana, and Park County, Wyoming: Montana Bureau of Mines and Geology Open-File Report 529, 27 p., 1 sheet, scale 1:100,000.

Khalil, M., 2017, 2D electrical resistivity tomography and VLF-EM survey in Virginia City, Montana: Montana Technological University—Geophysical Engineering Field Camp Report, 38 p.

Khalil, M., Bobst, A., and Mosolf, J., 2018, Utilizing 2D electrical resistivity tomography and very low frequency electromagnetics to investigate the hydrogeology of natural cold springs near Virginia City, southwest Montana: Pure and Applied Geophysics, v. 175, no. 10, p. 3525–3538.

Kharaka, Y.K., Thordsen, J.J., and White, L.D., 2002, Isotopes and chemical compositions of meteoric and thermal waters and snow from the greater Yellowstone National Park region: USGS Open-File Report 02-194.

Kline, K. (Montana Rural Water Systems, Inc.), 2016, Source water protection plan—Town of Virginia City public water system (PWSID#MT0000353), 40 p.

Lindsey, B.D., Jurgens, B.C., and Blitz, K., 2019, Tritium as an indicator of modern, mixed, and premodern groundwater age: USGS Scientific Investigations Report 2019-5090.

McCarthy, P.M., Dutton, D.M., Sando, S.K., and Sando, R., 2016, Montana StreamStats—A method for retrieving basin and streamflow characteristics in Montana: U.S. Geological Survey Scientific Investigations Report 2015-5019-A, 16 p., doi: http://dx.doi.org/10.3133/sir20155019A.

Montana Bureau of Mines and Geology (MBMG), 2018, Montana Groundwater Information Center Water Well Data, http://nris.mt.gov/gis/ [Accessed November 7, 2018].

Montana Department of Environmental Quality (MDEQ), 2014, Circular DEQ 1 Standards for Water Works, available at https://deq.mt.gov/files/Water/WQInfo/Documents/Circulars/Circulars/2018DEQ-1.pdf [Accessed July 23, 2018].

Montana Department of Environmental Quality (MDEQ), 2018, Final 2018 water quality integrated report, available at https://deq.mt.gov/Portals/112/Water/WQPB/CWAIC/Reports/IRs/2018/2018_IR_Final.pdf [Accessed May 28, 2020].

Montana Department of Environmental Quality (MDEQ), 2019, Circular DEQ 7 Montana Numeric Water Quality Standards https://deq.mt.gov/Portals/112/Water/WQPB/Standards/PDF/DEQ7/DEQ-7.pdf [Accessed June 8, 2020].

Mosolf, J.G., 2021, Geologic map of the Virginia City 7.5’ quadrangle, Madison County, Montana: Montana Bureau of Mines and Geology Geologic Map 80, 1 sheet, scale 1:24,000.

Mosolf, J., Bobst, A., and Crowley, J., in prep, Landslide map of the Virginia City area, Madison County, Montana; MBMG Open-File Report.

National Oceanic and Atmospheric Administration (NOAA), 2018, NOAA 1981–2010 Climate Normals, https://www.ncdc.noaa.gov/cdo-web/datatools/normals [Accessed November 7, 2018].

Oster, H., Sonntag, C., and Munnich, K.O., 1996, Groundwater age dating with chloroflurocarbons: Water Resources Research, v. 32, no. 10, p. 2989–3001.

Patton, T., 1991, MBMG Memo to Melinda Tichenor (Virginia City Council), 3 p.

PRISM, 2018, PRISM Climate Data: http://www.prism.oregonstate.edu/ [Accessed November 7, 2018].

Rozanski, K., Araguás-Araguás, L., and Gonfiantini, R., 1993, Isotopic patterns in modern global precipitation: Climate change in continental isotopic records, v. 78, p. 1–36.

Ruppel, E.T., and Liu, Y., 2004, The gold mines of the Virginia City mining district, Madison County, Montana: Montana Bureau of Mines and Geology Bulletin 133, 83 p., 2 sheets.

Rutherford, B., and Speece, M., 2017, A seismic survey in Virginia City, Montana, to investigate the origin of natural springs: Montana Technological University—Geophysical Engineering Field Camp Report, 53 p.

SNOTEL, 2018, Snow Telemetry (SNOTEL) and snow course data and products: https://www.wcc.nrcs.usda.gov/snow/ [Accessed November 7, 2018].

Speece, M., 2018, A seismic refraction survey in Virginia City, Montana, to investigate stream bed hydrologic conditions along Alder Creek: Montana Technological University— Geophysical Engineering Field Camp Report, 50 p.

Sugarbaker, L.J., Constance, E.W., Heidemann, H.K., Jason, A.L., Lukas, V., Saghy, D.L., and Stoker, J.M., 2014, The 3D elevation program initiative—A call for action: U.S. Geological Survey Circular 1399, 35 p., doi: http://dx.doi.org/10.3133/cir1399.

Timmer, J., 2020, MBMG analytical laboratory: Quality assurance manual: Montana Bureau of Mines and Geology Open-File Report 729, 8 p.

Vuke, S.M., 2013, Landslide map of the Big Sky area, Gallatin and Madison Counties, Montana: Montana Bureau of Mines and Geology Open-File Report 632, 1 sheet, scale 1:24,000.

Walker, G.P., 1971, Compound and simple lava flows and flood basalts: Bulletin of Volcanology, v. 35, no. 3, 579–590.

Weir, K.L., 1982, Maps showing geology and outcrops of part of the Virginia City and Alder quadrangles, Madison County, Montana: U.S. Geological Survey Miscellaneous Field Studies Map MF-1490.

Yates, M.V., Yates, S.R., and Gerba, C.P., 1988, Modeling microbial fate in the subsurface environment: Critical Reviews in Environmental Science and Technology, v. 17, no. 4, p. 307–344.

APPENDIX A
WATER QUALITY

Table A1. MBMG laboratory analytical parameters and abbreviations.

Major Ions and Nutrients (mg/L)	
Calcium*	Ca
Magnesium*	Mg
Sodium*	Na
Potassium*	K
Iron	Fe
Manganese	Mn
Silica*	SiO_2
Bicarbonate*	HCO_3
Carbonate	CO_3
Chlorine*	Cl
Sulfate*	SO_4
Nitrate*	as N
Fluoride	F
Orthophosphate	as P

Field Parameters		
Specific Conductivity*	Fld SC	µS/cm
pH*	Fld pH	---
Water Temperature*	Temp	°C

Laboratory Parameters		
Lab Specific Conductivity	Lab SC	µS/cm
pH	Lab pH	---

Water Isotopes		
Deturium Fraction*	δD	per mil; ‰
^{18}O Fraction*	$\delta^{18}O$	per mil; ‰

Trace Elements (µg/L)	
Aluminum	Al
Antimony	Sb
Arsenic*	As
Barium	Ba
Beryllium	Be
Boron	B
Bromide	Br
Cadmium	Cd
Cerium	Ce
Cesium	Cs
Chromium	Cr
Cobalt	Co
Copper	Cu
Gallium	Ga
Lanthanum	La
Lead	Pb
Lithium	Li
Molybdenum	Mo
Nickel	Ni
Niobium	Nb
Neodymium	Nd
Palladium	Pd
Praseodymium	Pr
Radon*	Rn
Rubidium	Rb
Silver	Ag
Selenium	Se
Strontium	Sr
Thallium	Tl
Thorium	Th
Tin	Sn
Titanium	Ti
Tungsten	W
Uranium	U
Vanadium	V
Zinc	Zn
Zirconium	Zr

mg/L, milligrams per liter (ppm).
µg/L, micrograms per liter (ppb).
µS/cm, microSiemens per centimeter at 25°C.
*Parameters reported in this appendix (B).
Other parameters are available from the GWIC database: http://mbmggwic.mtech.edu/

Table A2. Composite monthly water isotopes of precipitation.

Gwic ID	Map #	Site Name	Date	Sample Mass (g)	$\delta^{18}O$	δD	d
					‰		
291772	1	VIRGINIA CITY UPPER PRECIP GAGE	5/1/17	NR	-18.2	-140	5.6
291772	1	VIRGINIA CITY UPPER PRECIP GAGE	6/1/17	306	-14.9	-112	7.2
291772	1	VIRGINIA CITY UPPER PRECIP GAGE	7/1/17	554	-16.4	-124	7.2
291772	1	VIRGINIA CITY UPPER PRECIP GAGE	8/1/17	316	-8.0	-66	-2
291772	1	VIRGINIA CITY UPPER PRECIP GAGE	9/1/17	84	-13.1	-113	-8.2
291772	1	VIRGINIA CITY UPPER PRECIP GAGE	10/1/17	468	-19.9	-150	9.2
291772	1	VIRGINIA CITY UPPER PRECIP GAGE	11/1/17	217	-17.0	-127	9
291772	1	VIRGINIA CITY UPPER PRECIP GAGE	5/1/18	492	-16.8	-130	4.4
291772	1	VIRGINIA CITY UPPER PRECIP GAGE	6/1/18	648	-10.5	-95	-11
291772	1	VIRGINIA CITY UPPER PRECIP GAGE	10/1/18	265	-13.8	-101	9.4
291772	1	VIRGINIA CITY UPPER PRECIP GAGE	11/1/18	546	-17.0	-127	9
291763	2	VIRGINIA CITY LOWER PRECIP GAGE	4/1/17	NR	-18.7	-147	2.6
291763	2	VIRGINIA CITY LOWER PRECIP GAGE	5/1/17	NR	-17.5	-134	6
291763	2	VIRGINIA CITY LOWER PRECIP GAGE	6/1/17	668	-13.5	-101	7
291763	2	VIRGINIA CITY LOWER PRECIP GAGE	7/1/17	779	-12.1	-93	3.8
291763	2	VIRGINIA CITY LOWER PRECIP GAGE	8/1/17	218	-2.6	-49	-28.2
291763	2	VIRGINIA CITY LOWER PRECIP GAGE	9/1/17	165	-12.4	-105	-5.8
291763	2	VIRGINIA CITY LOWER PRECIP GAGE	10/1/17	497	-16.3	-127	3.4
291763	2	VIRGINIA CITY LOWER PRECIP GAGE	11/1/17	696	-16.0	-128	0
291763	2	VIRGINIA CITY LOWER PRECIP GAGE	12/1/17	714	-15.8	-116	10.4
291763	2	VIRGINIA CITY LOWER PRECIP GAGE	1/1/18	501	-22.0	-170	6
291763	2	VIRGINIA CITY LOWER PRECIP GAGE	2/1/18	327	-18.8	-146	4.4
291763	2	VIRGINIA CITY LOWER PRECIP GAGE	2/28/18	104	-19.6	-157	-0.2
291763	2	VIRGINIA CITY LOWER PRECIP GAGE	3/31/18	659	-21.2	-165	4.6
291763	2	VIRGINIA CITY LOWER PRECIP GAGE	5/1/18	777	-18.8	-147	3.4
291763	2	VIRGINIA CITY LOWER PRECIP GAGE	6/1/18	596	-16.1	-123	5.8
291763	2	VIRGINIA CITY LOWER PRECIP GAGE	7/1/18	1177	-9.4	-83	-7.8
291763	2	VIRGINIA CITY LOWER PRECIP GAGE	8/1/18	8	-4.7	-68	-30.4
291763	2	VIRGINIA CITY LOWER PRECIP GAGE	9/1/18	718	-15.1	-114	6.8
291763	2	VIRGINIA CITY LOWER PRECIP GAGE	10/1/18	17	-1.9	-61	-45.8
291763	2	VIRGINIA CITY LOWER PRECIP GAGE	11/1/18	331	-13.3	-109	-2.6

Note. d, deuterium excess, calculated as $\delta D - 8\delta^{18}O$. NR, not recorded.

Sample excluded from LMWL calculation due to low d value, indicating sample evaporation.

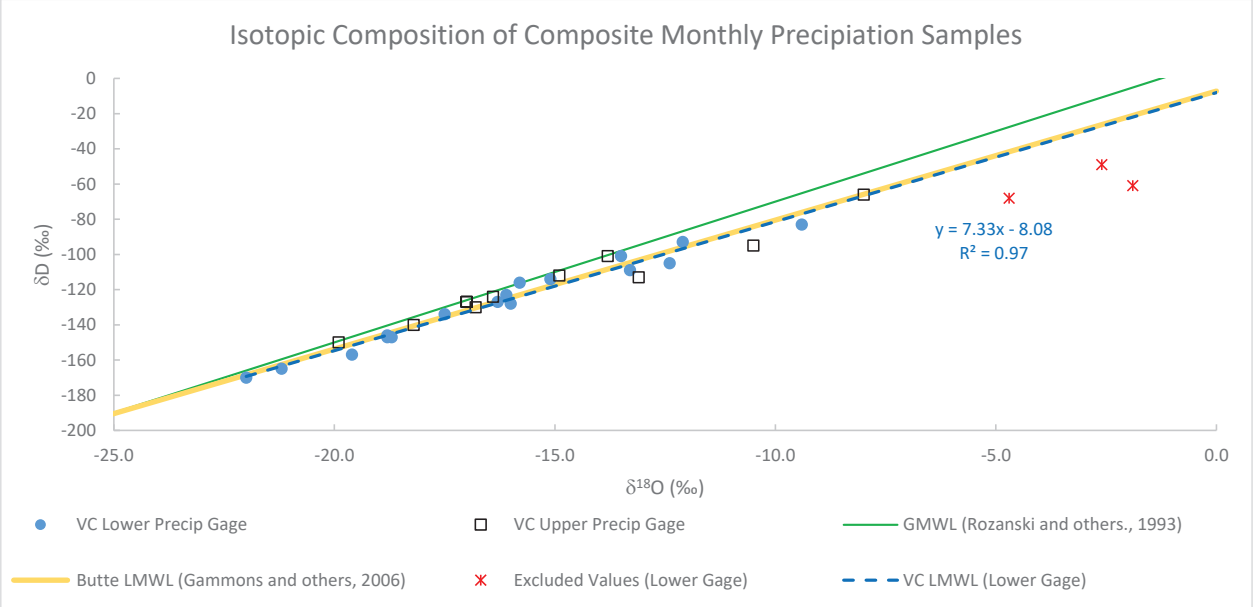

Table A3. Selected monitoring results for Springs 1 and 2.

Gwic ID	Map #	Site Name	Date	Discharge (gpm)	Temp (°C)	Fld pH	SC (µS/cm)	Ca	Mg	Na	K	SiO_2	HCO_3	SO4	Cl	NO_3-N	As (µg/L	^{222}Ra (pC/L)	$\delta^{18}O$	δD
								mg/L											‰	
262623	4	VIRGINIA CITY * SPRING 1	3/2/17		10.6	8.2	331	31.4	14.2	7.65	2.31	35.4	152	8.16	7.07	1.45	2.36	195	-19.1	-152
262623	4	VIRGINIA CITY * SPRING 1	3/28/17																-19.2	-152
262623	4	VIRGINIA CITY * SPRING 1	3/28/17																-19.2	-152
262623	4	VIRGINIA CITY * SPRING 1	4/25/17																-19.4	-152
262623	4	VIRGINIA CITY * SPRING 1	5/22/17		10.6	8.3	335	31.5	14.2	7.38	2.17	34.8	173	5.59	6.34	1.31	2.35		-19.4	-152
262623	4	VIRGINIA CITY * SPRING 1	6/28/17		11.0	8.1	292												-19.2	-151
262623	4	VIRGINIA CITY * SPRING 1	7/24/17		11.0	8.3	334												-18.9	-150
262623	4	VIRGINIA CITY * SPRING 1	8/16/17		10.9	8.2	324	28.9	13.0	6.99	1.84	34.0	173	5.10	6.42	1.36	2.35		-18.7	-149
262623	4	VIRGINIA CITY * SPRING 1	10/16/17																-19.3	-150
262623	4	VIRGINIA CITY * SPRING 1	11/20/17		11.1	8.1	283	30.8	13.7	7.29	2.06	33.6	171	5.30	6.67	1.38	2.62		-19.3	-151
262623	4	VIRGINIA CITY * SPRING 1	12/18/17		10.2	8.1	291											168	-19.2	-151
262623	4	VIRGINIA CITY * SPRING 1	1/24/18																-19.2	-150
262623	4	VIRGINIA CITY * SPRING 1	2/13/18		9.9	7.8	297	30.8	13.9	7.38	2.2	33.8	173	5.44	6.53	1.34	2.25		-19.3	-151
262623	4	VIRGINIA CITY * SPRING 1	3/24/18		10.5	8.0	276												-19.4	-151
262623	4	VIRGINIA CITY * SPRING 1	4/25/18																-19.1	-149
262623	4	VIRGINIA CITY * SPRING 1	5/17/18		10.6	7.9	288	29.2	14.5	8	2.42	36.5	173	5.31	6.68	1.37	2.50		-19.3	-151
278204	3	VIRGINIA CITY * SPRING 2	3/2/17	40				30.6	13.7	7.57	1.59	29.9	166	5.65	5.80	1.44	2.42		-18.8	-149
278204	3	VIRGINIA CITY * SPRING 2	3/28/17																-18.9	-150
278204	3	VIRGINIA CITY * SPRING 2	4/25/17	41															-19.1	-150
278204	3	VIRGINIA CITY * SPRING 2	5/22/17	89	9.3	8.3	333	27.5	12.6	7.03	1.20	31.4	173	4.58	5.21	1.34	2.43		-19.3	-150
278204	3	VIRGINIA CITY * SPRING 2	6/28/17	35	10.1	7.8	273												-18.8	-148
278204	3	VIRGINIA CITY * SPRING 2	7/24/17	55	10.1	8.3	332												-18.7	-148
278204	3	VIRGINIA CITY * SPRING 2	8/16/17	24	10.6	8.1	317	28.8	12.9	7.51	1.39	29.8	173	4.18	5.40	1.37	2.46		-18.9	-148
278204	3	VIRGINIA CITY * SPRING 2	10/16/17		9.8	8.1	321												-18.8	-148
278204	3	VIRGINIA CITY * SPRING 2	1/24/18																-19.0	-148
278204	3	VIRGINIA CITY * SPRING 2	2/13/18		9.3	7.7	288	30.4	13.7	7.61	1.90	30.0	173	4.14	5.74	1.34	2.24		-19.0	-148
278204	3	VIRGINIA CITY * SPRING 2	3/24/18	40	9.2	8.0	285												-19.0	-148
278204	3	VIRGINIA CITY * SPRING 2	4/25/18	78															-18.9	-148

Table A4. Selected monitoring results for other springs.

Gwic ID	Map #	Site Name	Date	Discharge (gpm)	Temp (°C)	Fld pH	SC (µS/cm)	Ca	Mg	Na	K	SiO_2	HCO_3	SO_4	Cl	NO_3-N	As	$\delta^{18}O$	δD
								mg/L									(µg/L)	‰	
291688	6	SAWYER SPRING	4/25/17		8.6	7.5	525											-18.5	-147
291688	6	SAWYER SPRING	5/22/17		8.1	7.5	645	56.1	25.2	22.98	5.21	46.3	342	11.68	10.39	0.19	11.77	-18.5	-147
291688	6	SAWYER SPRING	7/24/17		8.9	7.5	636											-18.4	-146
291688	6	SAWYER SPRING	8/16/17		9.1	7.7	628	52.5	23.4	22.35	4.65	45.9	346	11.60	11.18	0.18	12.54	-17.8	-144
291701	7	MASON SPRING	4/25/17		9.6	7.7	317											-19.5	-154
291701	7	MASON SPRING	5/22/17		8.6	7.9	382	35.4	13.0	13.10	3.64	52.1	193	6.80	9.10	0.87	3.68	-19.9	-155
291701	7	MASON SPRING	7/24/17		8.9	7.8	382											-19.1	-152
291701	7	MASON SPRING	8/16/17		9.3	8.1	367	33.9	12.4	12.99	3.36	51.0	193	6.33	8.59	0.89	3.61	-19.5	-153
291701	7	MASON SPRING	1/24/18		6.4	7.5	550											-18.2	-145
291701	7	MASON SPRING	2/28/18		4.1	7.6	550											-18.6	-147
292170	8	NEVADA CITY SPRING	5/22/17		10	8.2	465	42.3	17.5	17.21	2.53	41.6	233	10.40	13.90	0.57	2.49	-19.3	-152
292170	8	NEVADA CITY SPRING	7/24/17		11.6	8.3	454											-19.2	-151
292170	8	NEVADA CITY SPRING	8/16/17		13.7	8.4	432	41.6	17.1	18.60	2.7	41.7	235	10.01	14.14	0.53	2.38	-18.6	-150
292170	8	NEVADA CITY SPRING	1/24/18		7.1	8.3	404											-18.9	-150
292170	8	NEVADA CITY SPRING	2/28/18		7.9	8.4	404											-19.0	-151
292170	8	NEVADA CITY SPRING	3/24/18		6.8	8.3	403											-19.0	-150
292170	8	NEVADA CITY SPRING	4/11/18		11.2	8.4	403											-19.0	-150
292170	8	NEVADA CITY SPRING	8/13/18	108															
298083	5	GILBERT SPRING	7/30/18	30*															
298083	5	GILBERT SPRING	7/20/21	51															
298083	5	GILBERT SPRING	8/2/21	60															
298083	5	GILBERT SPRING	8/16/21	51															
298083	5	GILBERT SPRING	9/4/21	49															
298083	5	GILBERT SPRING	9/17/21	49															

Note. Highlighted values indicate exceedance of the MCL.

*Estimated

Table A5. Selected monitoring results for wells.

Gwic ID	Map #	Site Name	HGU	Total Depth (ft)	Date	Temp (°C)	Fld pH	SC (µS/cm)	Ca	Mg	Na	K	SiO_2	HCO_3	SO_4	Cl	NO_3-N	As	$\delta^{18}O$	δD
									mg/L									(µg/L	‰	
108805	9	CHRISTMAN, RICH	Landslide	99	5/16/17	11.3	7.1	618	64.2	24.9	25.8	7.2	50.3	298	27.4	55.0	1.13	7.5	-18.7	-148
263446	11	KOCH, WILLIAM	Basement Rocks	318	5/16/17	11.1	7.5	788	3.0	1.2	197.2	1.8	9.4	504	20.9	7.3	ND (0.01)	15.3	-19.9	-158
263446	11	KOCH, WILLIAM	Basement Rocks	318	8/15/17	11.7	8.9	867	3.3	1.5	194.1	2.1	9.5	491	20.2	7.3	ND (0.01)	14.2	-19.2	-155
271932	12	MADISON COUNTY	Alluvium	109	5/16/17	9.6	6.6	1225	94.6	38.9	84.0	10.3	22.8	313	22.2	241.1	4.78	0.8	-16.6	-131
271932	12	MADISON COUNTY	Alluvium	109	8/16/17	12.1	7.6	1279	95.3	38.8	78.1	12.1	24.0	308	20.1	221.6	3.40	0.5	-16.6	-132
242217	13	NEVIN BUBBA	Basement Rocks	250	5/16/17	12.7	7.3	675	2.7	2.0	166.7	4.9	30.8	410	22.8	12.6	ND (0.01)	25.1	-20.0	-158
242217	13	NEVIN BUBBA	Basement Rocks	250	8/15/17	12.8	8.9	743	2.7	2.0	172.0	5.1	30.8	404	22.6	11.9	ND (0.01)	22.8	-19.6	-157
236720	14	BOWLING, ROBERT	Landslide	220	5/16/17	10.9	6.6	451	31.2	27.3	20.8	8.2	20.0	257	28.7	14.9	ND (0.01)	0.9	-19.1	-153
236720	14	BOWLING, ROBERT	Landslide	220	8/15/17	11.1	8.2	415	31.2	27.2	20.8	8.6	21.1	251	27.6	14.8	ND (0.01)	1.2	-18.5	-150
294417	19	MBMG BOWLING 1	Landslide	155	11/20/17	11.7	8.3	269	27.8	11.3	8.6	7.5	72.3	162	4.9	5.0	0.68	5.1	-19.8	-154
294418	20	MBMG BOWLING 2	Tuff	610	11/20/17	11.8	7.6	899	31.1	17.4	127.8	24.6	31.0	584	22.1	6.4	ND (0.01)	74.7	-19.9	-156
294418	20	MBMG BOWLING 2	Tuff	610	6/27/18	12.5	7.6	968	33.9	18.7	162.8	27.0	30.5	635	24.3	7.8	0.06	64.9	-19.9	-155
294419	21	MBMG BOWLING 3	Landslide	210	5/17/18	12.4	7.7	330	27.9	12.1	20.2	12.3	68.6	212	7.6	4.9	0.05	27.8	-19.6	-154
294421	22	MBMG BOWLING 4	Landslide	210	11/20/17	12.1	8.0	311	27.3	11.7	17.4	10.4	61.9	194	10.9	5.2	0.04	20.9	-19.6	-154

Note. Highlighted values indicate exceedance of the MCL.

Table A6. Selected monitoring results for streams.

Gwic ID	Map #	Site Name	Date	Stage (ft)	Discahrge (cfs)	Temp (°C)	Fld pH	SC (µS/cm)	Ca	Mg	Na	K	SiO_2	HCO_3	SO_4	Cl	NO_3-N	As (µg/L)	^{222}Ra (pC/L)	$\delta^{18}O$	δD
									mg/L											‰	
291773	23	DAYLIGHT CREEK #1	4/21/17	0.62																	
291773	23	DAYLIGHT CREEK #1	5/4/17	0.67		14.1		301												-18.3	-145
291773	23	DAYLIGHT CREEK #1	5/19/17	0.66		11.9	8.8	350	40.7	12.2	6.62	1.41	23.1	186	6.99	3.77	0.85	1.21		-18.6	-146
291773	23	DAYLIGHT CREEK #1	6/1/17	0.67		11.5	9.0	352												-18.4	-145
291773	23	DAYLIGHT CREEK #1	6/14/17	0.67		12.5															
291773	23	DAYLIGHT CREEK #1	7/6/17	0.68		13.7	8.4	357												-18.0	-143
291773	23	DAYLIGHT CREEK #1	7/18/17	0.68		11.2															
291773	23	DAYLIGHT CREEK #1	8/1/17	0.70		9.2	8.4	382												-17.6	-142
291773	23	DAYLIGHT CREEK #1	8/14/17	0.70		9.6	8.3	366	38.4	11.5	6.65	1.26	23.9	200	6.48	3.95	0.98	1.09		-17.9	-143
291773	23	DAYLIGHT CREEK #1	9/1/17	0.69		8.7		303												-18.3	-144
291773	23	DAYLIGHT CREEK #1	9/17/17	0.68		10.3	8.4	361												-18.4	-144
291773	23	DAYLIGHT CREEK #1	10/1/17	0.70		8.2															
291773	23	DAYLIGHT CREEK #1	10/29/21	0.69																	
291773	23	DAYLIGHT CREEK #1	11/11/17	0.67		8.0	8.4	370												-18.3	-144
291773	23	DAYLIGHT CREEK #1	12/18/17	0.69		5.4	8.6	320											66.99	-18.3	-143
291773	23	DAYLIGHT CREEK #1	1/24/18	0.68		6.6	8.6	319												-18.0	-143
291773	23	DAYLIGHT CREEK #1	4/11/18	1.65		0.1	7.6	38												-19.4	-151
291773	23	DAYLIGHT CREEK #1	5/30/18	0.80		11.7	7.9	294												-18.4	-144
291773	23	DAYLIGHT CREEK #1	6/11/18	0.77																	
291773	23	DAYLIGHT CREEK #1	7/2/18	0.99																	
291773	23	DAYLIGHT CREEK #1	8/13/18	1.00	0.290																
291773	23	DAYLIGHT CREEK #1	7/20/21	*	0.065																
291773	23	DAYLIGHT CREEK #1	8/2/21	*	0.071																
291773	23	DAYLIGHT CREEK #1	8/16/21	*	0.085																
291773	23	DAYLIGHT CREEK #1	9/4/21	*	0.071																
291773	23	DAYLIGHT CREEK #1	9/17/21	*	0.038																
291774	24	DAYLIGHT CREEK #2	4/18/17	0.50	0.95																
291774	24	DAYLIGHT CREEK #2	4/21/17	0.52	0.95																
291774	24	DAYLIGHT CREEK #2	5/4/17	0.58	0.97	13.3		355											27	-18.5	-146
291774	24	DAYLIGHT CREEK #2	5/19/17	0.52	0.78	8.7	8.5	448	42.4	16.9	10.14	3.10	32.9	214	8.98	13.22	0.68	3.17		-18.6	-147
291774	24	DAYLIGHT CREEK #2	6/1/17	0.52	0.78	12.6	9.0	416												-18.3	-146
291774	24	DAYLIGHT CREEK #2	6/14/17	0.51	0.89	10.5															
291774	24	DAYLIGHT CREEK #2	7/6/17	0.37	0.64	17.0	8.4	355												-18.3	-145
291774	24	DAYLIGHT CREEK #2	7/18/17	0.44	0.79	11.6	8.2														
291774	24	DAYLIGHT CREEK #2	8/1/17	0.39	0.69	11.3	8.7	397												-18.2	-144
291774	24	DAYLIGHT CREEK #2	8/14/17	0.42	0.91	11.5	8.7	379	36.2	13.9	7.64	2.29	31.6	196	6.87	9.63	0.75	2.47		-18.1	-144
291774	24	DAYLIGHT CREEK #2	9/1/17	0.42	0.78	13.4		319												-18.3	-145
291774	24	DAYLIGHT CREEK #2	9/17/17	0.53	0.77	9.1	8.7	390												-18.7	-147
291774	24	DAYLIGHT CREEK #2	10/1/17	0.39		7.8															
291774	24	DAYLIGHT CREEK #2	10/29/17	0.48	1.00																
291774	24	DAYLIGHT CREEK #2	11/11/17	0.50	1.04	5.0	8.7	435												-18.5	-146
291774	24	DAYLIGHT CREEK #2	12/18/17	0.54		3.1	8.7	347											ND (20)	-18.4	-146
291774	24	DAYLIGHT CREEK #2	1/24/18	0.49		2.5	8.7	346												-18.6	-146
291774	24	DAYLIGHT CREEK #2	4/11/18	1.06		1.5	8.1	90												-19.5	-152
291774	24	DAYLIGHT CREEK #2	5/7/18	0.55	2.10																
291774	24	DAYLIGHT CREEK #2	5/30/18	0.58	1.90	13.0	8.2	353												-18.3	-144
291774	24	DAYLIGHT CREEK #2	6/11/18	0.55	2.20																
291774	24	DAYLIGHT CREEK #2	7/2/18	0.60																	

*Staff gage no longer usable.

Table A6—*Continued.*

Gwic ID	Map #	Site Name	Date	Stage (ft)	Discahrge (cfs)	Temp (^{o}C)	Fld pH	SC (µS/cm)	Ca	Mg	Na	K	SiO_2	HCO_3	SO_4	Cl	NO_3-N	As	^{222}Ra	$\delta^{18}O$	δD
									mg/L									(µg/L)	(pC/L)	‰	
291775	25	DAYLIGHT CREEK #3	4/18/17	1.09	1.28																
291775	25	DAYLIGHT CREEK #3	5/4/17	1.09	1.39	11.2		413											46	-17.2	-148
291775	25	DAYLIGHT CREEK #3	5/19/17	0.90	0.73	6.6	8.6	551	46.6	18.9	16.19	3.58	33.7	241	11.82	21.72	0.64	3.92		-18.4	-145
291775	25	DAYLIGHT CREEK #3	6/1/17	1.05	0.66	12.3	8.8	459												-18.4	-146
291775	25	DAYLIGHT CREEK #3	6/14/17	1.11	0.95	9.3															
291775	25	DAYLIGHT CREEK #3	7/6/17	1.06	0.62	16.0	8.2	458												-18.2	-144
291775	25	DAYLIGHT CREEK #3	7/18/17	1.00	0.57	12.6	8.1														
291775	25	DAYLIGHT CREEK #3	8/1/17	0.60	0.59	11.8	8.6	419												-18.1	-144
291775	25	DAYLIGHT CREEK #3	8/14/17	1.00	0.86	12.6	8.6	397	41.4	15.9	10.93	2.94	31.5	208	7.67	11.96	0.57	3.10		-18.0	-144
291775	25	DAYLIGHT CREEK #3	9/1/17	0.97	0.54	14.1		338												-18.5	-145
291775	25	DAYLIGHT CREEK #3	9/17/17	1.10	1.00	8.3	8.5	441												-18.6	-146
291775	25	DAYLIGHT CREEK #3	10/1/17	1.15		7.5															
291775	25	DAYLIGHT CREEK #3	10/16/17	1.04	0.81	6.9	8.3	469												-18.3	-144
291775	25	DAYLIGHT CREEK #3	10/29/17	1.03	0.55																
291775	25	DAYLIGHT CREEK #3	11/11/17	1.04	1.22	4.1	8.5	608												-18.5	-145
291775	25	DAYLIGHT CREEK #3	12/18/17	1.05		2.3	8.6	390											ND (20)	-18.5	-145
291775	25	DAYLIGHT CREEK #3	1/24/18	ICE		0.9	8.6	386												-18.4	-145
291775	25	DAYLIGHT CREEK #3	4/11/18	1.63		5.2	8.4	182												-19.5	-152
291775	25	DAYLIGHT CREEK #3	5/7/18	1.15	1.30																
291775	25	DAYLIGHT CREEK #3	5/30/18	1.50	2.50	12.1	8.4	400												-18.3	-144
291775	25	DAYLIGHT CREEK #3	6/11/18	1.10	1.70																
291775	25	DAYLIGHT CREEK #3	7/2/18	1.03																	

Table A6—*Continued.*

Gwic ID	Map #	Site Name	Date	Stage (ft)	Discahrge (cfs)	Temp (°C)	Fld pH	SC (µS/cm)	Ca	Mg	Na	K	SiO_2	HCO_3	SO_4	Cl	NO_3-N	As (µg/l)	^{222}Ra (pC/L)	$\delta^{18}O$	δD
									mg/L											‰	
291776	26	ALDER GULCH #1	4/18/17	0.98	5.68																
291776	26	ALDER GULCH #1	5/4/17	1.09	6.26	7.8		285												-17.9	-139
291776	26	ALDER GULCH #1	5/19/17	1.33	11.30	4.4	8.5	382	31.8	13.7	3.19	2.32	12.5	176	8.73	1.34	0.09	0.41		-17.9	-139
291776	26	ALDER GULCH #1	6/1/17	1.29	12.32	9.7	8.7	320												-17.9	-139
291776	26	ALDER GULCH #1	6/14/17	1.27	10.88	8.4															
291776	26	ALDER GULCH #1	7/6/17	1.01	5.86	13.4	8.1	357												-17.6	-137
291776	26	ALDER GULCH #1	7/18/17	1.00	7.10	11.8	8.0														
291776	26	ALDER GULCH #1	8/1/17	0.88	4.54	12.4	8.1	364												-17.5	-137
291776	26	ALDER GULCH #1	8/14/17	0.70	4.97	13.0	8.4	358	40.8	16.7	3.31	4.05	13.5	216	8.35	2.28	0.05	0.58		-17.9	-138
291776	26	ALDER GULCH #1	9/1/17	0.73	2.79	15.3		320												-17.9	-138
291776	26	ALDER GULCH #1	9/17/17	0.90	3.75	10.1	8.4	378												-18.1	-139
291776	26	ALDER GULCH #1	10/1/17	1.01		8.5															
291776	26	ALDER GULCH #1	10/16/17	1.01	2.95	6.7	8.3	392												-17.8	-138
291776	26	ALDER GULCH #1	10/29/17	1.11	3.15																
291776	26	ALDER GULCH #1	11/11/17	1.13	4.18	2.9	8.3	430												-18.0	-139
291776	26	ALDER GULCH #1	12/18/17	1.17		0.8	8.3	324											45.69	-18.1	-139
291776	26	ALDER GULCH #1	1/24/18	0.99		0.5	8.3	329												-18.0	-139
291776	26	ALDER GULCH #1	4/11/18	0.98	3.23	7.1	8.7	309												-18.3	-141
291776	26	ALDER GULCH #1	5/17/18	1.80	21.80																
291776	26	ALDER GULCH #1	5/30/18	2.30	13.90	9.8	7.7	175												-18.1	-138
291776	26	ALDER GULCH #1	6/11/18	2.00	19.60																
291776	26	ALDER GULCH #1	7/2/18	1.78																	
			4/18/17	0.84	5.18																
291777	27	ALDER GULCH #2	5/4/17	0.90	6.01	9.8	8.4	316											23	-17.9	-140
291777	27	ALDER GULCH #2	5/19/17	1.20	12.30	4.5	8.6	382	33.9	14.4	4.54	2.46	14.1	186	9.04	3.00	0.11	0.75		-17.9	-139
291777	27	ALDER GULCH #2	6/1/17	1.18	10.82	10.6	8.8	337												-17.7	-139
291777	27	ALDER GULCH #2	6/14/17	1.20	10.60	7.0															
291777	27	ALDER GULCH #2	7/6/17	0.93	4.48	14.3	8.2	303												-17.4	-136
291777	27	ALDER GULCH #2	7/18/17	0.84	3.99	15.4	7.9														
291777	27	ALDER GULCH #2	8/1/17	0.72	3.00	17.4	8.6	342												-17.4	-137
291777	27	ALDER GULCH #2	8/14/17	0.72	3.49	15.9	8.3	354	36.8	16.3	4.71	2.68	15.0	212	7.80	3.22	0.05	1.07		-17.5	-137
291777	27	ALDER GULCH #2	9/1/17	0.76	1.86	15.3		316												-17.9	-138
291777	27	ALDER GULCH #2	9/17/17	0.92	3.16	7.5	8.5	393												-18.3	-142
291777	27	ALDER GULCH #2	10/1/17	1.10		8.1															
291777	27	ALDER GULCH #2	10/16/17	1.13	3.84	6.0	8.4	416												-18.1	-139
291777	27	ALDER GULCH #2	10/29/17	1.10	3.02																
291777	27	ALDER GULCH #2	11/11/17	1.07	3.18	2.5	8.5	467												-18.1	-140
291777	27	ALDER GULCH #2	12/18/17	0.96		0.2	8.2	348											39	-18.2	-140
291777	27	ALDER GULCH #2	1/24/18	0.95		0.1	8.4	354												-18.0	-140
291777	27	ALDER GULCH #2	4/11/18	1.30	5.14	6.2	8.8	311												-18.6	-144
291777	27	ALDER GULCH #2	5/7/18	1.68																	
291777	27	ALDER GULCH #2	5/30/18	1.75		7.9	7.7	247												-18.1	-139
291777	27	ALDER GULCH #2	6/11/18	1.30	23.30																
291777	27	ALDER GULCH #2	7/2/18	1.23																	

Table A7. Tritium values and ages from the $^{3}H/^{3}He^{*}$ method.

Gwic ID	Map #	Site Name	HGU	Date	Tritium (TU)	Tritium 1σ error (TU)	$^{3}He^{*}$ (TU)	Calculated Age (yr)[+]	Tritium Age Class[#]
262623	4	VIRGINIA CITY * SPRING 1	Landslide	3/2/17	0.14	0.11	-3.2	NA	Premodern
262623	4	VIRGINIA CITY * SPRING 1	Landslide	5/22/17	0.35	0.08	1.1	NA	MIxed
262623	4	VIRGINIA CITY * SPRING 1	Landslide	8/16/17	0.62	0.03	-14.1	NA	MIxed
262623	4	VIRGINIA CITY * SPRING 1	Landslide	11/20/17	0.48	0.03	-2.1	NA	MIxed
262623	4	VIRGINIA CITY * SPRING 1	Landslide	2/13/18	0.47	0.03	NR	–	MIxed
262623	4	VIRGINIA CITY * SPRING 1	Landslide	5/17/18	0.53	0.03	NR	–	MIxed
278204	3	VIRGINIA CITY * SPRING 2	Lava Flows	5/22/17	0.84	0.06	NR	–	MIxed
278204	3	VIRGINIA CITY * SPRING 2	Lava Flows	8/16/17	0.83	0.05	NR	–	MIxed
278204	3	VIRGINIA CITY * SPRING 2	Lava Flows	2/13/18	0.85	0.11	NR	–	MIxed
291688	6	SAWYER SPRING	Landslide	5/22/17	1.69	0.08	NR	–	MIxed
291688	6	SAWYER SPRING	Landslide	8/16/17	1.79	0.07	NR	–	MIxed
291701	7	MASON SPRING	Landslide	5/22/17	0.11	0.03	2.2	NA	Premodern
291701	7	MASON SPRING	Landslide	8/16/17	0.29	0.02	NR	–	MIxed
292170	8	NEVADA CITY SPRING	Landslide	5/22/17	0.84	0.08	2.2	NA	MIxed
292170	8	NEVADA CITY SPRING	Landslide	8/16/17	0.60	0.04	NR	–	MIxed
263446	11	KOCH, WILLIAM	Basement Rocks	5/16/17	ND	0.05	468	>60	Premodern
263446	11	KOCH, WILLIAM	Basement Rocks	8/15/17	ND	0.02	100	>60	Premodern
271932	12	MADISON COUNTY	Alluvium	5/16/17	6.38	0.29	NR	–	Modern
271932	12	MADISON COUNTY	Alluvium	8/16/17	5.60	0.46	NR	–	Modern
242217	13	NEVIN BUBBA	Basement Rocks	5/16/17	ND	0.03	3698	>60	Premodern
242217	13	NEVIN BUBBA	Basement Rocks	8/15/17	ND	0.01	2581	>60	Premodern
236720	14	BOWLING, ROBERT	Landslide	5/16/17	ND	0.03	NR	>60	Premodern
236720	14	BOWLING, ROBERT	Landslide	8/15/17	0.12	0.05	403	>60	Premodern
294419	21	MBMG BOWLING #3	Landslide	5/17/18	6.57	0.47	NR	–	Modern

$^{3}He^{*}$ = Tritiogenic helium calculated using the excess air model

[+] Ages calculated using the excess air model.

NR, not reported.

NA, not applicable; low nobel gas indicates air stripping.

ND, results were below the method detection limit (0.1 TU).

[#]Lindsey and others, 2019.

Table A8. CFC values and interpreted ages.

Gwic ID	Map #	Site Name	Date	# of Samples	Avg CFC-11 (pptv)	CFC-11 Age Range (yr)	Avg CFC-12 (pptv)	CFC-12 Age (yr)	Avg CFC-113 (pptv)	CFC-113 Age (yr)	Age Range (yr)
262623	4	VIRGINIA CITY * SPRING 1	5/22/17	2	182	33–40	550	29	56	29–31	29–40
262623	4	VIRGINIA CITY * SPRING 1	8/16/17	3	175	34–37	492	21–29	46	30–32	21–37

Note. pptv, parts per trillion by volume.

Table A9. Dissolved inorganic carbon dating results.

Gwic ID	Map #	Site Name	Date	pMC*	$\delta^{13}C$ (o/oo)	Apparent Radiocarbon Age (yr)
262623	4	VIRGINIA CITY * SPRING 1	5/22/17	80.1 ± 0.3	-13.1	<1790
262623	4	VIRGINIA CITY * SPRING 1	9/1/17	80.7 ± 0.3	-11.7	<1720
278204	3	VIRGINIA CITY * SPRING 2	5/22/17	79.5 ± 0.3	-13.8	<1850
291688	6	SAWYER SPRING	9/1/17	94.0 ± 0.3	-12.5	<500

*pMC, percent modern carbon.

APPENDIX B
WELL HYDROGRAPHS

Appendix B. Virginia City Well Hydrographs (pg 1 of 4)

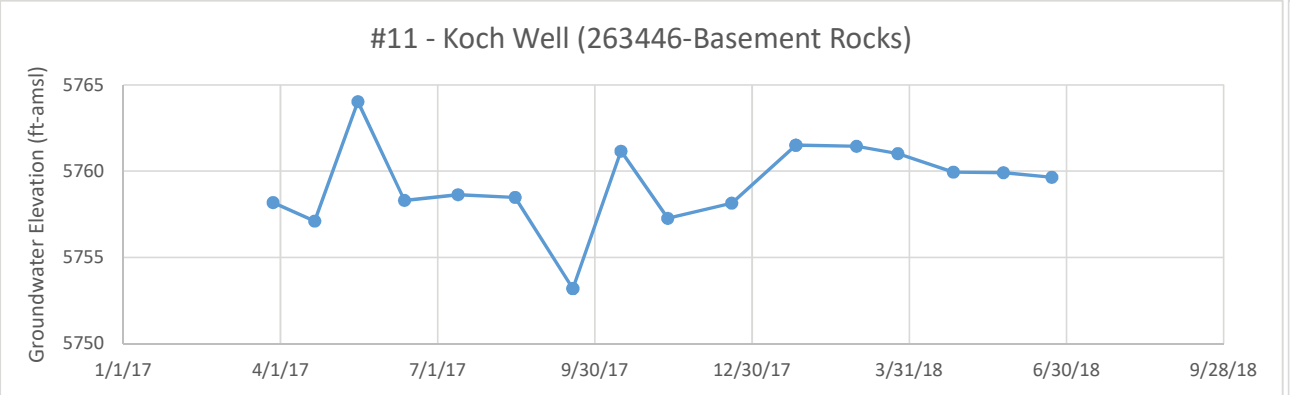

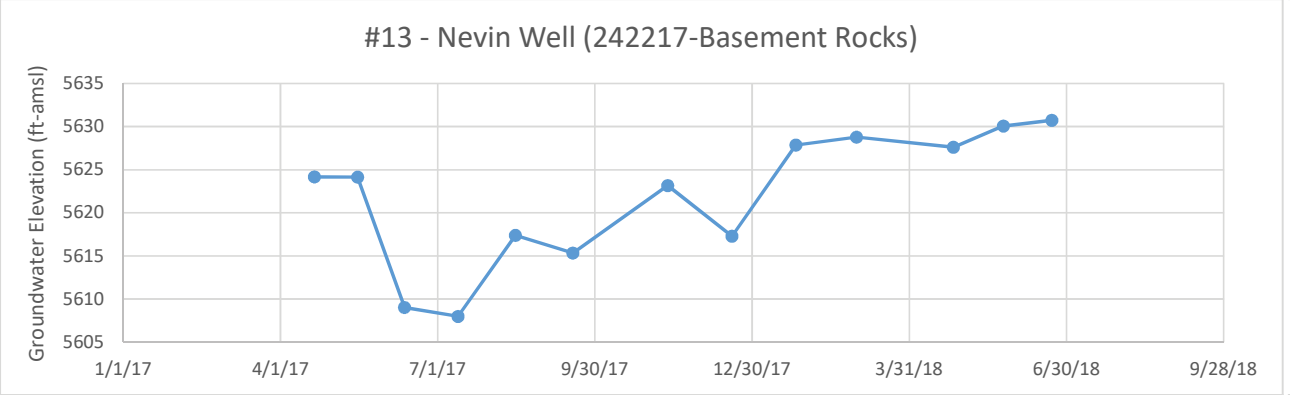

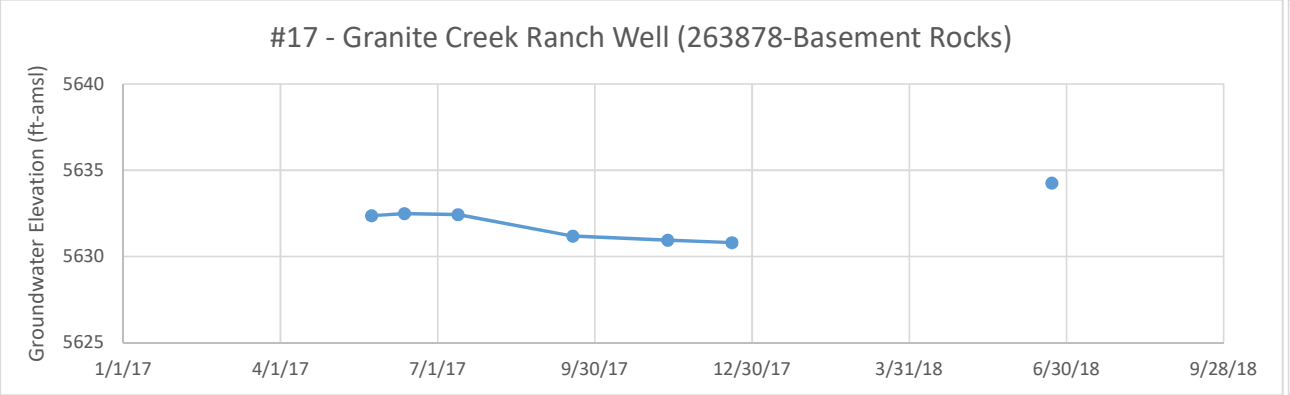

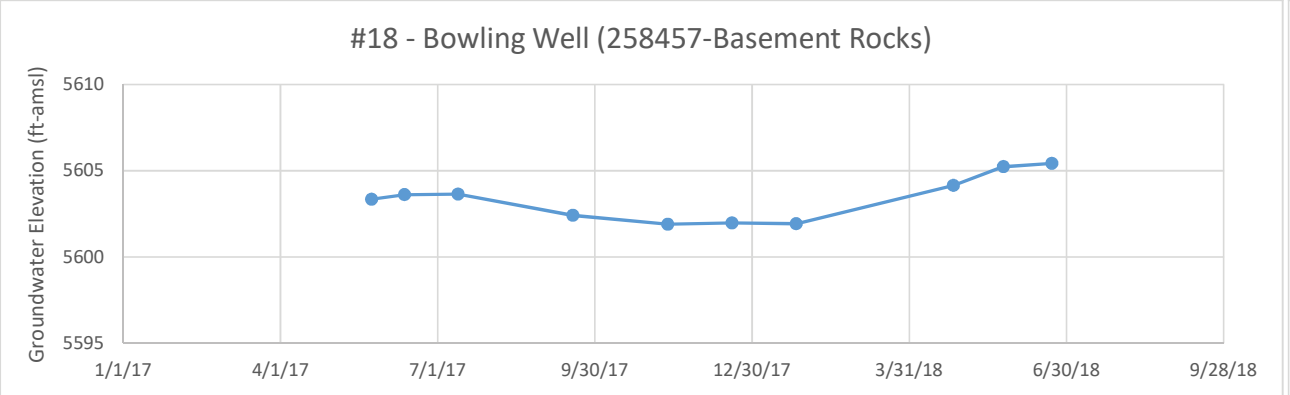

Appendix B. Virginia City Well Hydrographs (pg 2 of 4)

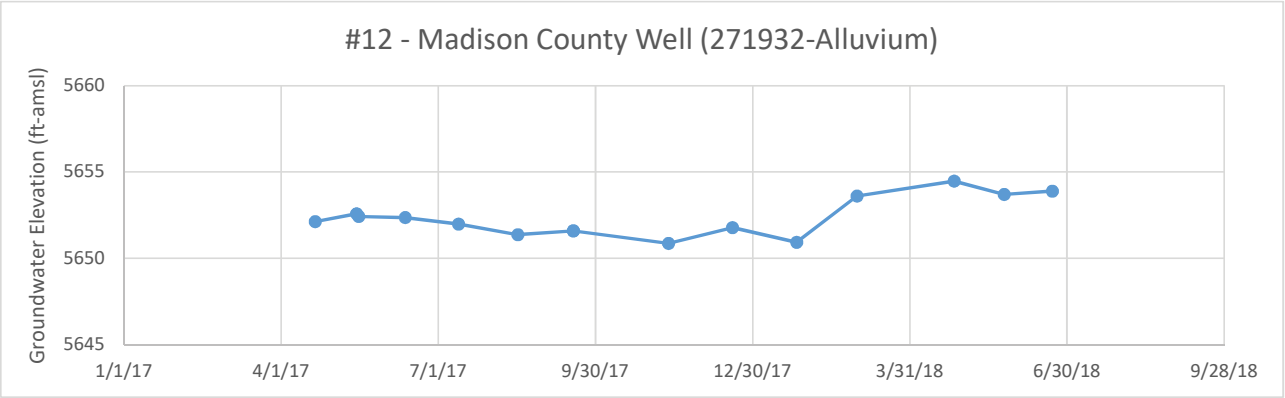

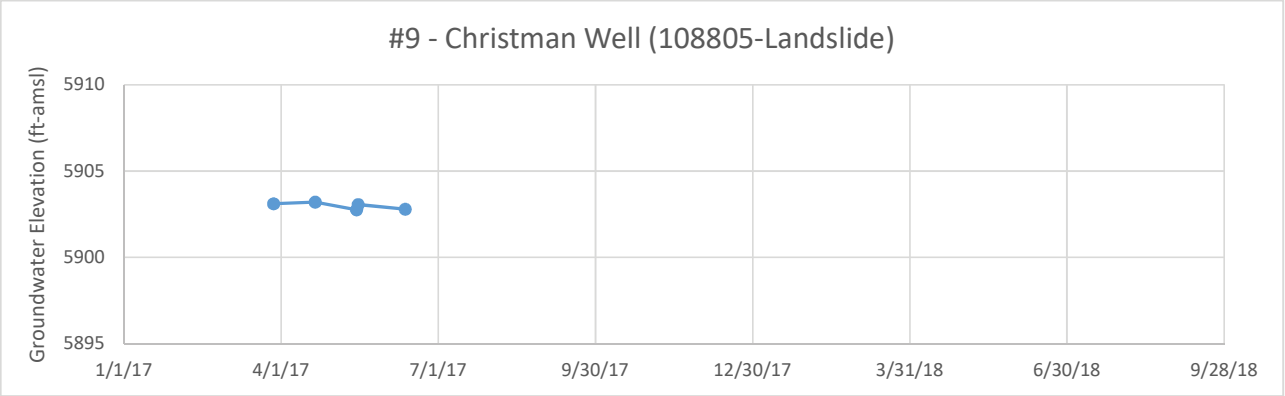

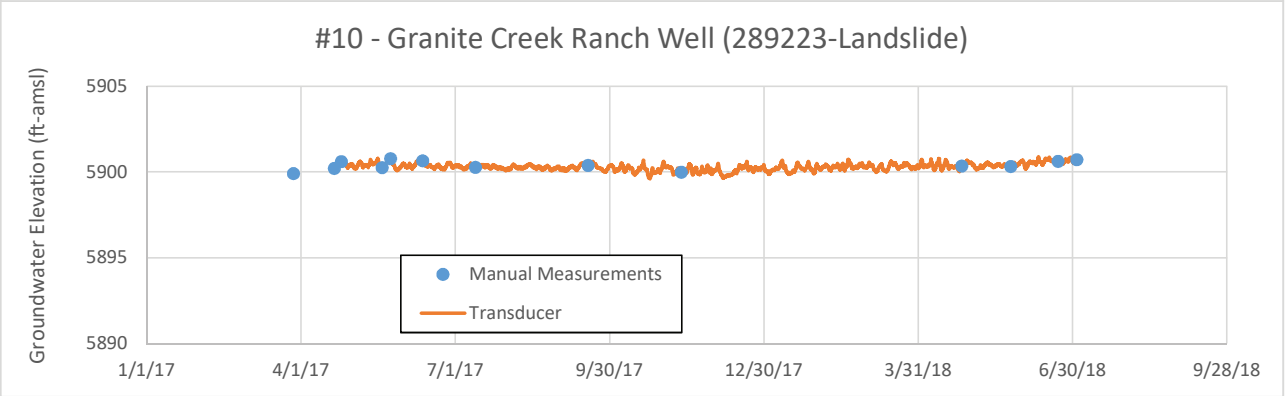

Appendix B. Virginia City Well Hydrographs (pg 3 of 4)

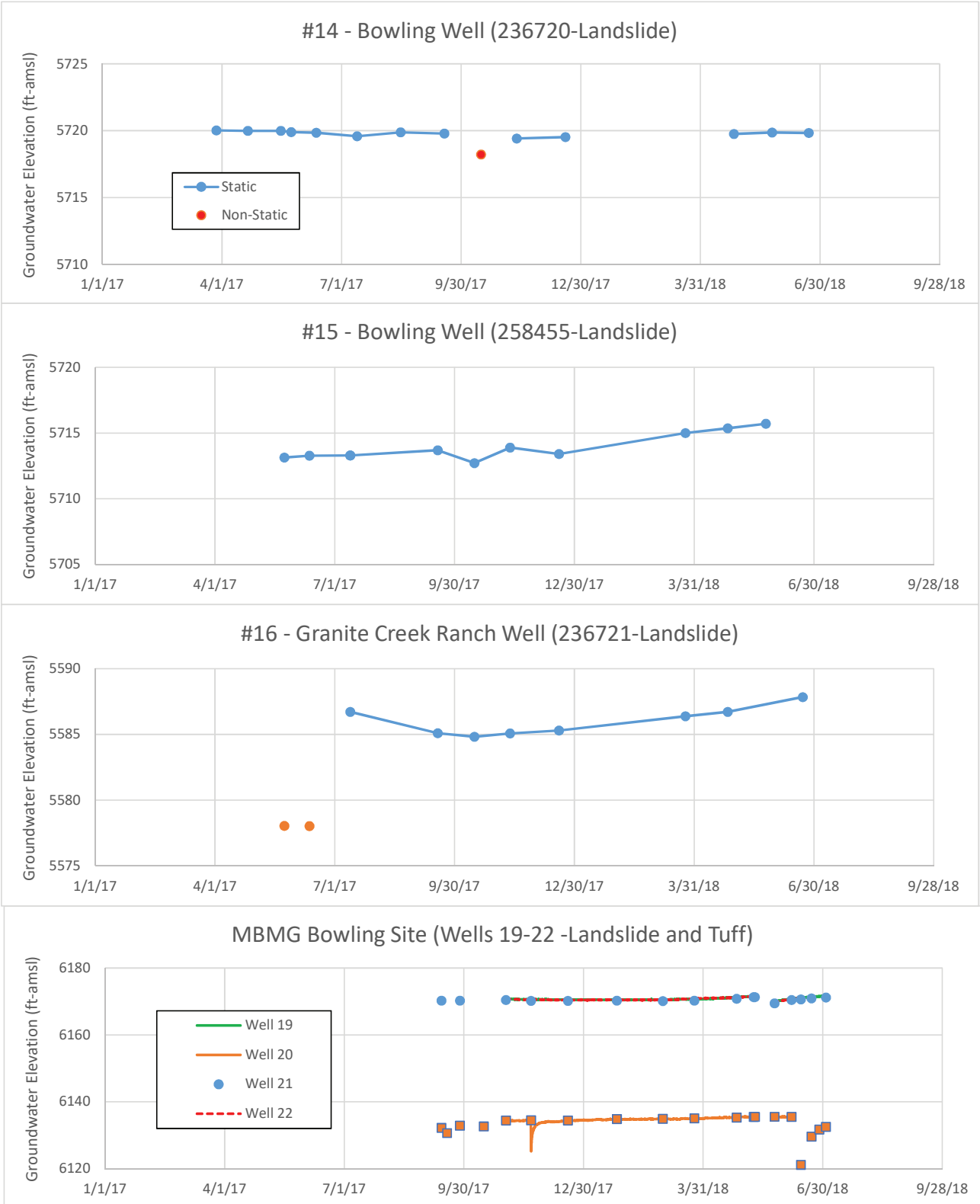

Appendix B. Virginia City Well Hydrographs (pg 4 of 4)

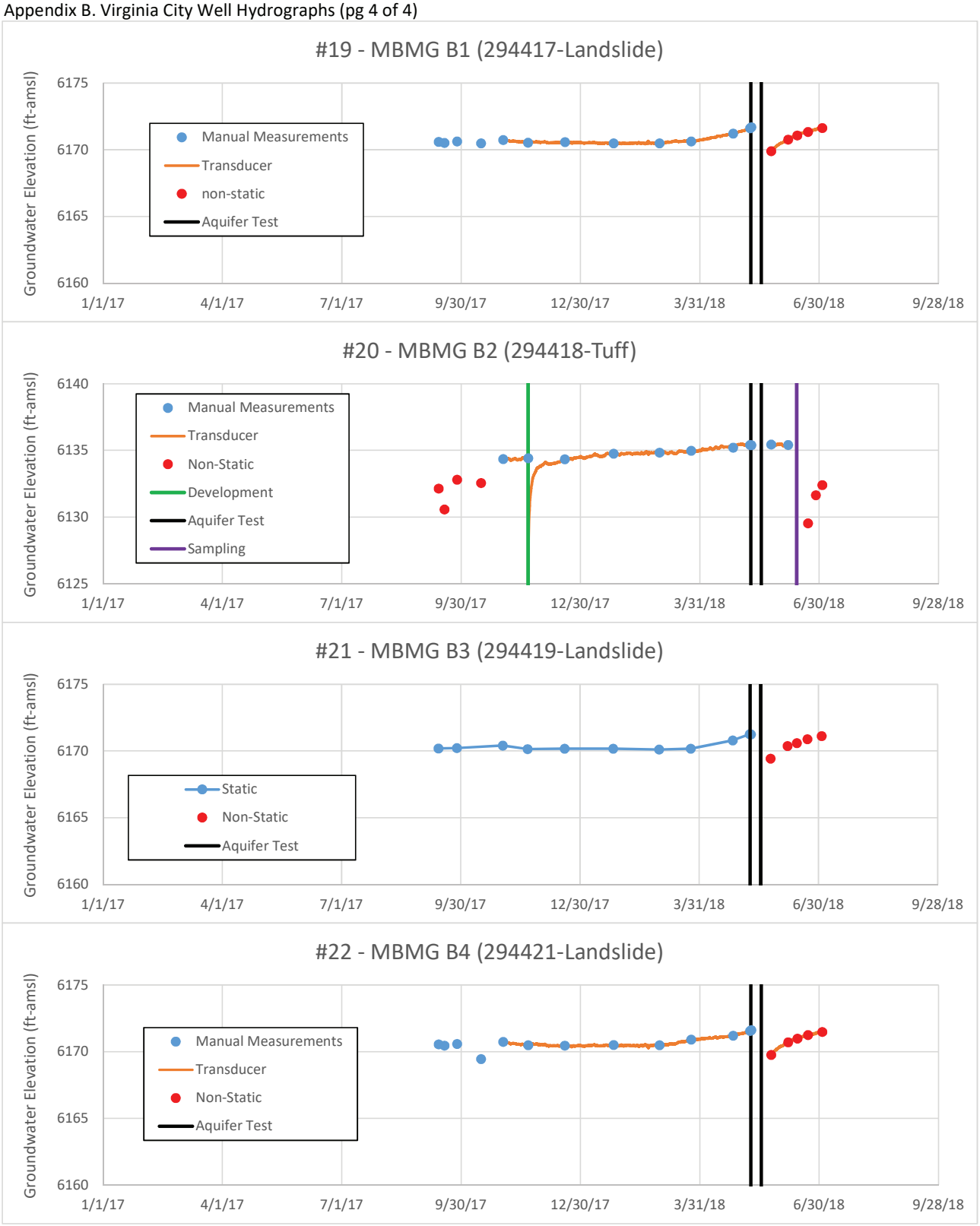

APPENDIX C

SPRINGS AND STREAMS, HYDROGRAPHS, AND THERMOGRAPHS

Appendix C. Virginia City Surface-Water Hydrographs—Daylight Creek (page 1 of 6)

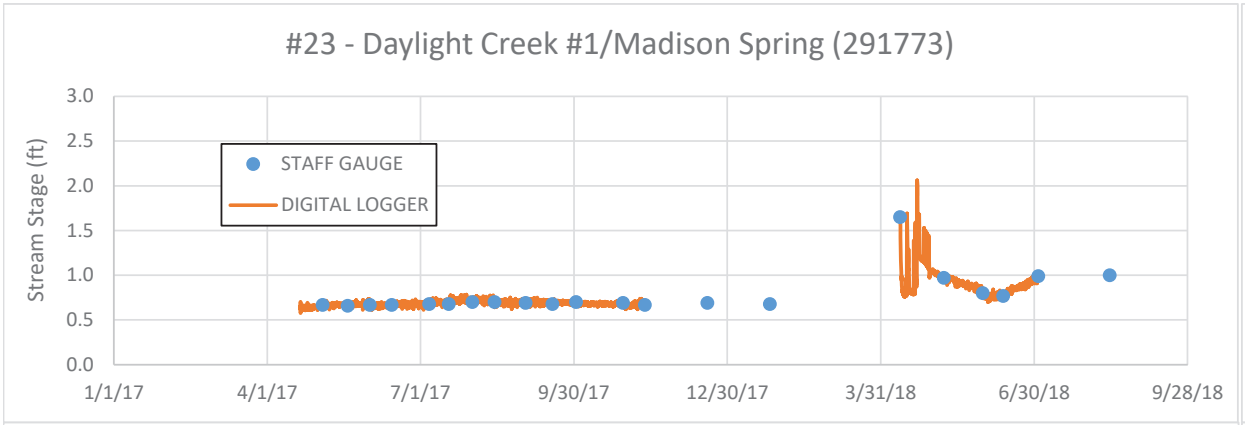

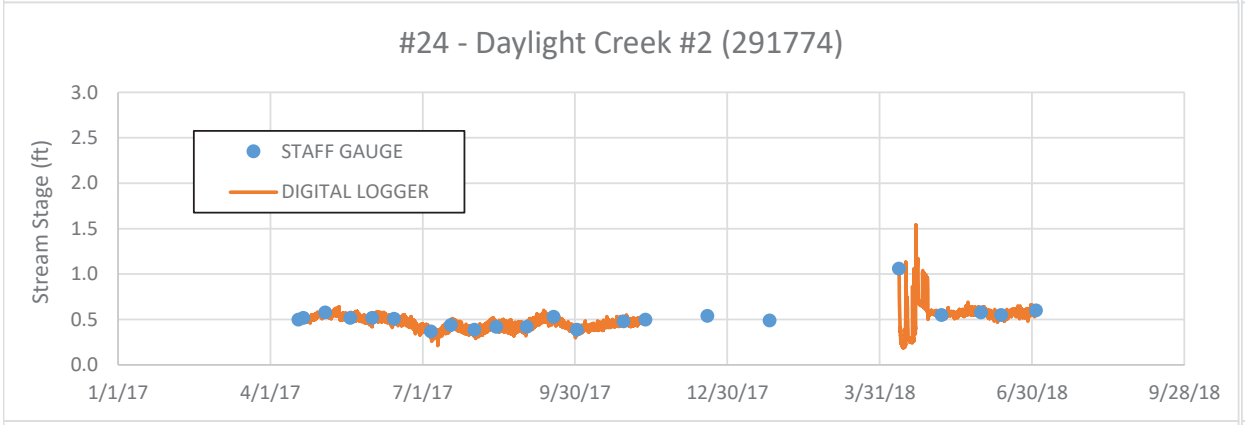

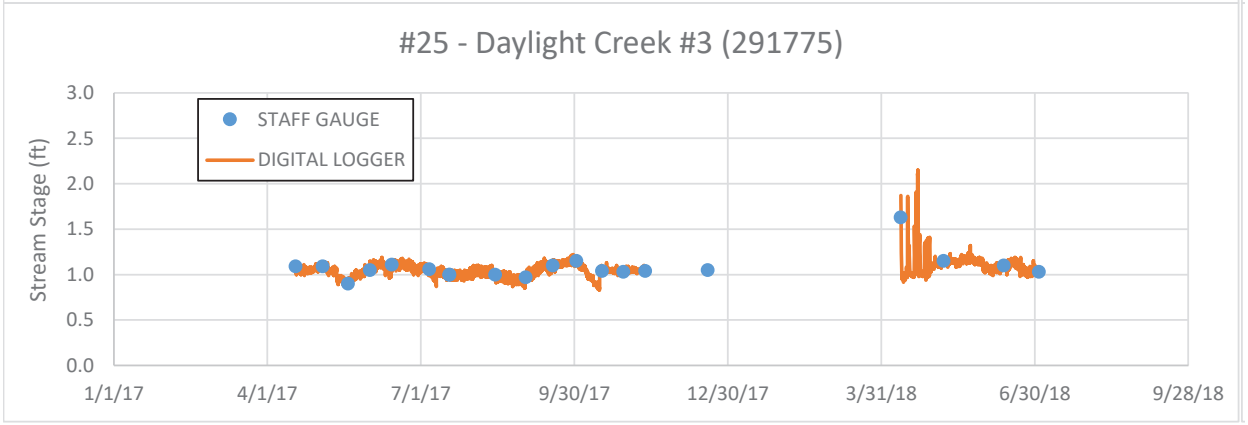

Appendix C. Virginia City Surface-Water Hydrographs—Alder Gulch (page 2 of 6)

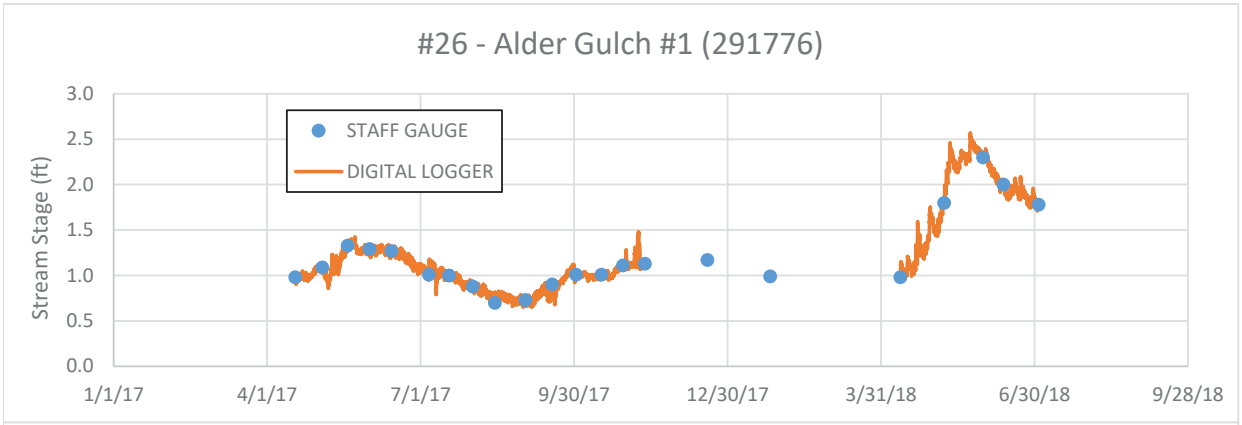

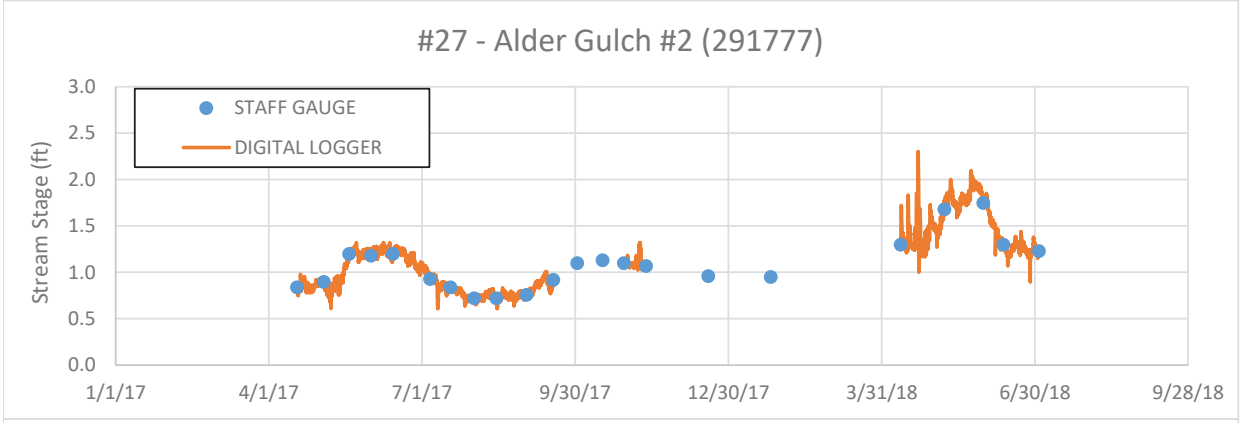

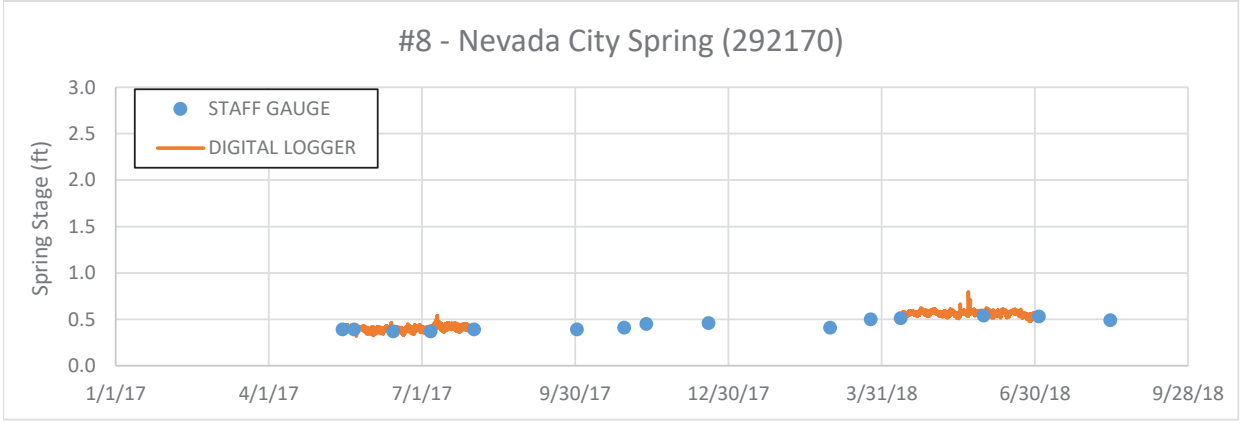

Appendix C. Virginia City Surface-Water Hydrographs—Daylight Creek (page 3 of 6)

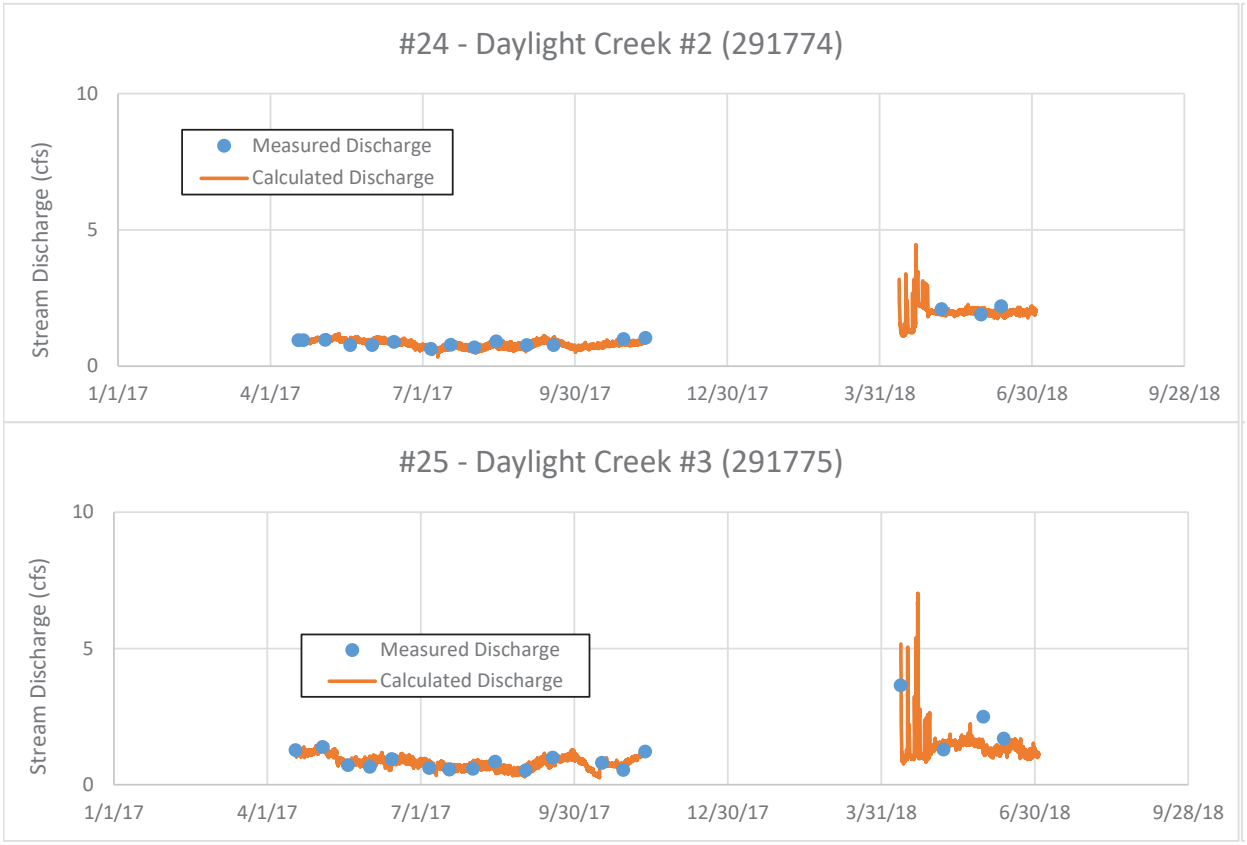

Note: Discharge was not normally measured at the Daylight Creek #1 site since the flow was low.

Appendix C. Virginia City Surface-Water Hydrographs—Alder Gulch (page 4 of 6)

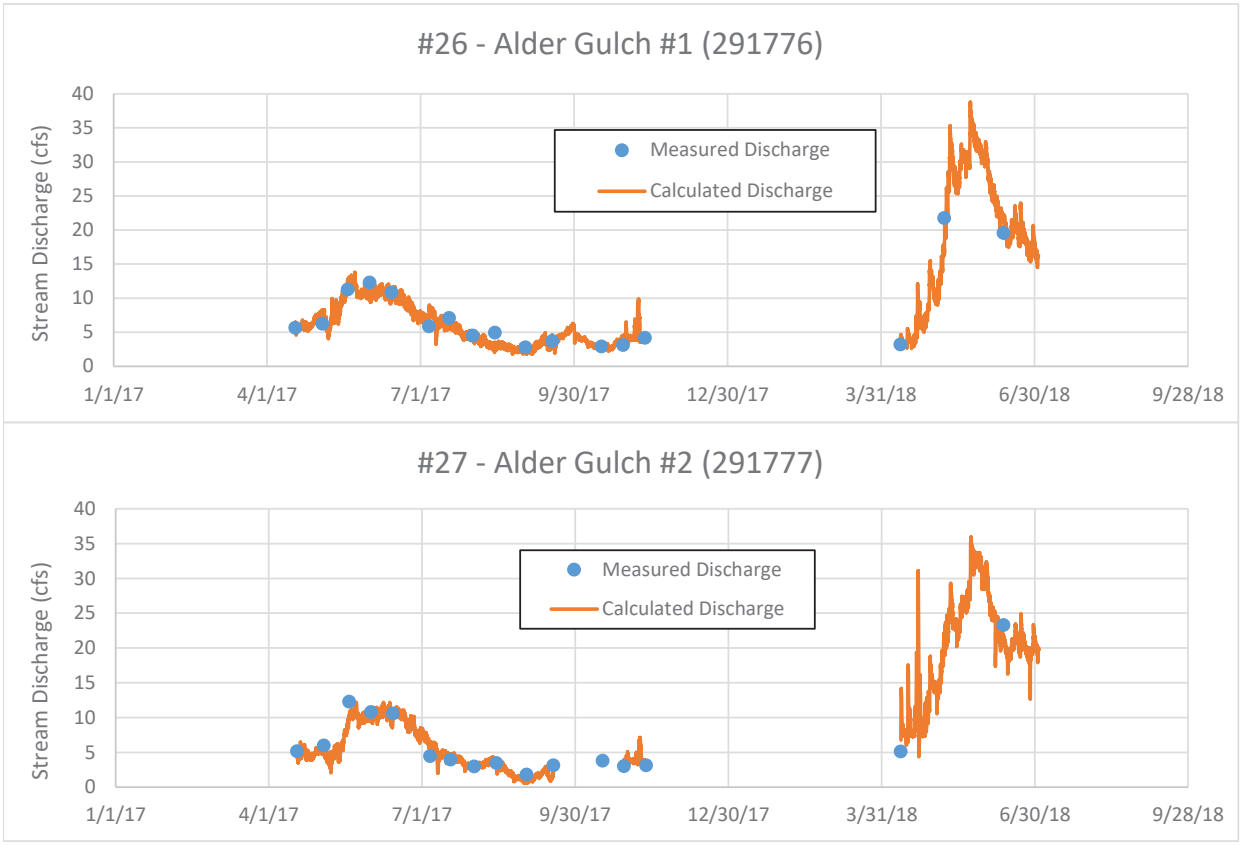

Appendix C. Virginia City Surface-Water Thermographs—Daylight Creek (page 5 of 6)

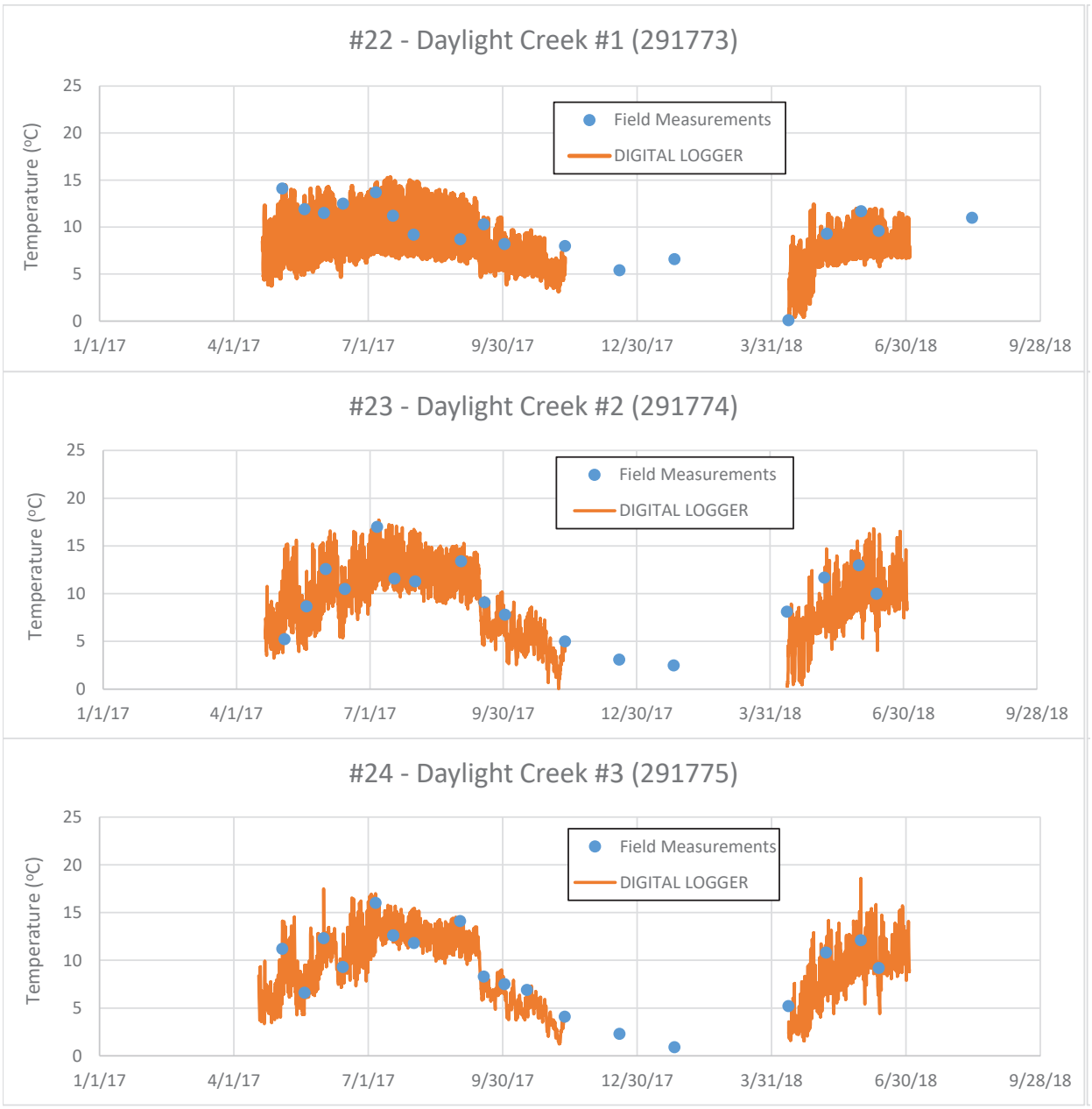

Appendix C. Virginia City Surface-Water Thermographs—Alder Gulch (page 6 of 6)